2010

Phenotype-dependent regulation of the system x_C^- cystine/ glutamate exchanger by glutathione levels in rat astrocyte primary cultures

Todd Seib
The University of Montana

PHENOTYPE-DEPENDENT REGULATION OF THE SYSTEM X_C^- CYSTINE/GLUTAMATE EXCHANGER BY GLUTATHIONE LEVELS IN RAT ASTROCYTE PRIMARY CULTURES

Todd Seib

B.S., Biochemistry, Duquesne University

M.S., Biochemistry, University of Montana

Submitted in partial fulfillment of the requirements for the

Degree of Doctor of Philosophy

Department of Biomedical and Pharmaceutical Sciences

University of Montana

2010

Seib, Todd M., Ph.D., August 2010 Dept. of BMED & Pharm. Sci.

Phenotype-dependent regulation of the System x_c^- cystine/glutamate exchanger by glutathione levels in rat astrocyte primary cultures

Research advisor: Richard J. Bridges, Ph.D.

The system x_c^- (Sx_c^-) transporter functions under normal physiological conditions in astrocytes to mediate the exchange of extracellular cystine (L-Cys_2) for intracellular glutamate (L-Glu). The internalized L-Cys_2 serves as a rate-limiting precursor in the biosynthesis of glutathione (GSH), while the externalized L-Glu can access EAA receptors and contribute to either excitatory signaling or excitotoxcity. Although the regulation of Sx_C^- has been studied in a variety of cells, particularly as related to xenobiotic exposure, much less is known about its regulation in astrocytes. In the present study the influence of phenotype (culturing in the presence of dibutyryl-cAMP) and GSH levels on the expression of Sx_C^- was investigated in cultures of primary astrocytes prepared from neonatal rats. We report that Sx_C^- activity in the dbcAMP-treated cells was nearly 7-fold greater than in untreated astrocytes (100 ± 21 and 15 ± 4 pmol/min/mg protein respectively) and that this uptake was further upregulated (~3-fold) in these cells following the depletion of intracellular GSH levels with buthionine sulfoximine (BSO, 500 μM, 24 hrs). Changes in Sx_C^- activity correlated with: increases in both protein and mRNA levels of the xCT subunit of the Sx_C^- heterodimer, an increase in the V_{max} for Sx_C^--mediated L-Glu uptake (147 ± 5 in untreated astrocytes to 350 ± 15 pmol/min/mg protein in dbcAMP-treated), and was linked temporally to alterations in GSH levels. The GSH depletion-induced induction of Sx_C^- was not mimicked by tBHQ or non-specific oxidants and was partially preventable by the co-administration of cell permeant thiols GSH-ethyl ester (5 mM) and N-acetylcysteine (NAC). These findings demonstrate that the expression of Sx_C^- on astrocytes is dynamically regulated by intracellular GSH levels in a cell- and phenotype-dependent manner. The presence of this pathway likely reflects the inherent vulnerability of the CNS to oxidative damage and raises interesting questions as to the functional consequences of changes in Sx_C^- activity in CNS injury and disease.

ACKNOWLEDGEMENTS

This work, like most endeavors, would not of been possible without the help of family, friends, and colleagues. First, I owe my gratitude to Vernon Grund and the Department of Biomedical and Pharmaceutical Sciences for giving me the opportunity to participate in this research program. Under the guidance of Richard Bridges, I have learned much about experimental design, scientific writing, and enzyme kinetics. I also am grateful to Rich for his patience with and dedication to my project. My graduate experience would not of been complete without the contributions and camaraderie of lab members Brady Warren, Fred Rhoderick, Sarjubhai Patel, Shailesh Agarwal, Wes Smith, Ran Ye, and Melissa Pathmajeyan, thank you all for your support and memories. Thanks to Jean Pfau, Darrell Jackson, Fernando Cardozo-Paelez, and Michele McGuirl for advice and insight regarding the development of this project. I would also like to thank Teri Girtsman, David Holley, Greg Leary, and Tom Rau for their enhancement of the lab experience. Thanks to the Departmental staff, including Kate Stewart, Lou Herritt, and Corbin Schwanke for their hard work and ready assistance. I would also like to thank faculty members John Shumpert, Andrij Holian, Craig Johnson, Chuck Thompson, and Keith Parker for their informative lectures and mentorship. I would like to thank my parents, Duane and Debbie Seib, and Cheri and Timothy Hanks, for introducing me to the natural world and to books. The lifelong support and encouragement from my family is greatly appreciated. I also thank my wife, Ilsa, who makes time fly when she's around and stand still when she's not. Her support and perspective were likely the most instrumental toward the completion of my graduate education.

TABLE OF CONTENTS

LIST OF TABLES

LIST OF FIGURES

Chapter 1. Introduction

1.1 System x_C^- functional characteristics

Membrane transporters on neurons and glia serve to regulate both intracellular and extracellular environments of the CNS. Uptake provides a route of entry for needed metabolites, as well as a mechanism through which synaptic and extrasynaptic concentrations of neuroactive molecules can be controlled. The system x_c^- (Sx_c^-) transporter functions under normal physiological conditions to mediate the exchange of extracellular L-cystine (L-Cys_2) for intracellular glutamate (L-Glu).

Much of the initial identification and comprehensive characterization of Sx_C^- was first described in IMR-90 cells by Shiro Bannai and colleagues (Bannai 1984; Bannai 1986a; Bannai and Kitamura 1980; Bannai and Kitamura 1981). Their initial kinetic and amino acid analysis revealed that: 1.) L-Cys_2 and L-Glu are exchanged in a 1:1 molar ratio at a single carrier and act as competitive substrates for one another on either side of the plasma membrane, 2.) the exchange process is independent of sodium ion availability and dependent on chloride ions (chloride component demonstrated by Waniewski and Martin (Waniewski and Martin 1984)), 3.) exchange is electroneutral and dependent on each substrate having a net negative charge which in turn is dependent on pH, and 4.) internally transported L-Cys_2 is reduced to L-cysteine (L-CysH) (often by reacting with glutathione (GSH) to form a GSH-CysH disulphide and free L-CysH), which, in turn serves as the rate-limiting precursor for the synthesis of GSH.

The first isolation of mouse xCT (the protein subunit of Sx_C^- responsible for substrate specificity) by expression cloning was obtained from mouse macrophages stimulated with LPS (Sato et al. 1999). The human variants of xCT (xCTa and xCTb) were subsequently cloned from WI26VA4 lung fibroblasts (Sato et al. 2000) and U87 glioma cells (Kim et al. 2001) respectively. Sx_c^- has now been identified in a wide variety of CNS cells (e.g., astrocytes (Allen et al. 2001; Cho and Bannai 1990; Gochenauer and Robinson 2001), microglia (Piani and Fontana 1994), retinal Muller cells (Kato et al. 1993), immature cortical neurons (Murphy et al. 1990), and glioma cell lines (Cho and Bannai 1990; Ye et al. 1999)), as well as fibroblasts, macrophages, hepatocytes and endothelial cells (Bannai 1986b; Hosoya et al. 2002; Sasaki et al. 2002; Sato et al. 1999). Sx_c^- is also present (and inducible) at the blood brain barrier, where it may serve as a point of entry for L-Cys_2, as well as structurally related drugs and neurotoxins (Guebel and Torres 2004; Hosoya et al. 2002; Nagasawa et al. 2005; Warren et al. 2004).

Following the initial findings that identified L-Glu and L-Cys_2 as endogenous substrates of Sx_C^-, numerous pharmacological studies have continued to probe the specificity of the transporter. Structure-activity studies employing amino acid analogs of the endogenous substrates have demonstrated that L-aspartate acts as neither a substrate nor inhibitor, and that L-homocysteate, L-alpha-aminoadipate, L-alpha-aminopimelate, quisqualate, 4-S-carboxyphenylglycine (4-S-CPG), ibotenate, (RS)-4-Br-homoibotenate, (RS)-5-Br-willardine, are competitive inhibitors (Bannai 1986a; Cho and Bannai 1990; Patel et al. 2004; Ye et al. 1999). A structurally unrelated compound, sulfasalazine, has also been shown to act as a potent inhibitor

of Sx_C^- (Chung et al. 2005). While a number of inhibitors have been defined, the lack of selectivity among them poses a challenge to performing experiments using physiological preparations. For example, quisqualate acts as an AMPA and mGluR agonist (Balazs et al. 2006), ibotenate acts as an NMDA and mGluR agonist (Ebert et al. 1991), and 4-S-CPG is a Group I mGluR antagonist (Bedingfield et al. 1995) (for pharmacology review see Bridges and Patel 2009).

Sx_C^- is a heterodimer composed of the two proteins, xCT and 4F2hc (aka CD98) (Sato et al. 1999). The xCT subunit (502 a.a., ~ 40 kDa) is a member of solute carrier family 7 (SLC7), which is divided into two subgroups, the cationic amino acid transporters (CAT) and the light chains of the heteromeric amino acid transporters (HAT) (human genome mapping workshop designation SLC7A11) (for review see Verrey et al. 2004). xCT and members of this "light chain" family are characteristically hydrophobic, contain 12-transmembrane-spanning domains, non-glycosylated, and require one of two disulphide-linked heavy chain type-II N-glycoproteins (4F2hc or rBAT) for surface expression (Fig. 1.1). In the case of xCT, unlike some members of the HAT family, the 4F2hc subunit is required both for trafficking of xCT to the plasma membrane (Nakamura et al. 1999) and for Sx_C^- function. Sato and coworkers isolated cDNA from mouse macrophages and demonstrated that L-Cys_2/L-Glu exchange is observed only when both xCT and 4F2hc proteins are expressed together in xenopus oocytes, but not separately (Sato et al. 1999). Similar experiments with the human homolog of Sx_C^- (hxCT) (Bassi et al. 2001) demonstrated that the expression of both subunits was required to develop a stably transfected mammalian line (Bridges and Zalups 2005). The evidence for the

ability of xCT to be functionally expressed with rBAT remains inconclusive (Bassi et al. 2001; Wang et al. 2003). Amino acid transport appears to serve as only one of the many potential functions of the 4F2hc protein. With a nearly universal expression profile in tissues and cell lines, the additional roles (of which amino acid transport could be potentially related) of the heavy chain subunits in tumor proliferation, lymphocyte activation and proliferation, differentiation, and adhesion, implicate these subunits in the potential pathologies of a number of organ systems (for review see Deves and Boyd 2000).

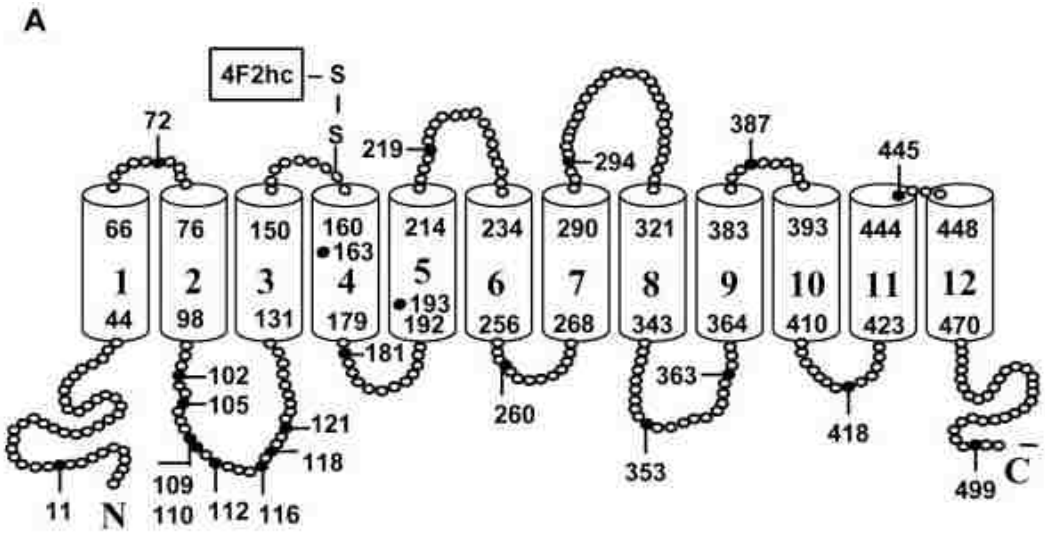

Figure 1. 1. Topology model of xCT. Both the N and C termini of xCT are located intracellularly and the 12-transmembrane domains are numbered and include the residues that define the limits of each segment. The CysH residue that forms the disulphide bond with 4F2hc is shown ($CysH^{158}$). The re-entrant loop between TM2 and 3, as well as regions of TM8 of the xCT subunit are thought to be responsible for substrate binding and transport activity (Gasol et al. 2004; Jimenez-Vidal et al. 2004).

1.2 Physiological features of the exchanger

L-Cys_2 and L-Glu act as competitive substrates/inhibitors (i.e., K_m's for L-Cys_2 and L-Glu in the 50-100 μM range) for one another at Sx_C^-, therefore the direction of L-Glu/L-Cys_2 exchange through the antiporter is determined by the concentration gradients of either substrate across the plasma membrane (Fig. 1.2) (Bannai 1986b). Under normal physiological conditions, the system XAG- transporters (aka EAATs) function to concentrate L-Glu into neurons and glia. This establishes a concentration gradient where intracellular L-Glu concentration (mM) greatly exceeds that of the extracellular space (Danbolt 2001). This and the nearly undetectable levels of L-Cys_2 in the CSF (Sagara et al. 1993a; Wang and Cynader 2000) dictate that the transporter exchanges one molecule of extracellular L-Cys_2 for one of intracellular L-Glu. As a consequence of this bidirectional transport, Sx_C^- mediates two distinct actions -- the influx of L-Cys_2, which once reduced intracellularly to L-CysH, acts as the rate-limiting precursor for the synthesis of GSH, an antioxidant important for both glial and neuroprotection, and, the efflux of L-Glu, which, depending on spaciotemporal conditions and concentration, may contribute to both extrasynaptic signaling and excitotoxicity (Baker et al. 2002a; Baker et al. 2002b; Choi 1990; Chung et al. 2005; Sontheimer 2008).

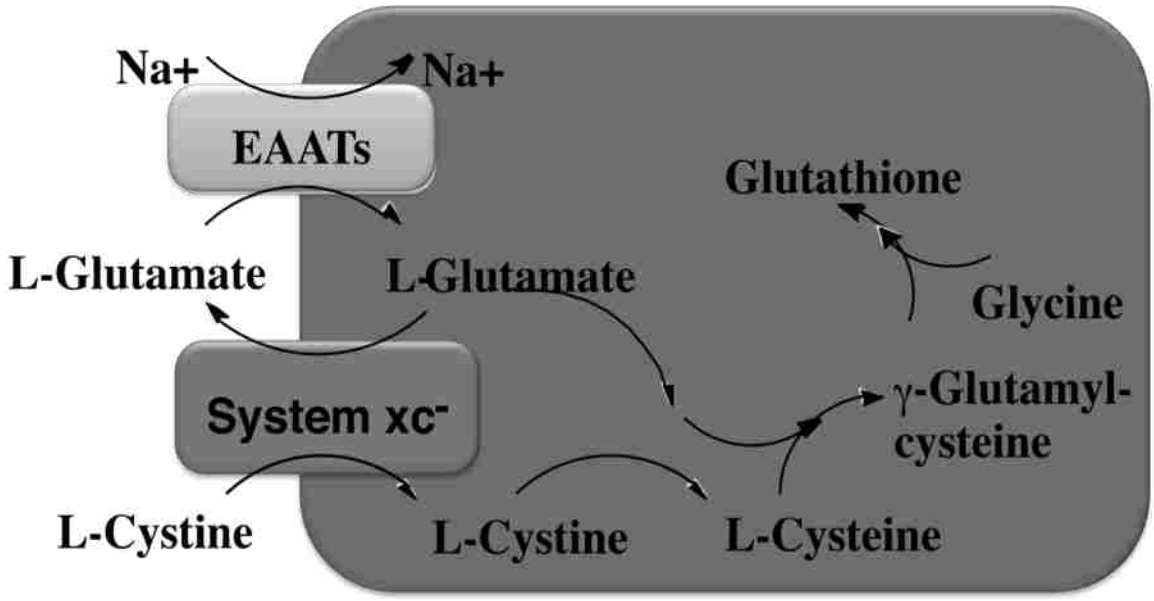

Figure 1.2. The physiological significance of Sx_C^- is related to the import of L-Cys_2 and the export of L-Glu. Sx_C^- can undergo homo- or hetero-exchange with both L-Cys_2 and L-Glu depending on concentration gradients. Under normal physiological conditions, the low levels of extracellular L-Cys_2 coupled with the high intracellular levels of L-Glu (established by the activity of the EAATs), dictate that Sx_C^- functions by exchanging an intracellular L-Glu molecule for one extracellular L-Cys_2.

1.2.1 GSH

GSH is synthesized in two ATP-dependent steps to form a tripeptide comprised of the amino acids L-Glu, L-CysH, and L-glycine and is present in virtually all cell types (Fig. 1.4). In the CNS, GSH is the most prevalent antioxidant (it comprises 97% of the acid-soluble thiols in the cerebral cortex and approximately 80% of the total soluble thiol groups and in whole brain, the concentration of total glutathione, consisting of both oxidized and reduced forms, ranges from 0.5 to 3.4 μmoles/gm tissue (for reviews see Dringen et al. 2000; Meister and Anderson 1983; Orlowski and Karkowsky 1976). Depending on culture conditions and analytical methods used,

intracellular GSH levels in CNS derived cell cultures and immortalized lines can range from ~7-50 nmoles/mg protein (Cho and Bannai 1990; Dringen et al. 1999; Gegg et al. 2005; Sagara et al. 1993a; Sagara et al. 1993b). Consistent with the localization of Sx_C^- on glia (Sato et al. 2002), the majority of GSH in the brain is also found in astrocytes (Ben-Yoseph et al. 1996; Sagara et al. 1993b; Slivka et al. 1987), which consequently can withstand higher levels of H_2O_2 induced toxicity than neurons (Desagher 1996; Philbert et al. 1991; Raps et al. 1989).

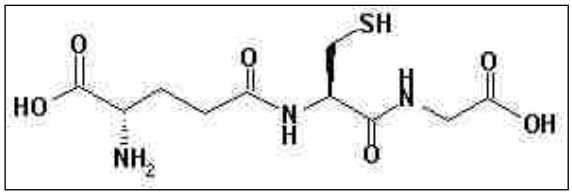

Figure 1.3. The chemical structure of glutathione (GSH).

For a seemingly simple molecule, GSH serves as a multifaceted detoxification strategy for the cell. Much of this is due to the L-CysH moiety which allows GSH to react non-enzymatically with oxidants such as the highly damaging hydroxy and peroxynitrite radicals (for reviews see Juurlink and Patterson 1998; Meister and Anderson 1983; Orlowski and Karkowsky 1976). Peroxides, by-products of aerobic respiration and superoxide metabolism and potential precursors for more reactive radicals, are detoxified enzymatically by glutathione peroxidase and GSH (Juurlink and Patterson 1998; Meister and Anderson 1983; Orlowski and Karkowsky 1976). There are a large group of metals and reactive electrophiles, many of which are known or suspected carcinogens, that are also efficiently conjugated and removed by the action of glutathione-S-transferase (GST) enzymes (Hayes et al. 2005).

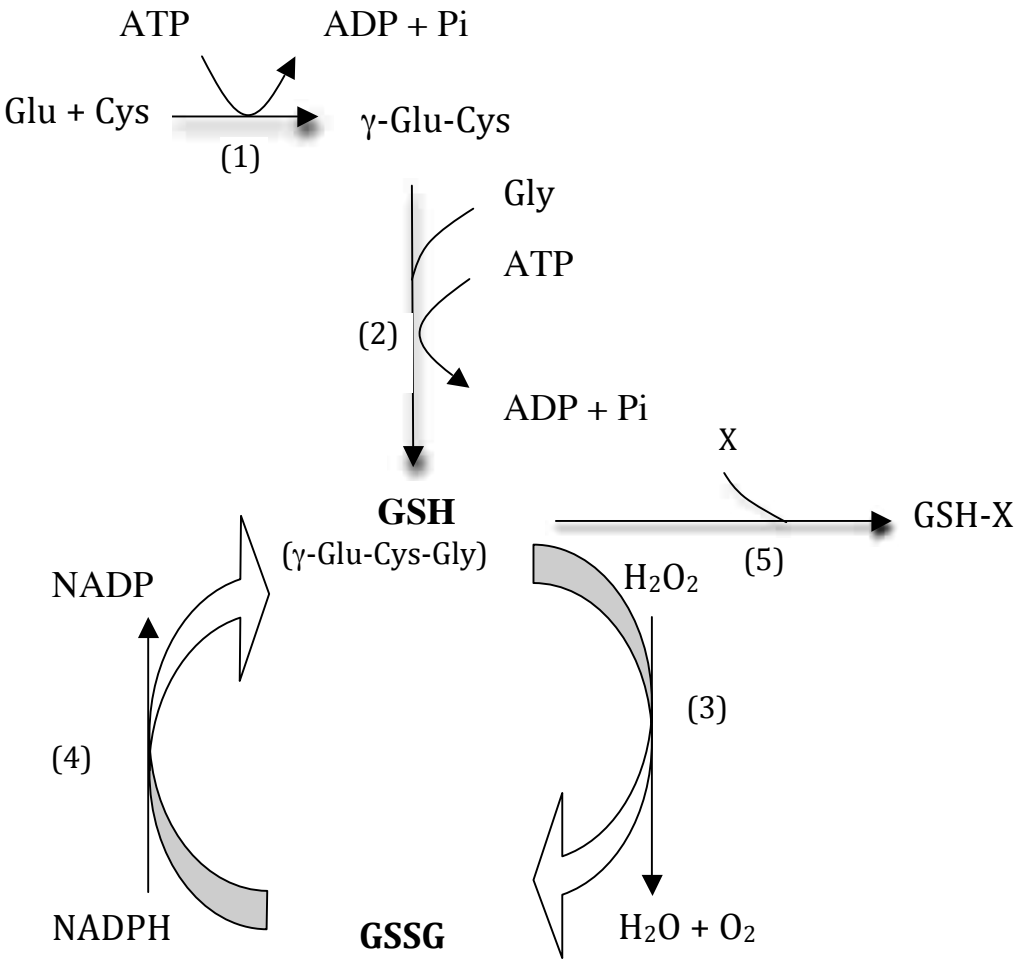

Figure 1.4. Glutathione synthesis and detoxification reactions. The rate-limiting reaction for GSH synthesis is catalyzed by γ-glutamylcysteine synthetase (1.) γ-Glutamylcysteine and glycine then react to form the final product in the second synthesis step, which is catalyzed by GSH synthetase (2.). As GSH scavenges oxidants and free radicals it is converted to the oxidized form GSSG through the action of GSH peroxidase (3.). Regeneration of GSH from GSSG requires the reducing cofactor NADPH and the enzyme GSH reductase (4.). Additionally, GSH also reacts with xenobiotics including electrophiles and metals (X) through the GSH-S-transferase (GST) family of enzymes to detoxify and remove these compounds (5).

1.2.1.1 GSH cycling between astrocytes and neurons – the L-Cys_2/L-CysH shuttle

Maintaining intracellular GSH levels is largely dependent upon the availability of the rate-limiting precursor L-CysH (Bannai 1986a; Orlowski and Karkowsky 1976). Instead of transporting L-CysH directly, L-Cys_2, transported into astrocytes through Sx_C^-, is reduced intracellularly and serves as the primary source of L-CysH for GSH synthesis (Cho and Bannai 1990; Kranich et al. 1998; Sagara et al. 1993a). In fact, culturing cells in L-Cys_2 -free media or applying a high concentration of extracellular L-Glu are both effective means by which to deplete cellular GSH levels (Cho and Bannai 1990; Sagara et al. 1993a; Sagara et al. 1993b). Consistent with this, mice that do not express xCT, exhibit plasma levels of L-Cys_2 that are double that of wildtype controls, as well as GSH levels half that of wildtype mice (Sato et al. 2005). Interestingly, depriving neuronal cultures of L-Cys_2 does not result in depleted levels of neuronal GSH (Sagara et al. 1993b). When astrocytes are grown in co-culture with neurons, neuronal GSH increases, and this can be mimicked by supplying neuronal cultures with L-CysH (Dringen et al. 1999; Sagara et al. 1993b). However, L-CysH levels in astrocyte media or CSF decrease if Sx_C^- is inhibited by L-Glu or if L-Cys_2 is removed (Dringen et al. 1999; Sagara et al. 1993a; Sagara et al. 1993b; Wang and Cynader 2000). The link between extracellular L-CysH generation and Sx_C^- function appears to be the synthesis and efflux of GSH. Current evidence suggests that extracellular L-CysH is a metabolic product of extracellular GSH that, once released from astrocytes can react: 1.) non-enzymatically with extracellular cystine to form L-CysH and GSH-CysH, or 2.) with γ-glutamyltranspeptidase (γGGT)

to produce cysteinylglycine, which is then subject to additional cleavage by a dipeptidase into L-CysH (Dringen et al. 1999; Wang and Cynader 2000). Therefore, the generation of extracellular L-CysH completes the cycle of thiol exchange between astrocytes and neurons, briefly: L-Cys_2 uptake via Sx_C^- determines intracellular and subsequently, extracellular GSH levels. Extracellular L-CysH arises as a byproduct of reactions with GSH on the cell surface and extracellular space, and neurons utilize extracellular L-CysH for GSH synthesis (Fig. 1.5). In this way glial cells are primarily responsible for maintaining neuronal GSH level (Chen 2001; Drukarch et al. 1997; Sagara et al. 1993b). Sx_C^- has been found to localize primarily on cellular membranes facing the CSF (Sato et al. 2002), the origin of L-Cys_2 for CNS transport. This specialized localization and efficient activity of Sx_C^- may explain the nearly undetectable levels of L-Cys_2 in the CSF (Sagara et al. 1993a; Wang and Cynader 2000).

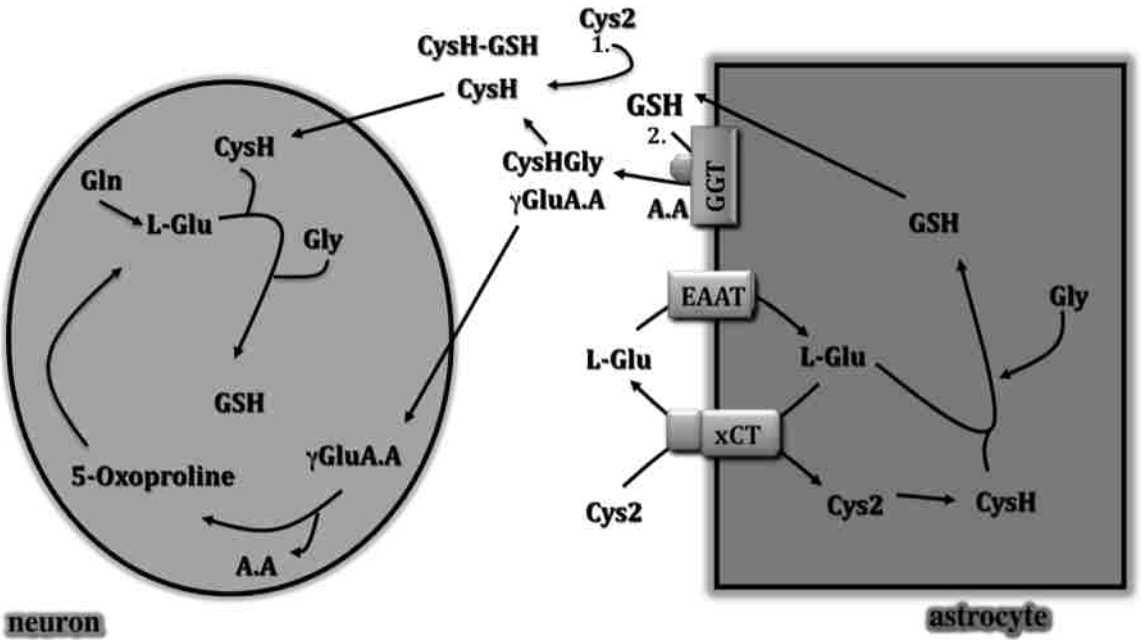

Figure 1.5. The L-Cys_2/L-CysH shuttle. The influx of L-Cys_2 through Sx_C^- provides an intracellular source of L-CysH for GSH synthesis in glia. Upon release from astrocytes, GSH can react nonenzymatically with extracellular L-Cys_2 to form L-CysH and CysH-GSH (1.), as well as undergo enzymatic catabolism (through the action of γ-glutamyltranspeptidase (GGT)) (2.) to result in the formation of γ-glutamyl amino acids (if the nucleophilic acceptor is an amino acid (A.A)), γ-glutamyl-GSH (if GSH is the acceptor), or L-Glu (if H_2O acts as the nucleophile) and L-CysHGly, which is subsequently cleaved by a dipeptidase. L-CysH is not thought to be released by glia directly (Wang 2000). The L-CysH produced as a result of reactions 1. and/or 2. then enters neurons for use in the synthesis of GSH.

1.2.1.2 Sx_C^- confers neuroprotective function to astrocytes

Two main features of the CNS make it especially vulnerable to oxidative damage; (1) the capacity for reactive oxygen species production is great, owing in part to specialized ROS generating systems (i.e. MAO and nNOS) and the high aerobic metabolic demands of the CNS, and (2) the neuronal specialization present in the CNS is membrane based, the primary components of which (lipids and protein) are

targets of oxidants (see Halliwell 1992 for review). Synaptic transmission, from the establishment of the action potential to the termination of the signal is highly dependent on membrane function and integrity. As the most abundant antioxidant in the mammalian CNS, GSH serves to protect neurons from oxidative damage. Accordingly, astrocytes play a critical neuroprotective role in the CNS as neurons rely heavily upon astrocytes for GSH precursors (for review see Dringen et al. 2000). Using co-culture systems, a number of studies have demonstrated the profound ability of astrocytes to protect neurons from oxidative stress (H_2O_2) and L-DOPA. Indeed, a cellular ratio of as few as 1 astroglial cell to 20 neurons has been shown to be protective against H_2O_2 toxicity (Desagher 1996). As the primary L-Cys_2 transport system in glia, it is perhaps not surprising that Sx_C^- function has been directly linked to the neuroprotective capabilities of astrocytes. For instance, glia are able to protect neurons from neurotoxic levels of L-Glu (3 mM) and H_2O_2 (30 μM) following the expression of Phase II detoxification and antioxidant related genes, including xCT (Shih et al. 2003). While a diverse list of genes are known to be induced in this scenario (xCT, GST, NQO1, HO-1, γGCS, GSHS, GGT, etc), the protective effect of glia is lost when GSH levels are depleted, suggesting that the protective effects are linked to those genes involved in either the synthesis or maintenance of GSH levels. In support of this, *in vitro* data has shown that xCT overexpression alone is sufficient to achieve neuroprotection in these toxicity paradigms (Shih et al. 2006).

1.2.2 L-Glu

In addition to the uptake of L-Cys_2 by Sx_C^- and the subsequent production of GSH, the other side of the exchange reaction, the export of L-Glu, is now being shown to be critically important for signaling processes within the CNS. A longstanding problem for neurochemists has been resolving the cellular source and function of extrasynaptic L-Glu in the CNS. Recently, microdialysis studies in the nucleus accumbens and striatum indicate that the primary source of *in vivo* extrasynaptic L-Glu is glial, specifically originating from the efflux activity of Sx_C^-. Through a mechanism of tonic stimulation of mGlurR2/3 receptors, L-Glu is thought to negatively regulate the synaptic release of both L-Glu and dopamine (Baker et al. 2002b). This signaling capability has been best demonstrated by its effect on withdrawal and relapse behavior in models of cocaine addiction (Baker et al. 2003; Moran et al. 2005).

1.3. Alteration of Sx_C^- function and neuropathology

Likely as a consequence of its contribution to both GSH and L-Glu levels, situations characterized by the loss of as well as increases in Sx_C^- activity are thought to mediate a number of pathologies and clinical phenomena, including neurodegeneration, the prevention and potentiation of addiction relapse, gliomas, and neuroinflammation. For example, the loss of functional xCT protein during development (Chintala et al. 2005) has been associated with reduced brain size and is associated with cortex thinning, striatum shrinkage, and ventricle enlargement

(Shih et al. 2006). There is also data to suggest that the motor neuron degeneration and spastic paraparesis observed in human neurolathyrism may involve the inhibition of Sx_C^- (Warren et al. 2004). Additionally, withdrawal from chronic cocaine administration reduces extracellular glutamate levels in the nucleus accumbens of rats by decreasing Sx_C^- activity. This reduction in activity is in turn associated with susceptibility to relapse. Conversely, increased Sx_C^- function is capable of preventing cocaine-induced drug seeking behavior (Baker et al. 2003; Moran et al. 2005).

There are also situations where increases in Sx_C^- activity may be detrimental, such as in cancers of the CNS. High-grade tumors have increased metabolic demands for glucose and oxygen and these features underlie both diagnostic and treatment strategies. Likely as a result of higher metabolic demand, gliomas and astrocytomas also exhibit increased levels of Sx_C^- activity (Ye et al. 1999) and intracellular GSH levels, both of which increase as the grade of the tumor increases (Sontheimer 2008 for review). In fact, there is growing support for the idea that the proliferative potential of a cell is related to the reduction state of cell, i.e. GSH levels could be part of what directs a cell toward cancer (Nkabyo et al. 2005). Increased GSH synthesis enables tumors to maintain rapid metabolic rates by protecting cells from endogenously produced reactive oxygen and nitrogen species, while at the same time, by endowing tumors with enhanced resistance to radiation and chemotherapy it frustrates certain therapeutic approaches that rely on overwhelming the GST and GSH-mediated mechanisms (Sontheimer 2008). Additionally, extracellular L-Glu derived from increased Sx_C^- activity may contribute to the development of

excitotoxicity and further promote cancer growth in the CNS (Choi and Rothman 1990; Chung et al. 2005; Chung and Sontheimer 2009; Lo et al. 2008; Lyons et al. 2007). The release of L-Glu via glioma cells has been linked to both peritumoral seizures and excitotoxic injury and death to surrounding neurons, potentially resulting in new space for increased tumor growth. Recent experiments using treatments that selectively inhibit Sx_C^- have resulted in decreased L-Glu efflux and GSH levels and have successfully reduced tumor growth and volume *in vivo* (Chung et al. 2005; Chung and Sontheimer 2009; Sontheimer 2008). This association between GSH and L-Glu levels and glioma growth suggests a connection between a cell's proliferative capability and Sx_C^- activity (Nkabyo et al. 2005). In support of this it has been shown that cells (astrocytes, fibroblasts, and meningeal cells) isolated from mice with deficient (Sato et al. 2005) or mutated xCT (Shih et al. 2006) are unable to proliferate normally in culture, while the overexpression of Sx_C^- enables a cell to evade cell cycle arrest (Lastro et al. 2008).

Excessive glutamate release within the CNS, as well as outside the CNS, may also contribute to pathology incurred by neuroinflammation and injury. Inflammation is commonly considered to be a non-specific protective response to antigen exposure (for reviews see Haslett et al. 1989; Ryan and Majno 1977). However, acute and chronic inflammation are also thought to contribute to pathology, including the neurotoxicity observed in CNS infections and in certain neurodegenerative diseases such as Alzheimer's and Multiple Sclerosis (Matyszak 1998; Skaper 2007). Microglia, the primary antigen presenting cells of the CNS, mediate the inflammatory response in the CNS. In response to infection, infiltrating microglia/macrophages express high

levels of Sx_C^- (Barger and Basile 2001; Piani and Fontana 1994) and in addition to pro-inflammatory factors, also release L-Glu (Piani et al. 1991). Therefore, the excitotoxic damage and neuroinflammation often associated with CNS infections and injury may be a consequence of glutamate release via Sx_C^-. Additionally, excessive levels of L-Glu levels outside the CNS may also direct the final outcome of CNS infection/injury. Under normal conditions, activated T-cells are thought to act in a neuroprotective capacity following infection/injury (Pacheco et al. 2007). However, when L-Glu is released from antigen presenting cells (APCs) via Sx_C^- (in response to LPS or other inducers (Pacheco et al. 2006; Sato et al. 1995), it can bind to mGluR5 receptors located on resting T-cells and subsequently impair T-cell activation, proliferation, and cytokine production (likely through the inhibition of ERK and JNK and activation of NF-KB) (Aandahl et al. 2002). In this way, L-Glu promotes a high threshold for T-cell activation. Therefore, deregulation of L-Glu release through Sx_C^- could promote neurotoxic outcomes in two ways, first, as a result of microglia-mediated inflammation and excitotoxicity, and second, by mediating alterations in the protective T-cell response.

In both cases, where either Sx_C^--activity and GSH levels are compromised or when Sx_C^- and GSH production are robust, resolving whether or not the changes in Sx_C^- (and consequently in GSH) are part of the disease mechanism or a compensatory cellular response to reduce disease progression, remains a major challenge. Additionally, depending on the overall effect (up- or down-regulation of Sx_C^- in balance with other modulators of L-Glu) of Sx_C^- function, the resulting changes in GSH and L-Glu levels can contribute to both therapeutic outcomes (neuroprotection,

preventing oxidative stress and relapse behavior) as well as pathology (tumor chemoresistance and growth, dysfunctional immune response, and susceptibility to drug-induced relapse). The tight balance between protection and pathology belies the inherent challenges and opportunities for therapeutic intervention at the level of GSH, L-Glu and Sx_C^-. Therefore, in order to study Sx_C^-, an increased understanding as to how Sx_C^- is regulated under normal conditions and in response to injury and disease is important, and may yield information useful for therapeutic intervention in neuropathology.

1.4. Regulation of Sx_C^-

Given the link between GSH production and Sx_C^- activity, it is perhaps not surprising that some of the first investigations into the induction of Sx_C^- involved the treatment of cells with electrophilic agents in an attempt to deplete GSH (Bannai 1984). In the late 1980's and early 1990's research began to link the ability of electrophilic compounds to induce phase II enzymes such as glutathione-S-transferases (GSTs), NAD(P)H: quinone oxidoreductase (NQO1), epoxide hydrolase, and UDP glucuronosyltransferases (Prochaska et al. 1985; Spencer et al. 1991; Talalay 1989; Talalay et al. 1988). At around the same time, cis-acting upstream enhancer elements of mouse and rat liver GST genes that respond to these electrophilic inducers were identified as nearly identical 41-bp segments termed the EpRE (electrophile response element and the antioxidant-response element (ARE) respectively (Prestera et al. 1993; Prestera and Talalay 1995). These sites were

shown to be distinct from AP-1 binding sites and tert-butylhydroquinone (tBHQ) was identified as one of a number of electrophiles shown to activate the EpRE (Prestera and Talalay 1995) via the transcription factor Nrf2 (see Itoh et al. 2004 for review). Consistent with the up-regulation of GSH-dependent enzymes and other detoxification mechanisms, Sx_c^- was also among the proteins known to be regulated through the EpRE (Ishii et al. 2000; Sasaki et al. 2002)(For a more detailed historical discussion into the regulation of Sx_C^- by Nrf2 and other transcription factors, see appendix). However, this level of regulatory control appears to differ among cell types (Qiang et al. 2004; Sasaki et al. 2002; Wang et al. 2006) and accumulating evidence suggests other mechanisms for Sx_C^- regulation exist. For example, similar to tBHQ and other electrophiles, LPS is also capable of inducing Sx_C^- in macrophages (Sato et al. 1995). However, this same induction is also observed in macrophages from mice deficient in Nrf2 (Ishii et al. 2000). In addition, there is now evidence that the up-regulation of Sx_C^- through L-Cys_2 deprivation, assumed to be mediated by the amino acid response element (AARE), is mediated not by Nrf2 but by the transcription factor ATF4 (Lewerenz and Maher 2009; Sato et al. 2004).

Sx_C^- is also up-regulated in primary astrocyte cultures following treatment with dibutyryl-cAMP (dbcAMP) (Gochenauer and Robinson 2001) presumably through the activation of the cAMP response element (CRE) (Daniel et al. 1998). The addition of dbcAMP to the culture medium results in a pronounced morphological and functional differentiation of astrocytes that is thought to model a more *in vivo* cell-type (for reviews see Hertz et al. 1998; Juurlink and Hertz 1985), specifically a reactive phenotype, a specialized glial subtype that accompany pathological

situations such as stroke, MS, and neuroplasia (Daginakatte et al. 2008). Astrocytes cultured in the presence of dbcAMP express increased levels of GFAP (Le Prince et al. 1991), glutamate transporters (Schlag et al. 1998; Swanson et al. 1997), glutamine synthetase (GS)(Stanimirovic et al. 1999), GABA(A) receptors (Hosli et al. 1997), and Sx_C^- (Gochenauer and Robinson 2001). It is likely that dbcAMP induces changes in protoplasmic astrocytes similar to those resulting from noradrenergic innervation *in vivo* (Hertz et al. 1998) and the action of the pituitary adenylate cyclase-activating polypeptide (PACAP), a peptide synthesized by neurons which selectively acts on astroglia involved in glutamate turnover (Figiel and Engele 2000). The functional consequences of dbcAMP-induced changes in glial phenotype may result in the enhancement of several neuroprotective and neurotrophic functions, transforming these highly pleiotropic cells into a reactive cell type with potentially increased abilities to promote neuron survival and recovery from injury (for review see Escartin and Bonvento 2008). For example, in the CNS, glutamatergic neurotransmission is terminated predominantly by the rapid uptake of synaptically released glutamate into astrocytes through the Na^+-dependent excitatory amino acid transporters (EAAT1 and EAAT2, also designated GLAST and GLT-1 respectively). It is subsequently converted into glutamine by the enzyme glutamine synthetase (GS). The only condition known to affect the expression of glial glutamate transporters and GS is the co-culturing of glia with neurons or exposure to dbcAMP (Schlag et al. 1998; Stanimirovic et al. 1999; Swanson et al. 1997). In addition to EAATs and GS, astrocytes treated with dbcAMP are also known to support increased neurite outgrowth (Miller et al. 1994), exhibit increased

immunoreactivity for the GABA(A)- receptor (Hosli et al. 1997). Sx_C^- may represent another of these important functional changes brought about by culturing astrocytes with dbcAMP. The changes in Sx_C^- seen upon dbcAMP administration may represent an important strategy for synthesizing GSH and combating oxidative stress, of which the CNS is highly susceptible.

Chapter 2. Rationale and Specific Aims

2.1 Rationale

Changes in GSH status have been associated with a number of pathological conditions. Sufficient GSH concentrations in astrocytes are critical for the survival of dopaminergic neurons, and neuronal GSH loss tends to correlate with disease severity in Parkinson's Disease (PD) patients (for review see Schulz et al. 2000b). Interestingly, GSH is also decreased during the preclinical asymptomatic phase of the disease, suggesting an early role for GSH in pathogenesis. Decreases in GSH have also been observed in schizophrenics *in vivo* as well as in *in vitro* models (Do et al. 2000) and polymorphisms in GSH-metabolism and synthesis genes (i.e. GSTT1, GCLC, and GCLM) are associated with increased susceptibility to the disorder (Berk et al. 2008). Conversely, in cancers of the CNS, GSH content increases as the glioma grade increases (for review see Sontheimer 2008). There is now growing support for the idea that the proliferative potential of a cell is related to reduction state of cell, i.e. GSH levels could be part of what directs a cell toward cancer (Nkabyo et al. 2005).

If a regulatory relationship exists between Sx_C^- and GSH levels, then the above situations characterized by either a decrease or an increase in GSH may involve a dysfunction in the GSH-dependent regulatory control of Sx_C^- transport, potentially altering the ability of the cell to act in a neuroprotective or neuropathological role. Relatively little is known about the relationship between GSH levels and Sx_C^- activity

in astrocytes and the data appears to be inconsistent both between and among cells types. For example, GSH-depletion has been reported to have no effect on L-Cys_2 transport in BHK21 fibroblasts (Sasaki et al. 2002) and rat kidney fibroblasts (Kang and Enger 1992), an inductive-effect in astrocytes (no dbcAMP) (Allen et al. 2001), C1 cells (Qiang et al. 2004) and brain homegenates (Limon-Pacheco et al. 2007), and a down-regulatory effect in astrocytes (treated with dbcAMP) (Bender et al. 2000) and HAIN-6 lung fibroblasts (Bannai 1984). We hypothesize that Sx_C^-, likely as a consequence of its role in GSH supply in the CNS, will be regulated via GSH or through a thiol-mediated event, in primary astrocytes. This hypothesis is supported by recent evidence suggesting the redox state of protein sulfhydryl moieties can serve as signaling intermediates in a number of transcriptional activation events (Ahn and Thiele 2003; Delaunay et al. 2002; Limon-Pacheco et al. 2007; Tachibana et al. 2009).

In the present study we used a dbcAMP treated astrocyte model to examine the potential regulatory relationships between GSH levels and Sx_C^- activity. Astrocyte cultures were treated with buthionine sulfoximine (BSO), an efficient and selective strategy for GSH depletion (Meister 1991) in culture models (BSO does not cross the BBB) that avoids the complicating effects of other GSH-depletion agents (i.e. non-selectivity and the propensity to activate GSH enzymes as a consequence of electrophilic properties) (Bannai 1984; Ishii et al. 2000; Meister 1991). Therefore by using BSO to inhibit GSH synthesis directly, GSH was able to be depleted and repleted directly, allowing the examination of how these changes affected Sx_C^- in both cell phenotypes. We find that Sx_C^- activity in the dbcAMP-treated cells was

nearly 7-fold greater than in untreated astrocytes (100 ± 21 and 15 ± 4 pool/min/mg protein respectively) and that uptake was up-regulated further in dbcAMP-treated cells (~3-fold) following GSH depletion (BSO, 500 μM, 24 hrs). The changes in Sx_C^- activity correlated with increases in both protein and mRNA levels of the xCT subunit, an increase in the V_{max} for L-Glu (147 ± 5 in untreated astrocytes to 350 ± 15 pmol/min/mg protein in dbcAMP-treated), and was linked temporally to GSH levels. The effect of GSH depletion was not mimicked by tBHQ or oxidants in this phenotype and was not preventable by exogenously added GSH. However, the BSO-effect was partially preventable by GSH-ethyl ester (5 mM) and N-acetylcysteine (NAC). The results suggest not only that the regulation of Sx_C^- is highly dynamic and phenotype-dependent, but also, in the instance of dbcAMP differentiated astrocytes, that GSH plays a distinct role in the regulation of cystine transport. This regulation may be particularly relevant in interpreting the contributions and consequences of changes in GSH and Sx_C^- in CNS disease mechanisms.

2.2 Specific Aims

Aim I. Evaluate the effect of GSH-depletion on Sx_C^- activity in primary astrocytes cultured with and without dbcAMP

Specific Experiments:

1. Examine time dependence of dbcAMP treatment on Sx_C^- activity by employing Na^+-independent [^{3}H]-L-glutamate transport assays as a measure of Sx_C^- activity

2. Deplete GSH in both untreated and dbcAMP-treated astrocytes and examine differences in content and disappearance

3. Determine if intracellular GSH levels in untreated and dbcAMP-treated cells are dependent on precursor (cysteine or cystine) availability or Sx_C^- inhibition

4. Quantify changes in Sx_C^- activity in GSH-depleted astrocytes cultured with and without dbcAMP

5. Determine if effect on Sx_C^- is dependent on dosing order of dbcAMP and/or BSO

6. Quantify changes using well characterized EpRE-mediated inducers of Sx_C^- activity i.e. tBHQ

7. Determine if changes in Sx_C^- are consistent with Sx_C^- pharmacology

8. Perform GSH-depletion and uptake experiments under Na^+-dependent conditions to see if changes are unique to Na^+-independent transport

Hypothesis:

Astrocytes cultured in the presence of dbcAMP, likely as a consequence of representing a more *in vivo* phenotype, exhibit a more sensitive feedback response to GSH-depletion by upregulating Sx_C^- activity in order to provide for more intracellular cysteine for GSH synthesis.

Aim II. Characterize the response of Sx_C^- to GSH-depletion in dbcAMP–treated astrocytes

Specific Experiments:

1. Perform a kinetic analysis of Sx_C^- transport to determine if the changes in response to GSH-depletion are related to the V_{max} or K_m of the transporter

2. Determine if GSH-depletion results in functional changes in Sx_C^- - mediated accumulation of extracellular L-glutamate in response to L-cystine availability using a fluorescence-coupled assay

3. Determine whether or not the changes in Sx_C^- activity correspond to changes in protein by performing immunoblots for both xCT and 4F2hc

4. Analyze mRNA changes in response to GSH-depletion using RT-PCR

5. Determine if Sx_C^- uptake recovers to control levels as GSH levels are restored

6. Determine the ability of GSH, GSH-metabolites, thiols, and antioxidants to prevent the effect of GSH-depletion on Sx_C^- activity

7. Evaluate the relationship between the level of ROS production and GSH-depletion in dbcAMP-treated astrocytes using carboxy-H2DCFDA

8. Determine if the effect of BSO on Sx_C^- can be mimicked by ROS, electrophiles, and L-cystine uptake inhibition

Hypothesis:

The change in Sx_C^- activity as a result of GSH-depletion may be a consequence of increased ROS and/or the removal of constitutive thiol-mediated regulation of the transporter. Cultures exposed to ROS, or transporter inhibition, should mimic the effect of BSO and a pre-treatment with GSH or GSH metabolites that bypass the BSO-mediated inhibition should prevent it.

Chapter 3. Materials and Methods

3.1 Cell culture and treatment regimen

Primary astrocytes were isolated and cultured from the cerebral cortices of 1-3 day old Sprague-Dawley rats using a standard protocol (McCarthy and de Vellis 1980). Briefly, cortices were removed and dissociated by repeated trituration with a borosilicate glass pipette and distributed into 150 cm^2 flasks containing DMEM/F12 (Invitrogen) supplemented with 15% FBS (Hyclone). Following a 24 hr incubation, the medium was replaced with DMEM/ F12 w/ 10% FBS to remove non-adherent cells. Cultures were maintained at 37^o C for approximately two weeks with medium changes occurring twice a week until 80%-90% confluency was achieved. The cultures were then shaken at 280 rpm for 24 hrs at 37^o C to remove contaminating cell types. At 100% confluency astrocyte cultures were plated as follows: 12-well plates, 3.0-4.0 x 10^4 cells/well; 100 mm dishes, 3.0-5.0 x 10^5 cells/dish; and 96-well plates, 5.0 x 10^3 cells/well. Ten to fourteen days post-plating astrocytes reached confluency and were designated as experimental day 0. Starting on day 0 and every 3 days afterward, culture media was changed and cultures either were given media alone or media containing 250 mM dbcAMP for a total of 7 days. Unless indicated otherwise, astrocytes receiving buthionine sulfoximine (BSO, Sigma-Aldrich), GSH-ethyl ester (Sigma-Aldrich), tert-butylhydroquinone (tBHQ, Alfa Aesar), N-acetylcysteine (NAC, Sigma Aldrich), glutathione (GSH, Sigma Aldrich), or other agents, were added to the astrocyte cultures for the final 24 hrs of the 7-day

regimen. Astrocyte cultures were >95% positive for glial fibrillary acidic protein (GFAP) and exhibited the well described polygonal to stellate change in morphology following exposure to dbcAMP (Hertz et al. 1998).

3.2 Transport activity assays

Sx_c^- activity was assayed using a protocol previously described (Patel et al. 2004; Warren et al. 2004). Briefly, on the day of the assay, growth media (DMEM/F12 w/ 10% FBS) was removed from cells grown in 12-well culture plates and replaced with a Na^+-free buffer (mM), $CaCl_2$ (1.1), KCl (5.36), KH_2PO_4 (0.77), $MgSO_4$ (0.71), choline chloride (137.5), D-glucose (11), HEPES (10), pH 7.4. Following a 5 minute pre-incubation in Na^+-free buffer (30° C), the buffer was aspirated and replaced with buffer containing 100 μM [^{3}H]-L-glutamate (New England Nuclear). Following a 5-min incubation at 30° C, the assays were terminated by three sequential 1-mL washes with ice-cold buffer and then the cells were dissolved in 1 mL of 0.4 M NaOH for 24 hrs. An aliquot (200 μL) was transferred into a 5-mL glass scintillation vial and neutralized with 5 μL glacial acetic acid, followed by the addition of 3.5 mL Liquiscint scintillation fluid (National Diagnostics) to each sample. Incorporation of radioactivity was quantified by liquid scintillation counting (LSC, Beckman LS 6500). All transport activity rates were normalized for protein determined via the BCA method (Pierce). Values are reported as mean pmol/min/mg protein ± SEM and are corrected for nonspecific uptake (e.g., leakage and binding) by subtracting the amount of [^{3}H]-L-glutamate accumulated at 4° C. To determine EAAT activity, a protocol identical to the above was employed, with the exception of using the

appropriate Na^+-dependent ionic conditions ((mM), KCl (5.3), KH_2PO_4 (0.441), NaCl (137.9), Na_2HPO_4 (0.336), D-glucose (11), $CaCl_2$ (1.1), $MgSO_4$ (0.71), HEPES (10), pH 7.4) and substrate ([^{3}H]-D-aspartate, 25 μM). Maximal velocity and affinity (Km) determinations were performed using nonlinear curve fitting analyses (Kaleidagraph 3.6.5). Data plots followed Michaelis-Menten kinetics and were fitted to the equation: y = m1*m0/(m2+m0).

3.3 Glutathione determination

Intracellular levels of GSH were quantified using an enzymatic-recycling assay described by Anderson (Anderson 1985). At the incubation times indicated, the culture medium was removed from astrocytes grown in 12-well plates and the cells were rinsed 2x with Dulbecco's PBS. The plates were placed on ice and 500 μL ice-cold 1% sulfosalicylic acid (Sigma-Aldrich) was added to each well. Cells were harvested by scraping. Samples were subjected to one freeze-thaw cycle prior to assaying for total GSH levels (GSH/GSSG). On the day of the assay, samples were thawed and sonicated on ice for 10 seconds, and centrifuged (15,000 x g, 5 minutes, 4^o C). The assay was performed by combining 40 μL of sample supernatant, 40 μL 2x EDTA buffer (12.6 mM EDTA tetrasodium salt, 286 mM sodium phosphate, pH 7.8), 50 μL 2.4 mM DTNB (Sigma-Aldrich), 50 μL 0.8 mM NADPH (Sigma-Aldrich), and 20 μL GSH reductase (Roche) in individual wells of a 96-well microplate (Fisher). Final concentrations were as follows: 0.2 mM NADPH, 0.6 mM DTNB, 1.0 U/mL GSH reductase. The rate of TNB production was monitored at 405 nm for 5 min at 30^o C

on a ThermoMax plate reader (Molecular Devices) and represents total glutathione content. GSH values were normalized for protein using the BCA protein assay (Pierce).

3.4 L-Glutamate efflux determination

Fluorometric determination of extracellular L-Glu was quantified using a modification of a previously published procedure (Patel et al. 2004). Confluent monolayers of primary rat astrocytes grown in 12-well Costar tissue culture plates were washed 3X with a modified Krebs buffer ((mM), KCl (5.3), KH_2PO_4 (0.441), NaCl (137.9), Na_2HPO_4 (0.336), D-glucose (11), $CaCl_2$ (1.1), $MgSO_4$ (0.71), HEPES (10), pH 7.4) and then incubated in 500 μL of Na^+-free buffer with or without substrates/inhibitors for 15 min at 30° C. Following the incubation, the buffer was removed from each well and stored at -20°C for subsequent analysis of extracellular [L-Glu]. Fluorometric determinations of L-Glu were quantified using a Hitachi F-2000 fluorescence spectrophotometer fitted with a thermo-controlled cuvette holder and a 1 cm^2 electronically driven magnetic stirrer platform. Following equilibration of NADP+ (1mM) and glutamate dehydrogenase (GDH, 50U) in buffer for 200 seconds, 200 μL of individual samples were added to the cuvette through the injection port and the resulting NADPH fluorescence was recorded for 300 sec @ Ex 370nm and Em 450nm. Intracellular L-Glu levels were determined by lysing cells in 0.1% Triton-X for 1 hr at RT. Total nanomoles of intracellular or extracellular L-

Glu in the samples were then calculated using a standard curve generated from fluorescence readings of sequential additions of 4 nanomoles L-Glu.

3.5 Immunoblotting

Whole-cell and nuclear lysate samples were prepared from astrocyte cultures and analyzed for xCT, 4F2hc, and Nrf2 proteins. For the whole-cell lysate preparation, confluent cultures of astrocytes grown in 100 mm or 150 mm dishes were rinsed in DPBS and cells were harvested by scraping in pre-chilled DPBS/Cømplete lysis buffer (Roche). The crude lysate was centrifuged @ 1200 x g for 10 minutes, resuspended in 500 μL DPBS/Cømplete, triturated on ice through a 27G needle, and following protein quantification (Bradford assay, Pierce), lysates were stored at –20^{o} C until use. Nuclear extracts were obtained from 100 mm dishes of confluent astrocytes using NE-PER reagents supplemented with HALT protease inhibitor cocktail (Thermo Scientific). Nuclear lysate proteins were quantified with the BCA assay (Pierce). Whole-cell and nuclear lysate samples were subjected to SDS-polyacrylamide gel electrophoresis in Tris/glycine/SDS buffer using 4-15% Tris-HCl Ready Gels (Bio-Rad). Prior to loading, thawed whole-cell lysates were suspended in 2X reducing (containing 2-mercaptoethanol, (2ME)) or non-reducing Laemmli Buffer (Bio-Rad). Nuclear extract samples were boiled (2 min, 95^{o} C) and 10-30 μg of protein (for both whole-cell and nuclear samples) was loaded. Proteins were transferred to a Hybond-P PVDF membrane in Towbin buffer (Tris/glycine/20% methanol pH 8.3) and Kaleidoscope Molecular Weight Markers (Bio-Rad) were used

to monitor transfer. Immunoreactive proteins were visualized using enhanced chemiluminescence (ECL) LumiGLO reagents (Cell Signaling) on a Fuji LAS-3000 Intelligent Dark Box. Following detection, blots were often stripped using 2% SDS, 100 mM 2ME, and 62.5 mM Tris-HCl pH 6.8 (30 min @ 50° C), blocked and re-probed for loading standards or other proteins. Density differences between proteins of interest were determined with ImageGauge software. All samples were background subtracted and normalized against GAPDH. Antibodies used in this study included α-xCT (1:500, generated/purified by Bethyl Labs), α-CD98 (1:200, Santa Cruz Biotechnology (sc-7094)), GAPDH (1:500, sc-20357), α-Nrf2 (1:200, sc-722), donkey α-rabbit IgG-F(ab')2-HRP (1:2000, Cell Signaling) α-biotin (1:1000, Cell Signaling), donkey α-goat IgG-HRP (1:2000, SC-2020). The rabbit xCT polyclonal antibody was commercially generated and affinity purified (Bethyl Laboratories) against a 15 a.a. synthetic peptide near the N-terminus of hxCT (MVRKPVVSTISKGGY) as described elsewhere (Kim et al. 2001). Immunostaining specific to xCT was present in positive controls (cell lines and oocyte expression system) and were absent when preadsorbed with peptide (data not shown).

3.6 RNA extraction, cDNA synthesis, and real-time PCR analysis

Total RNA was isolated from astrocytes grown in 100mm dishes using TRIzol Reagent (Invitrogen) followed by clean-up using the E.Z.N.A Total RNA Kit I (Omega Bio-tek). Following RNA spectrophotometric quantification, the integrity of the RNA was verified through denaturing agarose gel electrophoresis performed on 1.5 mg of

RNA sample resulting in distinct 28s and 18s rRNA bands. A 500 ng aliquot of each RNA sample was used to generate cDNA using the qScript cDNA Supermix (Quanta) in a 10 μL reaction. The cDNA product was diluted 5-fold (50 μL) and 5 μL of each was used in subsequent PCR reactions. All real-time primers were designed using Roche ProbeFinder software. The following primers were used: xCT (NM_001107673.2) fwd 5'-TCCATGAACGGTGGTGTGT-3' rev 5'-CCCTTCTCGAGATGCAACAT-3', 4F2hc (AB015433.1) fwd 5'-CAGCTATGGGGATGAGCTTG-3', rev 5'-TCATTCCACAGCATGATGAATGG-3'; and GAPDH (M17701.1) fwd 5'-AGCTGGTCATCAATGGGAAA-3', rev 5'-ATTTGATGTTAGCGGGATCG-3.' The 25 μL PCR reaction volume contained 1x Universal Master, the appropriate probe corresponding to the primer set from the Roche Probefinder library, and primers at 0.2 mM final concentration. Real-time PCR reactions were performed on the BioRad iQ5 for 95^{o} C for 3 minutes, 95^{o} C for 15 seconds, and 60^{o} C for 1 minute. All signals were normalized to GAPDH from identical cDNA preparations and fold changes in xCT or 4F2hc expression were determined from CT values using the formula $2^{-\Delta\Delta Ct}$.

3.7 ROS detection

Carboxy-H_2DCFDA (Molecular Probes, Invitrogen, C400) was used as an intracellular indicator of ROS production. Briefly, primary astrocytes were seeded @ 5.0 x 10^3 cells/well in black, clear-bottomed 96-well plates (Corning). Astrocytes were either untreated or given dbcAMP treatments for 7-days and received BSO or BSO with antioxidants/thiols, for the final 24hrs of the time course. On day 7, cells

were rinsed with DPBS 2x, loaded with 10 μM carboxy-H_2DCFDA in 200 μL DPBS for 25 min @ 37° C. Following the incubation, cells were rinsed 2x in DPBS. Cells were incubated in a Gemini Thermomax microplate reader (Molecular Devices) @ 30° C with pre-warmed DPBS. Multiple fluorescence readings (once every 5 minutes, bottom read) were taken (Ex 485λ, Em 530λ) over a 30 min time course to determine the suitable preincubation time for esterase hydrolysis. Optimal dye response occurred following a 5 minute preincubation. Values were corrected for autofluorescence by subtracting fluorescence units from dye-free cell samples. A cell-free sample of DPBS containing Carboxy-H_2DCFDA was used to assess background fluorescence due to spontaneous or atmospheric oxidation. Values are reported in relative fluorescence units (RFUs).

Chapter 4. Results

4.1 Sx_C^--mediated uptake of [^{3}H]-L-glutamate increases in primary astrocytes treated with dbcAMP and BSO

To establish basal activity levels of system x_C^- (Sx_C^-) in primary astrocytes, rates of [^{3}H]-L-glutamate uptake were determined under Na^+-independent conditions (i.e. Na^+-free) in cultures maintained over a 7-day period in either normal growth media (DMEM/F12 w/ 10% FBS) or media supplemented with 250 μM dbcAMP (media replaced every 3 days). The change in morphological phenotype induced by dbcAMP is illustrated in Figure 4.1. As described in Methods, uptake rates reported represent specific transport; i.e., values that have been corrected for non-specific uptake and leakage determined at 4°C. Preliminary time-course experiments demonstrated that cultures grown in the presence of dbcAMP for 7 days exhibited the most robust and reproducible changes in Sx_C^- activity (Fig. 4.2). The specific uptake in the dbcAMP-treated cells at this time point was nearly 7-fold greater than in untreated astrocytes (100 ± 21 and 15 ± 4 pmol/min/mg protein respectively)(Fig. 4.2). This observed increase in Sx_C^- activity is consistent with previous reports (Gochenauer and Robinson 2001). With respect to the magnitude of the increase in uptake, it should be noted that the relatively low levels of activity present in the astrocytes not cultured with dbcAMP led to a high degree of variation between experiments, making it harder to quantify absolute levels of specific uptake. For example, the untreated astrocytes often exhibited non-specific rates of activity (i.e. rates measured at 4°C) that were 50% or more of the total activity (Fig. 4.3). By

comparison, dbcAMP-treated cells had non-specific rates that were typically less than 20% of total activity (Fig. 4.3). This is not characteristic of all forms of L-Glu transport processes however as the total levels of uptake are much higher and the relative levels of non-specific rates are much lower under Na^+-dependent conditions (to isolate EAAT activity)(Fig. 4.4). Given these low levels of activity and the observation that dbcAMP-treated cells exhibit many of the morphological (Fig. 4.1) and biochemical markers that typify astrocytes *in vivo* (e.g., increased expression of EAATs, glutamine synthetase, GABA-A, GFAP etc. (Daginakatte et al. 2008; Hosli et al. 1997; Le Prince et al. 1991; Miller et al. 1994; Stanimirovic et al. 1999; Swanson et al. 1997), subsequent experiments were primarily limited to astrocytes grown in the presence of dbcAMP.

Astrocytes were cultured under the conditions described above with and without the γ-glutamylcysteine synthetase inhibitor BSO (500 μM final concentration) during the final 24 hrs of the treatment regimen to deplete intracellular GSH levels (Griffith 1982; Meister 1991). As expected, the intracellular GSH content in both untreated and dbcAMP-treated astrocytes cultures was depleted to below 10% of that found in controls 24 hrs following an exchange of media that contained BSO (Fig. 4.5). There also appeared to be a difference in the rates at which the GSH levels decreased during the early part of the time course. For instance, at 2 hrs following the addition of BSO, intracellular GSH levels in untreated astrocytes were 86 ± 2 % of control levels compared to 62 ± 4 % of control in the dbcAMP-treated cells ($p = 0.002$) (Table 4.1). It is also worth noting that at the start of the 24 hr incubation (time 0 hr), the levels of intracellular GSH in the untreated astrocytes were less than

those in the dbcAMP-treated astrocytes (3.8 ± 0.4 vs. 5.2 ± 0.7 nmol/mg protein, p = 0.006). Further, in those cultures not administered BSO, this difference grew to almost 2-fold (192.0 ± 8.8 %, p = 0.004) in dbcAMP-treated astrocytes 24 hrs following the exchange of fresh media (Fig. 4.5). The levels of L-Cys2/L-CysH in the media (0.1 mM each) appear to be saturating in terms of intracellular GSH synthesis as additions of both (L-Cys2: 250 μM - 500 μM and L-CysH: 500 μM – 1000 μM) were unable to significantly influence GSH levels in both cell types (Table 4.2). Also, when both cell types were treated with the Sx_C^- inhibitor 4S-CPG, levels of total intracellular GSH are equally decreased. Therefore, even as both untreated and dbcAMP-treated astrocytes exhibit marked differences in Sx_C^- activity, both apparently rely equally on Sx_C^--mediated transport of $L\text{-}Cys_2$ for the synthesis of GSH. These findings demonstrate that intracellular GSH levels in primary astrocytes are altered by both dbcAMP and BSO. Additionally, in dbcAMP-treated astrocytes it appears that GSH can be maintained at higher levels and may have a shorter intracellular half-life, possibly owing to increased efflux, utilization and/or metabolism. As these results confirmed the intended effect of BSO on GSH levels in both cell models, this same 24 hr BSO treatment was used to assess the effect of GSH-depletion on Sx_C^--mediated (i.e. Na^+-independent) [^{3}H]-L-glutamate uptake.

When the dbcAMP-treated cells were assayed for Na^+-independent [^{3}H]-L-glutamate transport, cultures administered BSO (500 μM, 24 hrs, as described above) exhibited a nearly 3-fold increase in uptake rates compared to cells that did not (253 ± 29 vs. 100 ± 21 pmol/min/mg protein) (Fig. 4.6). The nearly complete loss of intracellular GSH likely was necessary for the induction, as uptake was measured at

an earlier time-point characterized by a 36% loss of intracellular GSH (Table 4.1), and no significant induction of Na^+-independent [^{3}H]-L-glutamate transport was observed. In order to verify that the increased transport activity could be attributed to Sx_C^-, parallel assays were conducted in the presence of two well known inhibitors of the transporter: the endogenous substrate L-Cys_2 and the non-substrate inhibitor 4-*S*-carboxyphenyl glycine (4S-CPG) (Patel et al. 2004). Under these conditions L-Cys_2 and 4S-CPG respectively reduced uptake to 9 ± 2% and 14 ± 4 % of control (i.e., 32 ± 12 and 36 ± 8 pmol/min/mg protein), consistent with Sx_C^- pharmacology (Fig. 4.6). Sx_C^- activity in cultures depleted of GSH over an extended time course (7 days of BSO treatment vs. 24hrs) were not significantly different than those treated for only 24 hrs (259 ± 31 and 213 ± 32 pmol/min/mg protein) (Fig. 4.7). Thus, the effect of GSH depletion by BSO (500 μM) on Sx_C^- appears to be acute. The addition of BSO also produced an increase in Na^+-independent [^{3}H]-L-glutamate uptake in astrocytes cultured in the absence of dbcAMP, although this increase was much smaller in both absolute and relative terms compared to the increase observed in the dbcAMP-treated astrocytes, and should be interpreted within the context of the lower signal to noise limitations mentioned above (Fig. 4.6).

While the effects of dbcAMP on the glial expression and activity of the EAATs have been reported (Schlag et al. 1998; Swanson et al. 1997), whether or not these activities, like Sx_C^-, are also altered by GSH-depletion has not been examined. The EAAT subtypes EAAT1 (GLAST) and EAAT2 (GLT-1) are the predominantly expressed isoforms in cultured astrocytes (see Danbolt 2001 for review). EAAT activity was quantified under Na^+-dependent conditions using [^{3}H]-D-aspartate as a

substrate (Koch et al. 1999). As expected, rates of EAAT-mediated uptake increased in the astrocytes cultured in the presence of dbcAMP (240 ± 51 *vs*. 686 ± 84 pmol/min/mg). In contrast to Sx_C^- activity, however, a similar addition of BSO (500 μM, 24hrs) did not produce significant differences in either the untreated or dbcAMP-treated astrocytes (251 ± 58 and 738 ± 76 pmol/min/mg, respectively) (Fig. 4.8). We also tested the effect of GSH-depletion on a highly plastic neuronal "stem cell-like" cell line (C17.2 cells) (see Steindler 2002 for review) and observed no significant change in Sx_C^- activity (Fig. 4.9). Taken together, these results demonstrate that Sx_C^-, but not the EAAT system, is sensitive to alterations in GSH levels in primary astrocytes. Additionally, while both Sx_C^- and EAAT systems increase as a result of dbcAMP administration, the relative percentage of Sx_C^- activity to the total activity contributed by both systems differs markedly between the two phenotypes: Sx_C^- comprises ~6% of the total uptake in untreated astrocytes, increases to ~15% following dbcAMP treatment, and upon the addition of BSO increases to ~26% of the total uptake (Table 4.3).

4.2 The actions of dbcAMP and BSO on Sx_C^- activity are distinct from those of the EpRE/ARE activator tBHQ

One of the best-studied models of Sx_C^- induction involves the use of an electrophile, such as tBHQ, to activate the EpRE/ARE (Electrophile Response Element/Antioxidant Response Element)-linked signal transduction pathway (Ishii et al. 2000; Shih et al. 2003). Characterized in a variety of cells, including astrocytes,

this pathway leads to the upregulation of proteins associated with oxidative protection and xenobiotic detoxification, including: e.g., glutathione-S-transferases (GSTs), NAD(P)H: quinone oxidoreductase (NQO1), epoxide hydrolase, and UDP glucuronosyltransferases (for reveiw see Itoh et al. 2004; Talalay et al. 1995). Consistent with previous reports, the addition of tBHQ (24 hrs) increased Sx_C^- activity, intracellular GSH levels, and the nuclear presence of the EpRE/ARE-associated transcription factor Nrf2 in the astrocytes that had been cultured in the absence of dbcAMP (Fig. 4.10, Fig. 4.12A,B). In contrast, when tBHQ was added to the astrocytes which had been differentiated with dbcAMP (and exhibited much higher levels of Sx_C^- activity compared to the untreated cells), a further increase in activity was not observed (Fig. 4.11, Fig. 4.12A). Similarly, the intracellular levels of GSH in the astrocytes cultured with dbcAMP were also comparatively higher, but were not significantly changed following exposure of tBHQ (Fig. 4.12B). The fact that nuclear levels of Nrf2 protein increased in these cells, suggests that any change in Sx_C^- activity was either masked by the much larger increase induced by dbcAMP or was limited in a way potentially related to dbcAMP induced cellular changes. Taken together, these results demonstrate that the phenotypic changes induced by dbcAMP include alterations in the manner in which these astrocytes regulate the Sx_C^- transporter.

4.3 BSO-induced depletion of GSH increases the V_{max} but not K_m for L-glutamate transport by Sx_C^- in the dbcAMP-treated astrocytes

To further define the nature of the observed increase in Sx_C^- activity in dbcAMP-treated astrocytes depleted of GSH with BSO, a more detailed kinetic analysis was carried out (Fig. 4.13). Rates of Sx_C^--mediated, Na^+-independent uptake were quantified as a function of the concentration of L-Glu and then analyzed by nonlinear curve fitting using the Michaelis-Menten equation (KaleidaGraph 3.6.5). The use of L-Glu as a substrate avoids the complications associated with $L\text{-}Cys_2$ (e.g., disulfide exchange, reduction, solubility, availability, etc.). The resulting V_{max} value for L-Glu uptake in the dbcAMP-treated astrocytes increased from 147 ± 5 to 350 ± 15 pmol/min/mg protein in those cultures exposed to BSO (500 μM) for 24hrs. In contrast, the K_m values determined for L-Glu in the presence or absence of BSO were not significantly different from one another (i.e., 17 ± 2 and 25 ± 5 μM, respectively), consistent with values previously reported in dbcAMP-treated astrocytes (Gochenauer and Robinson 2001) and significantly lower (i.e. reflecting a higher affinity for substrate), than those reported in glioma, astrocytoma, and other tumor lines (~50-100 μM) (Bannai et al. 1989; Patel et al. 2004).

4.4 BSO mediated increase in Sx_C^- activity results in extracellular L-glutamate accumulation

To complement these direct studies on the Sx_C^--mediated uptake of [^{3}H]-L-Glu into the cultured astrocytes, the ability of $L\text{-}Cys_2$ to exchange with (i.e., produce an efflux

of) intracellular L-Glu was quantified using a glutamate dehydrogenase (GDH)/$NADP^+$ coupled assay (Patel et al. 2004). L-Glu present in the buffer is enzymatically converted to α-ketoglutarate by GDH, which generates a molar equivalent of NADPH that can be quantified fluorometrically (Ex 370λ, Em 450λ) and equated to L-Glu concentrations with a standard curve. Thus, dbcAMP-treated astrocytes (12-well plates, total volume = 0.5 mL/well) were rinsed free of media and incubated for 15 minutes in Na^+-free buffer containing various concentrations of L-Cys_2. As shown in Figure 4.14, L-Cys_2 produced a dose-dependent increase the amount of L-Glu present in Na^+-free buffer surrounding the dbcAMP-treated astrocytes. When L-Cys_2 was incubated with astrocytes that were also treated with BSO (500 μM, 24hrs) it produced a markedly greater accumulation of extracellular L-Glu, consistent with the increased activity of Sx_C^-. For example, following a 15 min incubation with 100 μM L-Cys2, the extracellular concentration of L-Glu in the dbcAMP-treated astrocytes reached 6.3 ± 0.1 μM in the cells also given BSO, but only 3.0 ± 0.8 μM in those that did not. In both instances the extracellular accumulation of L-Glu was inhibited by the inclusion of 4S-CPG (100 μM) in combination with the L-Cys_2 (Fig. 4.14). Additionally the increased extracellular L-Glu levels in the dbcAMP + BSO-treated astrocytes is still below the levels observed in a cell line known to exhibit pathogenically high levels of Sx_C^- activity (SNB19 human glioblastoma cells) (Fig. 4.15). These findings demonstrate that increases in Sx_C^- activity following GSH-depletion can be quantified as a function of either the direct uptake of [^{3}H]-L-Glu (Fig. 4.6 and Fig. 4.13) or the physiologically relevant exchange of extracellular L-Cys_2 for intracellular L-Glu.

4.5 BSO-induced changes in Sx_C^- protein and mRNA expression

Sx_C^- is heterodimer compromised of a non-glycosylated xCT light chain (~35-55 kDa) (Kim et al. 2001; Lim et al. 2005; Mysona et al. 2009; Shih et al. 2006) and a glycosylated 4F2hc (aka CD98) heavy chain (80-90 kDa) (Kim et al. 2001; Nakamura et al. 1999; Shih et al. 2006). To determine if the observed increase in V_{max} in the astrocytes following the BSO-mediated depletion of GSH is associated with changes in protein expression of xCT and/or 4F2hc, immunoblot experiments were performed. As the two subunits of the heterodimer are disulphide-linked, analyses of whole cell lysates were carried out in the presence and absence of 2-mercaptoethanol (2ME) (Figure 4.16). In lysates prepared from astrocytes cultured in the absence of dbcAMP and exhibiting minimal activity, the xCT antibody revealed two distinct bands at an estimated molecular weight of 50 kDa and 45 kDa under both non-reducing and reducing conditions (Fig. 4.16A: lanes 1 and 2). In addition to these same 50 kDa and 45 kDa bands, lysates prepared from the dbcAMP-treated astrocytes under non-reducing conditions also exhibited a very prominent band at 135 kDa (Fig. 4.16A, lane 3), consistent with the molecular weight of the xCT and 4F2hc heterodimer. Under reducing conditions, the loss of the 135 kDa band in the dbcAMP-treated astrocytes coincided with the appearance of a prominent band at 40 kDa (Fig. 4.16A, lane 4). This multiple banding pattern has been documented previously (Kim et al. 2001; Lim et al. 2005; Mysona et al. 2009; Shih et al. 2006) and all bands were undetectable in peptide blocking control experiments (data not shown).

Taken together, the appearance of the 135 kDa band under non-reducing conditions and the 40 kDa band in the presence of 2ME correlated with the increased Sx_C^- activity observed in the uptake and exchange assays carried out with the dbcAMP-treated astrocytes (Fig. 4.6 and 4.14). When a similar analysis was carried out on the dbcAMP-treated astrocytes that had been depleted of GSH with BSO over 24hrs, a similar banding pattern was observed (Fig. 4.16A, lanes 5 and 6). While there was only a small change (~1.2-fold increase, as judged by densitometry) in the amount of the 135 kDa band in these cells, there was a more marked increase in the expression of the 40 kDa band under reducing conditions (Fig. 4.16A, lane 6, ~1.8 fold) in the cells depleted of GSH.

A parallel series of immunoblot studies were also carried out to examine potential changes in the expression of 4F2hc. In the astrocytes that had been treated with dbcAMP, the 4F2hc antibody also revealed a prominent band at 135 kDa under non-reducing conditions (Fig. 4.16B, lane 3), consistent with the presence of the intact heterodimer. As was observed with xCT, the inclusion of 2ME led the loss of this 135 kDa band and the appearance of the monomer, in this instance at a molecular weight appropriate for 4F2hc, ~90 kDa (Fig. 4.16B, lane 4). Astrocytes cultured in the absence of dbcAMP exhibited only very faint bands at 135 kDa and 90 kDa under either reducing or non-reducing conditions, respectively (Fig. 4.16B, lanes 1 and 2). In the dbcAMP-treated astrocytes that had been depleted of GSH with BSO, 4F2hc staining density for the 135 kDa band (non-reducing conditions) was essentially unchanged (~0.9-fold), while the 90 kDa band (reducing) exhibited only a modest increase of ~1.3-fold.

The findings from the immunoblots suggest that the increased presence of the heterodimer (and the coincident gain in activity) in cells cultured with dbcAMP correlates to the increased expression of both the xCT and 4F2hc, rather than a single, rate-limiting, subunit. The further increase in Sx_C^- activity observed in the dbcAMP-treated astrocytes that had also been depleted of GSH with BSO, correlated to a greater extent with the increased expression of the xCT subunit, rather then either 4F2hc or the heterodimer. To further investigate the nature of the change in expression BSO (500 μM, 24 hrs) was added to the dbcAMP-treated astrocytes in the presence and absence of 50 μM cycloheximide (Fig. 4.17). While the astrocytes administered BSO and cycloheximide still exhibited a higher level of transporter activity (145 ± 8.1 % of control astrocytes), the activity was markedly reduced from the levels observed in the absence of cycloheximide (256 ± 25 % of control), indicating that protein synthesis was, in part, required for the increased Sx_C^- activity observed following GSH depletion.

The results of Q-PCR analysis of xCT and 4F2hc cDNA in response to dbcAMP and BSO in primary astrocytes are depicted in Figure 4.18. Following 6 days in culture with or without dbcAMP, a subset of cells were treated with 500 μM BSO for an additional 24 hrs and RNA was extracted. RT-PCR and Q-PCR were performed as described in Methods. A 69.5 ± 9.6 fold increase in xCT message in astrocytes grown in the presence of dbcAMP was observed when compared to untreated cells (Fig. 4.18). Following the 24hr exposure to BSO, xCT expression increased by an additional 2-fold (144.0 ± 5.8 fold) as compared to the cultures treated with dbcAMP alone. In contrast, comparable changes in the levels of 4F2hc mRNA were

not observed in response to either dbcAMP or dbcAMP/BSO (Fig. 4.18). Indeed, a small decrease (-1.3 ± 0.07 fold) in expression of 4F2hc message occurred following dbcAMP treatment. When these cultures were also depleted of GSH with BSO, 4F2hc mRNA increased only by 1.3 ± 0.1 fold. These data indicate that the extent to which dbcAMP and dbcAMP/BSO treatments result in increased mRNA and protein expression differs between the protein subunits of Sx_C^-. Whereas the expression of the active heterodimer may potentially result from increased protein synthesis of both subunits, at this time point (24 hrs post-BSO) only xCT message was increased.

4.6 Restoration of intracellular GSH levels in BSO-treated cells restores Sx_C^- activity to control levels

The association between intracellular GSH concentrations and Sx_C^- activity was next examined by quantifying transporter activity as GSH was restored to normal levels. To do this, cultures were first treated in a manner identical to the depletion experiments, culturing cells for 7 days in the presence dbcAMP and BSO for the final 24 hrs. The cultures were then rinsed and supplied with fresh media free of BSO. Sx_C^- activity and intracellular GSH levels were then monitored as the cells recovered from γ-glutamylcysteine synthetase inhibition, most likely as a consequence of the *de novo* synthesis of new γ-glutamylcysteine synthetase. The results depicted in Figure 4.19 demonstrate a close temporal correlation between GSH levels and Sx_C^- activity. For example, at 72 hrs post BSO treatment, GSH levels had recovered to

51% of control while Sx_C^- activity had decreased to 143% of control. By 120 hrs, GSH levels and Sx_C^- activity had both reached nearly 100% of control values.

As an alternative to allowing GSH levels to be replenished as a function of BSO washout and the restoration of γ-glutamylcysteine synthetase activity, a series of compounds, including GSH precursors, derivatives, and antioxidants, were added to the cultures at the same time as the BSO to test their ability to prevent the increase in Sx_C^- activity and thereby provide insight into whether or not it is specifically a decrease in GSH that triggers the Sx_C^- response (Figs. 4.20, 4.21, and 4.23). Inclusion of GSH (which is not transported into cells intact) or γ-glutamylcysteine in the extracellular media produced only a modest decrease in the amount Sx_C^- activity normally induced by the BSO-mediated depletion (Fig. 4.20). In contrast, the cell permeable GSH "pro-drug" GSH-ethyl ester proved to be one of the most effective compounds in preventing the upregulation, reducing the observed increase in Sx_C^- activity from 262 ± 21 % to 146 ± 5 % of control (Fig. 4.20). Total GSH levels were measured to confirm that the addition of GSH-ethyl ester did indeed result in increased intracellular GSH. Treatment with 1 mM GSH-E resulted in increased GSH levels (2.2 ± 0.4 nmol/mg protein) as compared to levels from BSO-treated cultures (0.9 ± 0.3 nmol/mg protein). This increase was enhanced in cells treated with 5 mM GSH-E (11.2 ± 0.8 nmol/mg protein) and surpassed even the levels of GSH in cultures grown in the absence of BSO (6.9 ± 2.3 nmol/mg protein). As a consequence of GSH efflux, the restoration of intracellular GSH by GSH-E treatment may also contribute to increased levels of extracellular GSH, which conceptually could also be responsible for preventing the effect of BSO, although this possibility appeared to be

ruled out by earlier experiments. However, these experiments were performed in cells without the inhibition of γ-glutamyltranspeptidase (γ-GT), a membrane-bound enzyme that catabolizes γ-glutamyl bonds (in the case of GSH catabolism the result is the production of L-cysteinylglycine and often a γ-amino acid, depending on the nucleophilic acceptor (Tate and Meister 1981)). Therefore, exogenously applied GSH could have been metabolized by this enzyme, potentially resulting in the formation and transport of γ-glutamylcysteine (a known side product of the enzyme when both GSH and L-Cys_2 are present) which could bypass the BSO block on GSH synthesis and thereby prevent the induction of uptake (Tate and Meister 1981). To isolate this potential component of GSH treatment, cultures were treated with a known inhibitor (Acivicin, AC) of γ-GT 2 hours prior to the addition of GSH and BSO. Through transpeptidase inhibition, co-treatment with GSH essentially avoids metabolism and remains in the extracellular space. A significant level of prevention was achieved by this strategy, more so than with GSH alone and similar to the effect of GSH-E at the same concentration (Fig. 4.20). While this may indeed represent a GSH-mediated extracellular mechanism of prevention, further experiments are needed to substantiate that extracellular GSH levels remained intact during the duration of the experiment. The cell permeable cysteine "pro-drug" N-acetyl-cysteine produced an effect essentially indistinguishable from GSH-ethyl ester, where its inclusion also limited the increase in Sx_{C^-} to 147 ± 12 % of control (Fig. 4.21). To test whether or not the effect of the GSH-ethyl ester treatment was related specifically to GSH or to a non-selective thiol-mediated effect, the effect of 2-mercaptoethanol (2ME) was also tested. 2ME is thought to react catalytically with

extracellular L-Cys_2 forming a disulphide of L-CysH-2ME that then likely enters the cell through neutral amino acid transporters (Sato et al. 2005; Shih et al. 2006). Astrocyte growth media contains both L-Cys_2 and L-CysH (100 μM each), therefore both 2ME alone and in combination with higher doses of both amino acids was tested. No significant prevention in the BSO-induced induction of Sx_C^- was observed in either the case of 2ME alone or 2ME and additional L-Cys_2 (500 μM), however a significant increase in activity was observed when L-CysH was applied in combination with 2ME. Other reducing agents and thiols including DTT and L-Cys_2 (without 2ME present), were also tested and aside from a modest change with DTT, showed no significant decrease in activity compared to cells treated with BSO alone (Fig. 4.21).

As it is likely that the BSO-mediated depletion of GSH also leads to an increase in the presence of reactive oxygen species (ROS), which in turn could serve as an initiator for Sx_C^- induction, the ROS levels present in astrocytes were quantified with an ROS–sensitive dye (Carboxy-H_2DCFDA). As reported in Figure 4.22, the BSO-mediated depletion of GSH that lead to an increase in Sx_C^- activity was accompanied by about a 3-fold increase in intracellular ROS-associated fluorescence. This increase in fluorescence was not observed when GSH-ethyl ester (5 mM) was included in the extracellular media. As an additional control, H_2O_2 (50 μM) was added to the astrocytes culture to enhance the generation of ROS. Interestingly, while the addition of the H_2O_2 produced a similar increase in ROS-associated fluorescence as was observed in the BSO treated cultures, the Sx_C^- activity in these astrocytes did not change (Figure 4.24). Further, the concomitant treatment of cultures with the

antioxidants Vitamin C (1 mM), Trolox (100 μM), R-α-Lipoic acid (50 μM), and catalase (3000 U/mL) and BSO was ineffective in preventing the BSO-mediated increase in Sx_C^- activity (Fig. 4.23). These findings suggest that the induction of Sx_C^- in the dbcAMP-differentiated culture was likely not the result of a general increase in ROS species within the astrocytes. Another consequence of γ-glutamylcysteine synthetase inhibition by BSO in dbcAMP-treated cultures is the intracellular accumulation of the amino acids L-Glu and L-Cys2, the substrates for the γ-glutamylcysteine synthetase reaction. While the addition of L-Cys2 (0.5mM) had no influence on Sx_C^- activity compared to controls, L-Glu (1mM) led to an increase similar to that of BSO on Sx_C^- activity (Fig. 4.24). As a substrate for Sx_C^-, L-Glu likely inhibited the uptake of extracellular L-Cys2, effectively leading to a drop in GSH and mimicking the effect of BSO on GSH not the high intracellular levels of L-Glu. The oxidized form of GSH (GSSG, 1mM), and electrophiles diethylmaleate (DEM, 100 μM), tBHQ, and sodium arsenite were unable to fully reproduce the effect of BSO (Fig. 4.24).

A.

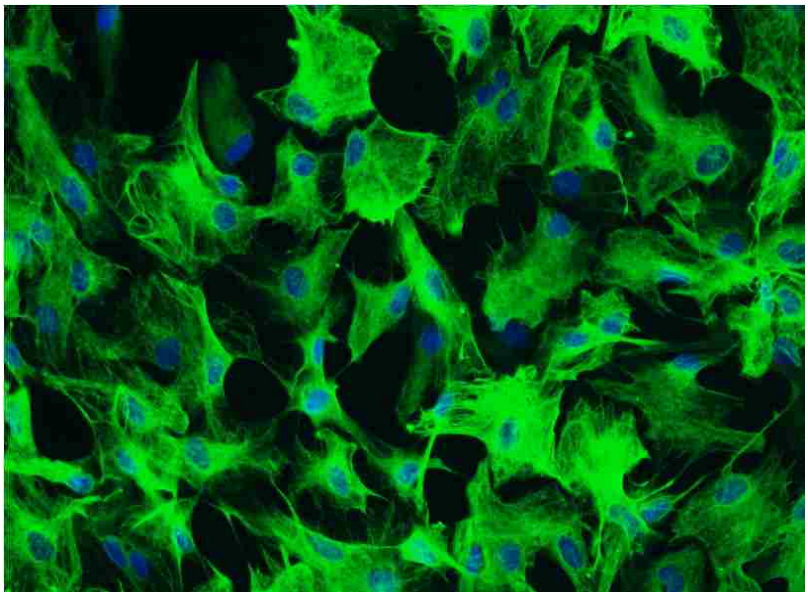

B.

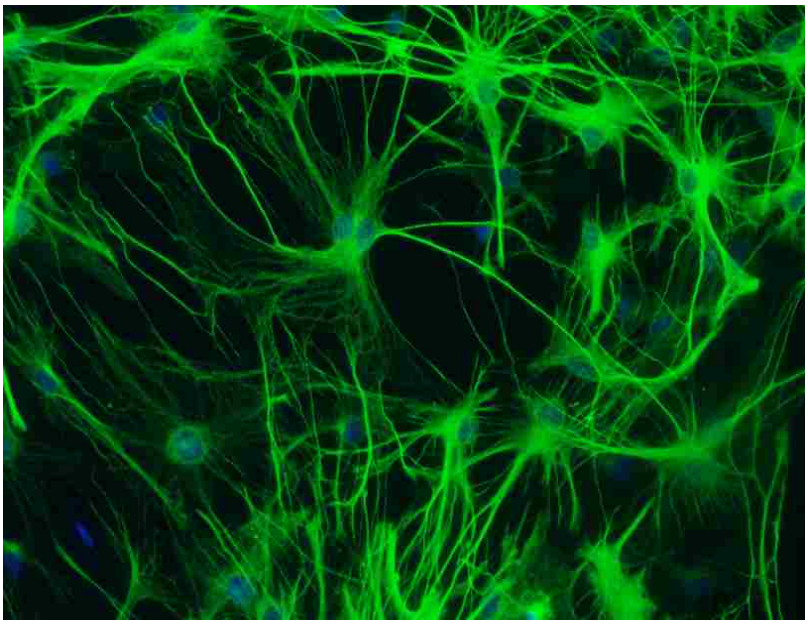

Figure 4.1. GFAP staining of primary astrocytes. Cells were cultured on poly-L-lysine-treated glass coverslips (18mm) in Costar 12-well culture plates either in the absence (A) or presence (B) of dbcAMP (250μM) for 7 days. Astrocytes were fixed with 4% paraformaldehyde, permeabilized in PBS/0.2% Triton-X for 5 min, and blocked in 3% BSA/PBS prior to anti-GFAP incubation (1:500, overnight, 4°C, DAKO Z0334). The secondary antibody used was Alexaflour 488 (1:500, Molecular Probes). A nuclear counterstain (DAPI 300nM) was applied prior to imaging. Images are @ 20x magnification.

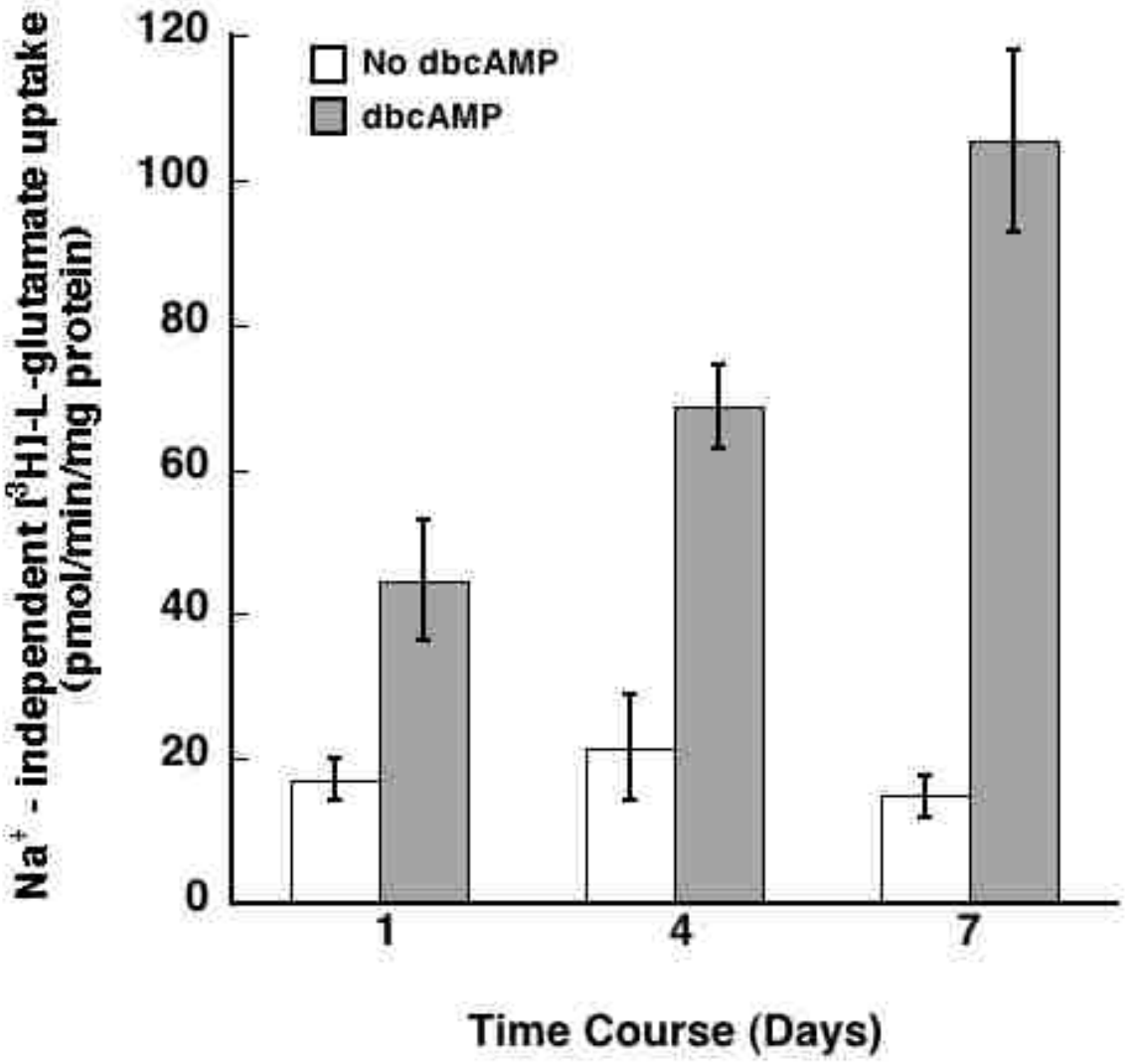

Figure 4.2. Time dependent effect of dbcAMP on Na^+-independent [^{3}H]-L-glutamate uptake in primary astrocytes. At 95%-100% confluency, astrocytes in 12-well culture dishes (Costar, Corning) were designated day 0 and given fresh culture media (DMEM/F12 with 10% FBS) alone or media supplemented with 250 μM (F.V.) dbcAMP. Culture media was changed accordingly every three days (days 0, 3, 6) and radiolabeled uptake assays performed on days 1, 4, and 7. Data presented represents n = 8-13.

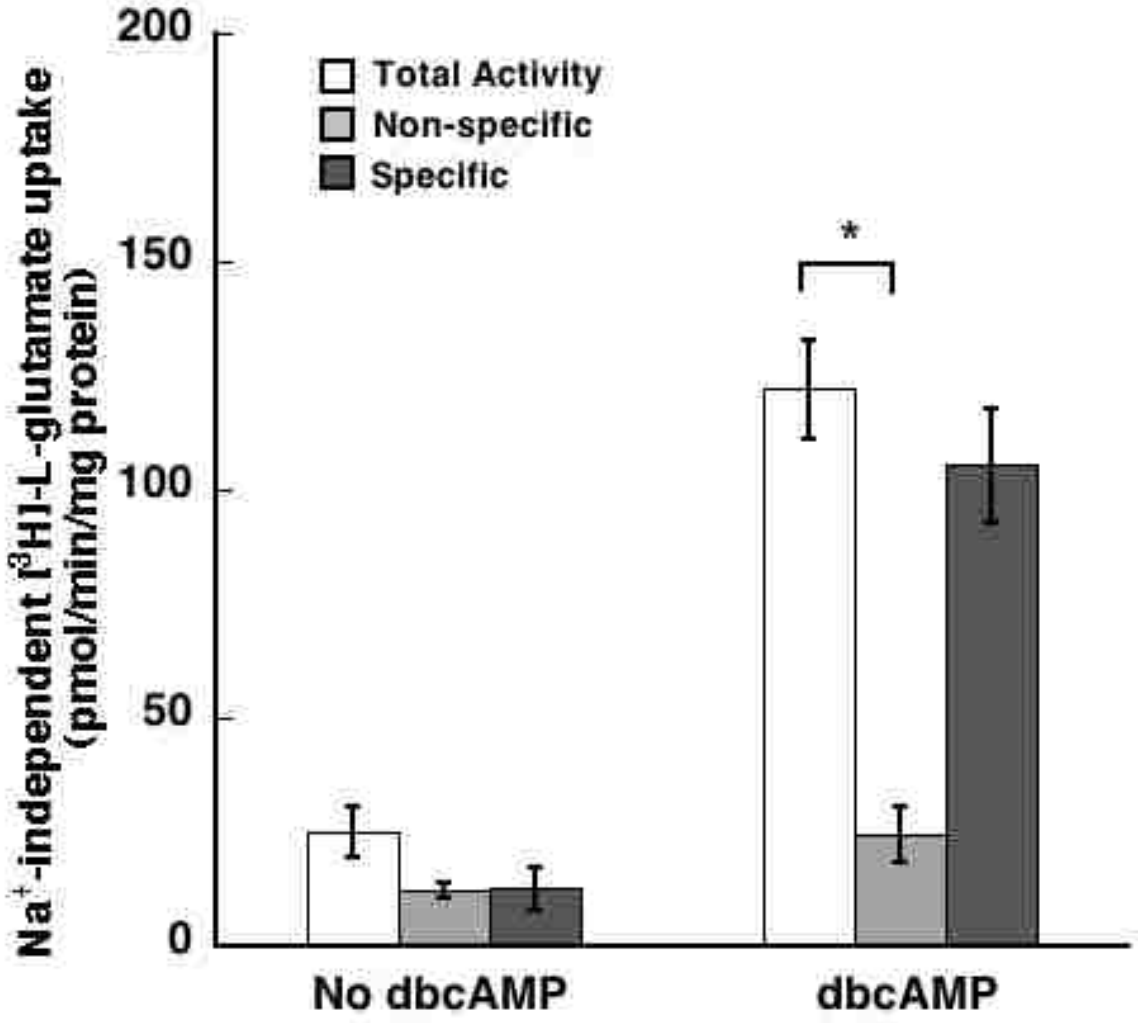

Figure 4.3. Total, non-specific, and specific Na^+-independent [^{3}H]-L-glutamate uptake activity in untreated and dbcAMP-treated astrocytes. Cells were grown in culture media (DMEM/F12 with 10% FBS) supplemented with 250 μM dbcAMP for 7 days prior to performing uptake experiments with (see Methods). There is no significant difference between total and non-specific rates of L-glutamate uptake in untreated astrocytes as determined by t-test. Data represent mean rates (pmol/min/mg protein) ± SEM, n = 11-13. *P <0.0001

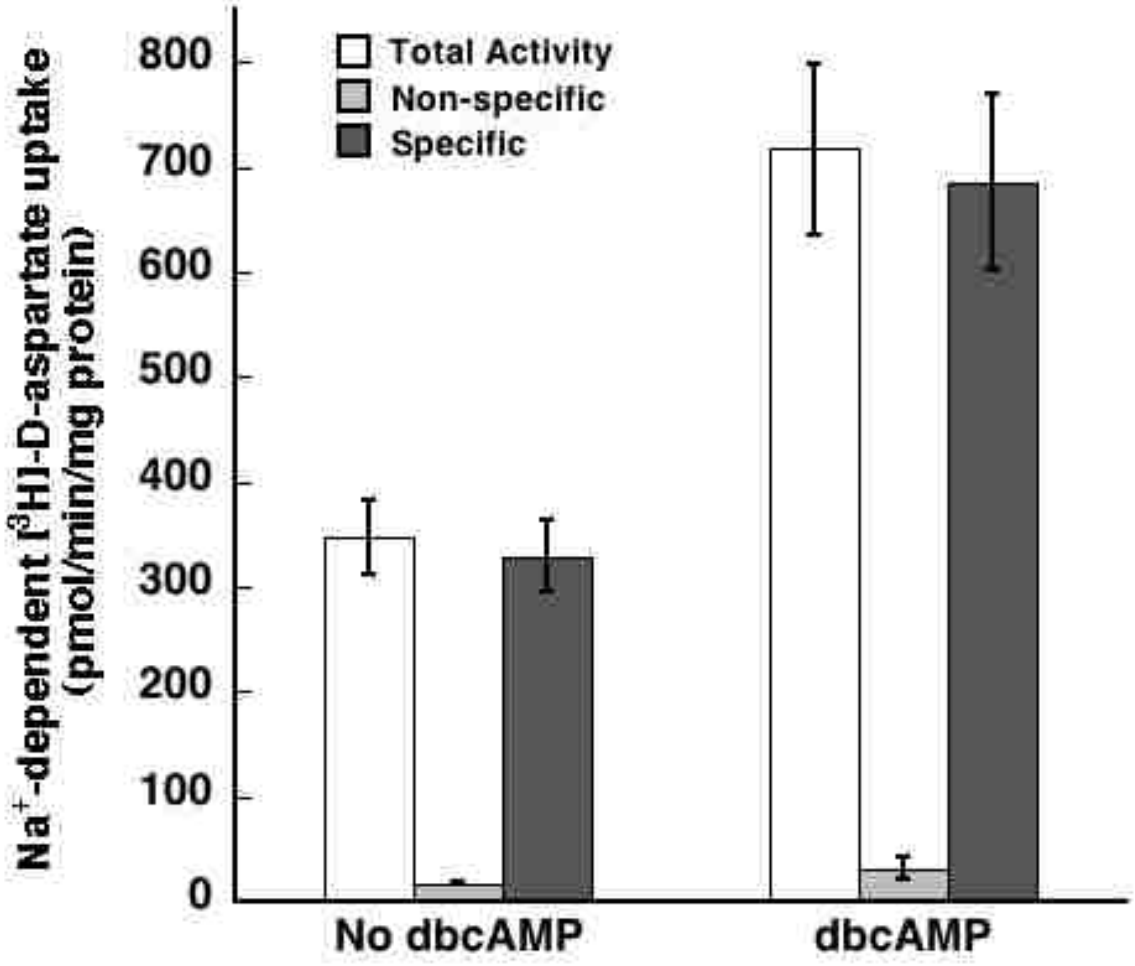

Figure 4.4. Total, non-specific, and specific Na^+-dependent [^{3}H]-D-aspartate uptake activity in untreated and dbcAMP-treated astrocytes. Cells were grown in culture media (DMEM/F12 with 10% FBS) supplemented with 250 μM dbcAMP for 7 days prior to performing uptake experiments (see Methods). Data represent mean rates (pmol/min/mg protein) ± SEM, n = 3-12.

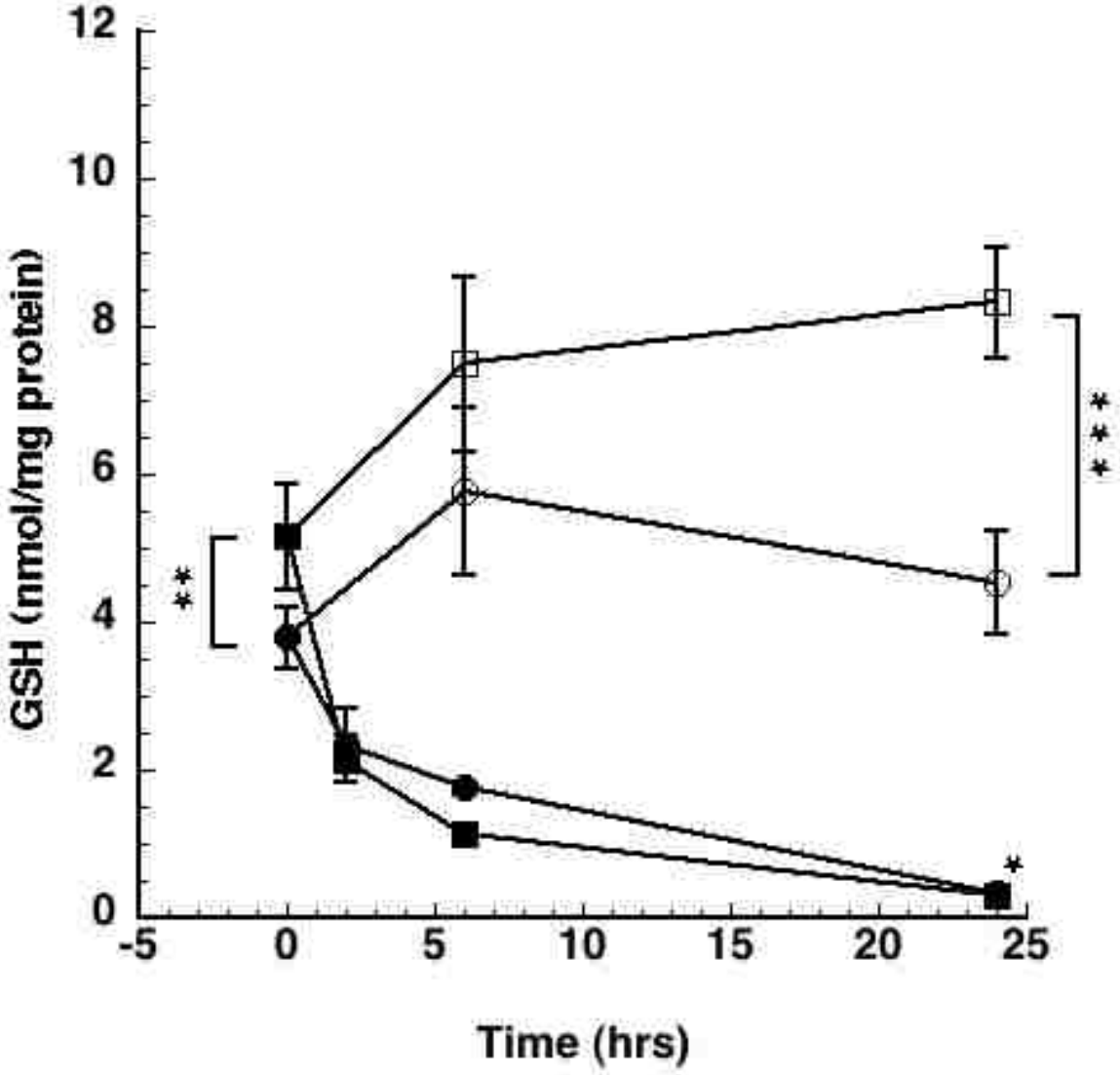

Figure 4.5. The effect of BSO on GSH levels in primary astrocytes. Following 7 days in culture with or without dbcAMP (250 μM), BSO (500 μM) was administered and astrocytes were assayed for intracellular GSH 0, 2, 6, and 24 hrs later. Data represents mean GSH levels (nmol/mg protein) ± SEM, n = 3-13. * P <0.0001 when comparing intracellular GSH levels at time 0hr to levels following 24 hrs of BSO-treatment in both untreated and dbcAMP treated cultures. ** P = 0.006 and *** P = 0.004 when comparing GSH levels in untreated to dbcAMP-treated astrocytes, at time 0hr, and 24 hrs. ○, Untreated; ●, Untreated + BSO; □, dbcAMP; ■, dbcAMP + BSO

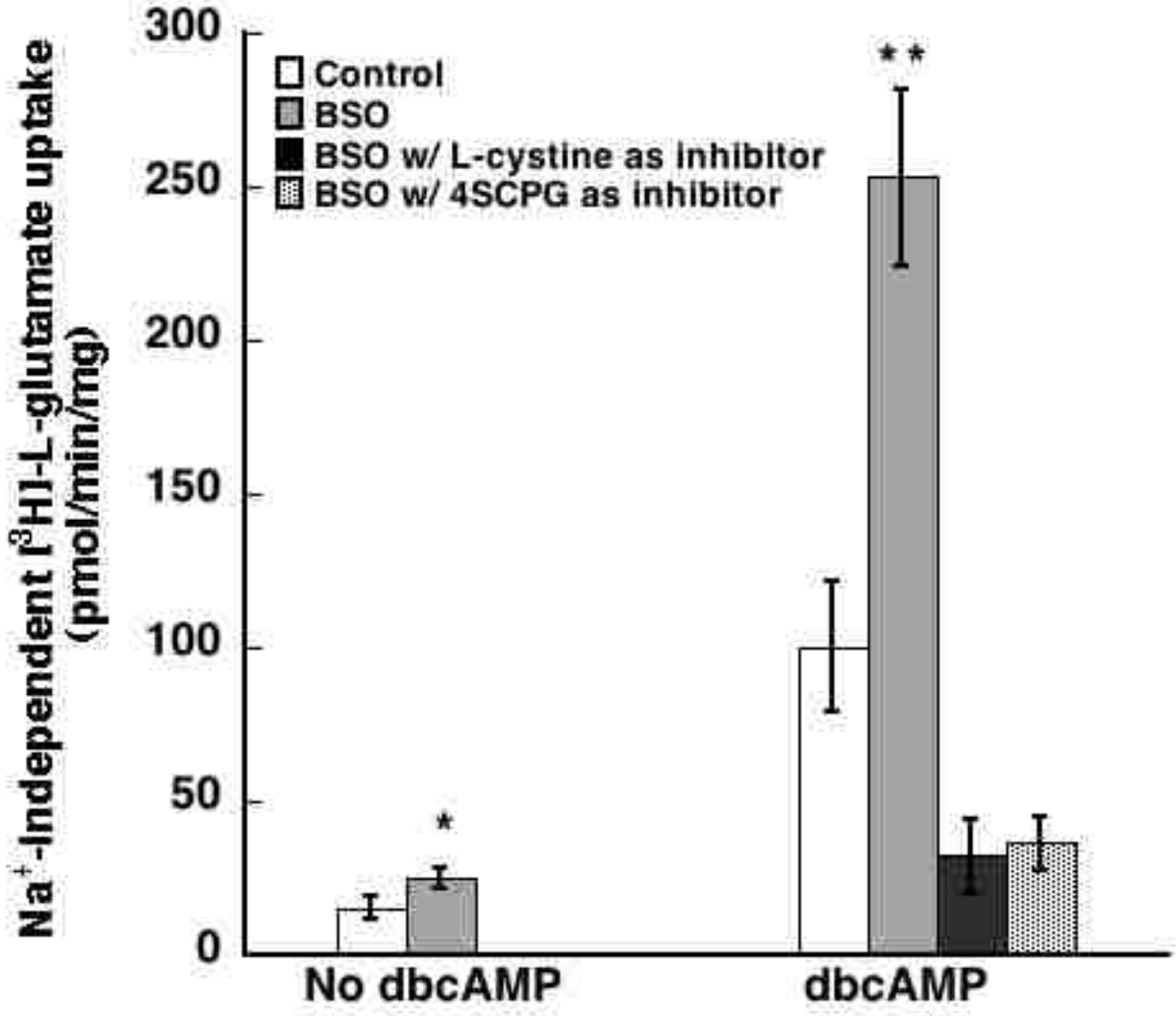

Figure 4.6. Na^+- independent [^{3}H]-L-glutamate uptake in primary astrocytes exposed to dbcAMP (7 days) and BSO (500 μM, final 24hrs). Pharmacological inhibition of [^{3}H]-L-glutamate uptake activity by L-cystine (500 μM) or 4S-CPG (100 μM) occurred in cells treated with BSO. Data represents mean rates (pmol/min/mg) ± SEM, n = 3-8. * P=0.006, ** P<0.0001 as determined by student t-test.

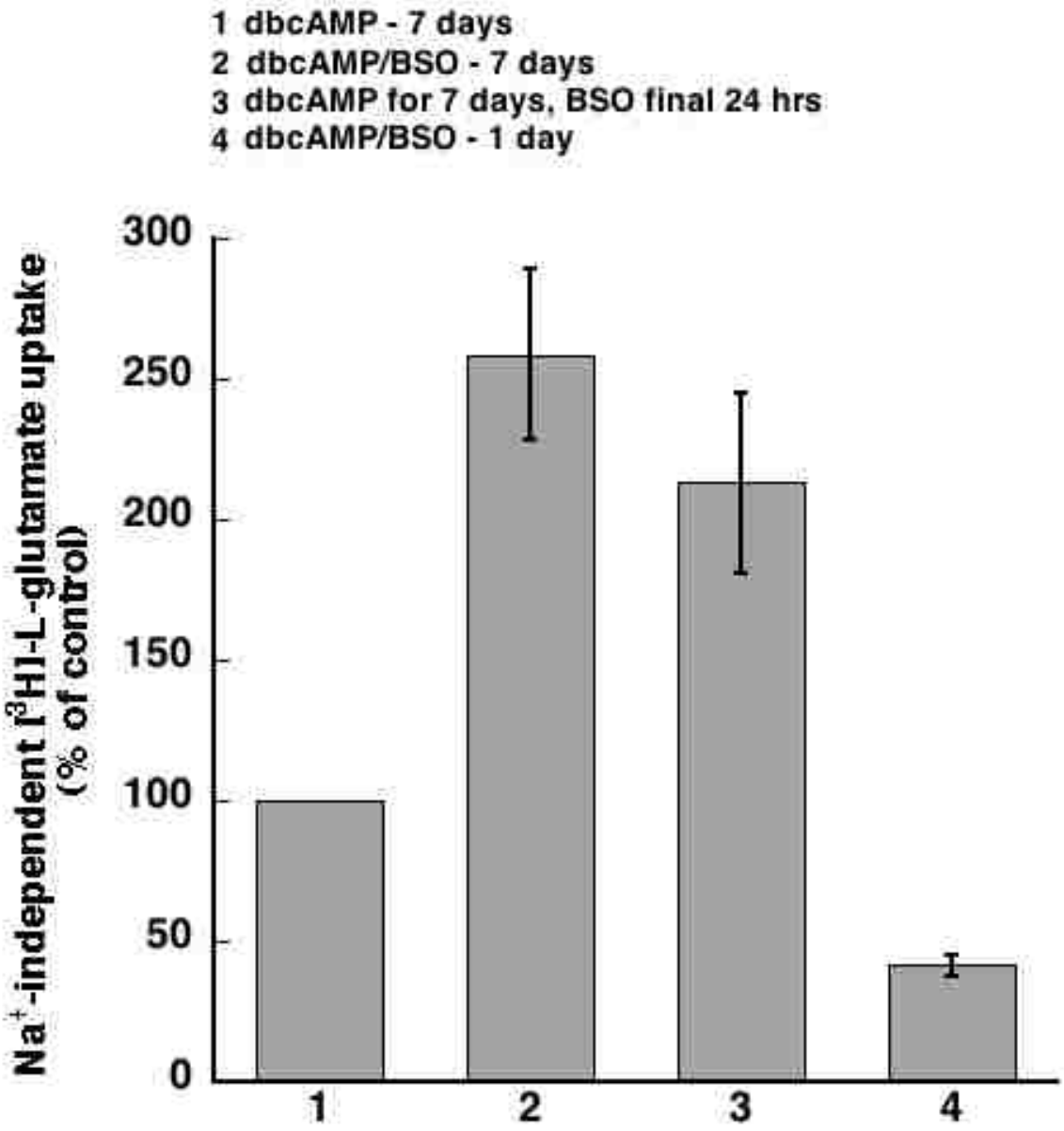

Figure 4.7. The effect of GSH depletion by BSO (500 μM) on Na^+-independent [^{3}H]-L-glutamate uptake. Astrocytes in culture were treated with dbcAMP alone for 7 days (1), a combination of dbcAMP + BSO (2), dbcAMP for 7 days with an addition of BSO for the final 24 hrs (3), or with dbcAMP + BSO on day 0 only (4) and assayed at the end of the 7 day time course. Data represents mean percent of control uptake ± SEM, n=3.

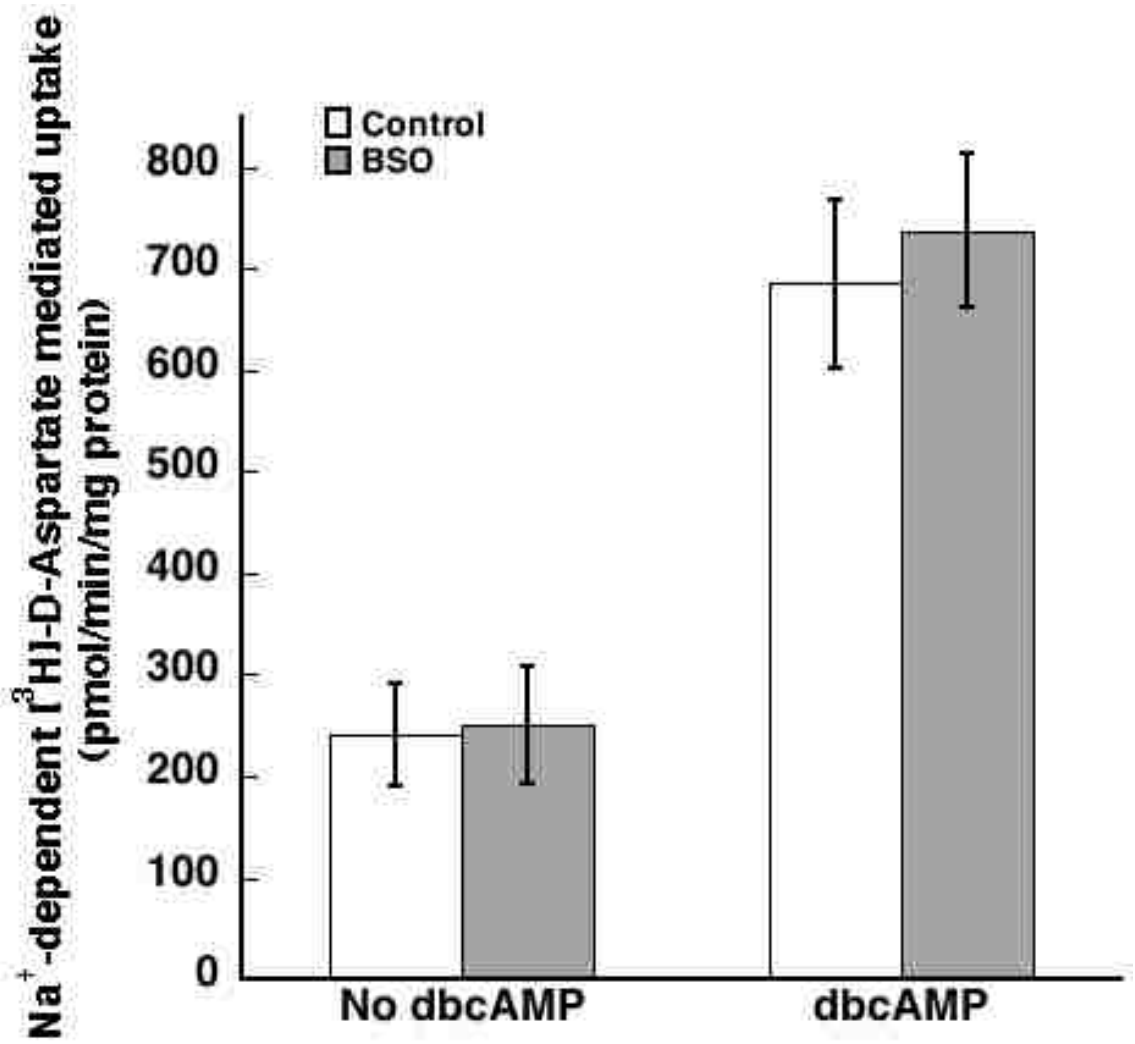

Figure 4.8. Na^+-dependent [^{3}H]-D-aspartate medicated uptake (EAAT-mediated) in primary astrocytes. Astrocytes grown in the presence or absence of dbcAMP for 7 days were treated with or without 500 μM BSO for the final 24 hrs and assayed for Na^+- dependent [^{3}H]-D-aspartate uptake activity. Data represents mean rates (pmol/min/mg protein) ± SEM, n = 3.

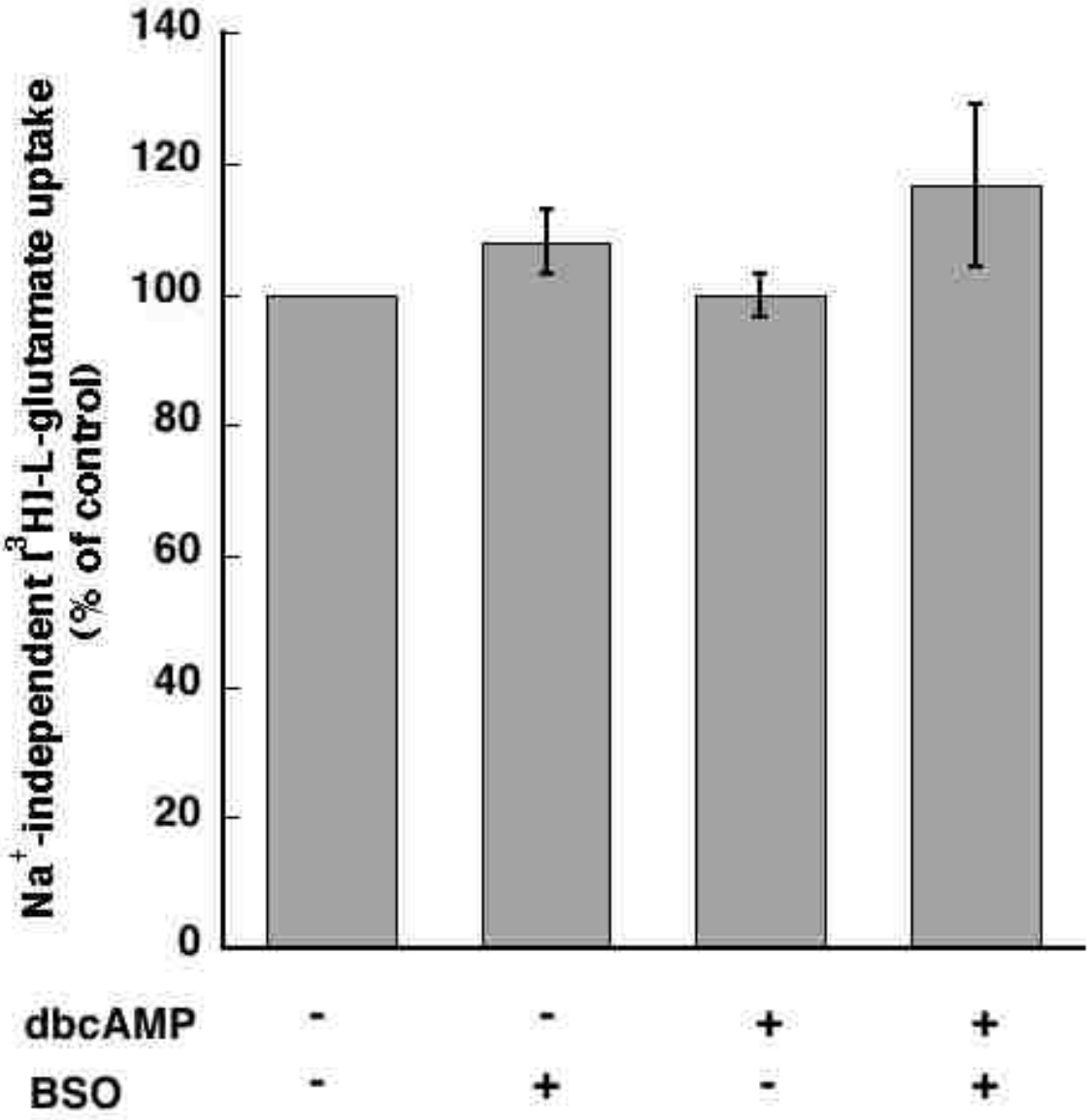

Figure 4.9. Na^+-independent [^{3}H]-L-glutamate uptake in C17.2 neuronal "stem cell-like" cells. C17.2 cells were cultured to confluency and treated with dbcAMP (250 μM), BSO (500 μM) or both dbcAMP + BSO for 24 hrs prior to performing the uptake assay, n =3.

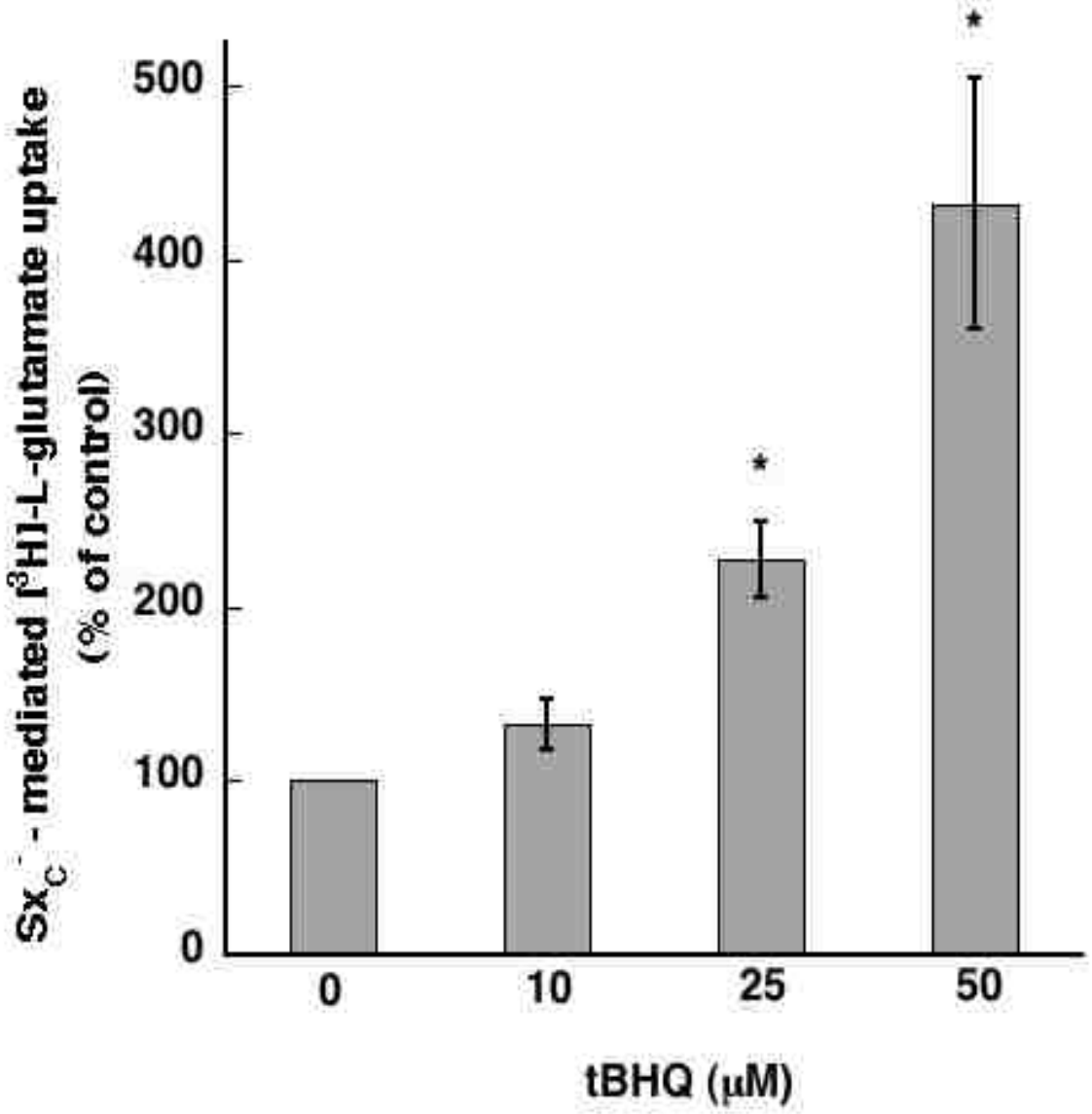

Figure 4.10. The effect of tBHQ on Sx_C^- -mediated uptake in primary astrocytes cultured without dbcAMP. Astrocytes received a dose (0-50 μM) of tBHQ for 24 hrs and were subsequently assayed for Sx_C^- -mediated [^{3}H]-L-glutamate uptake. Data represents mean % of control uptake, n = 4-8, *P ≤ 0.01 when 25 μM and 50 μM are compared to 0 μM and between 50 μM and 25 μM.

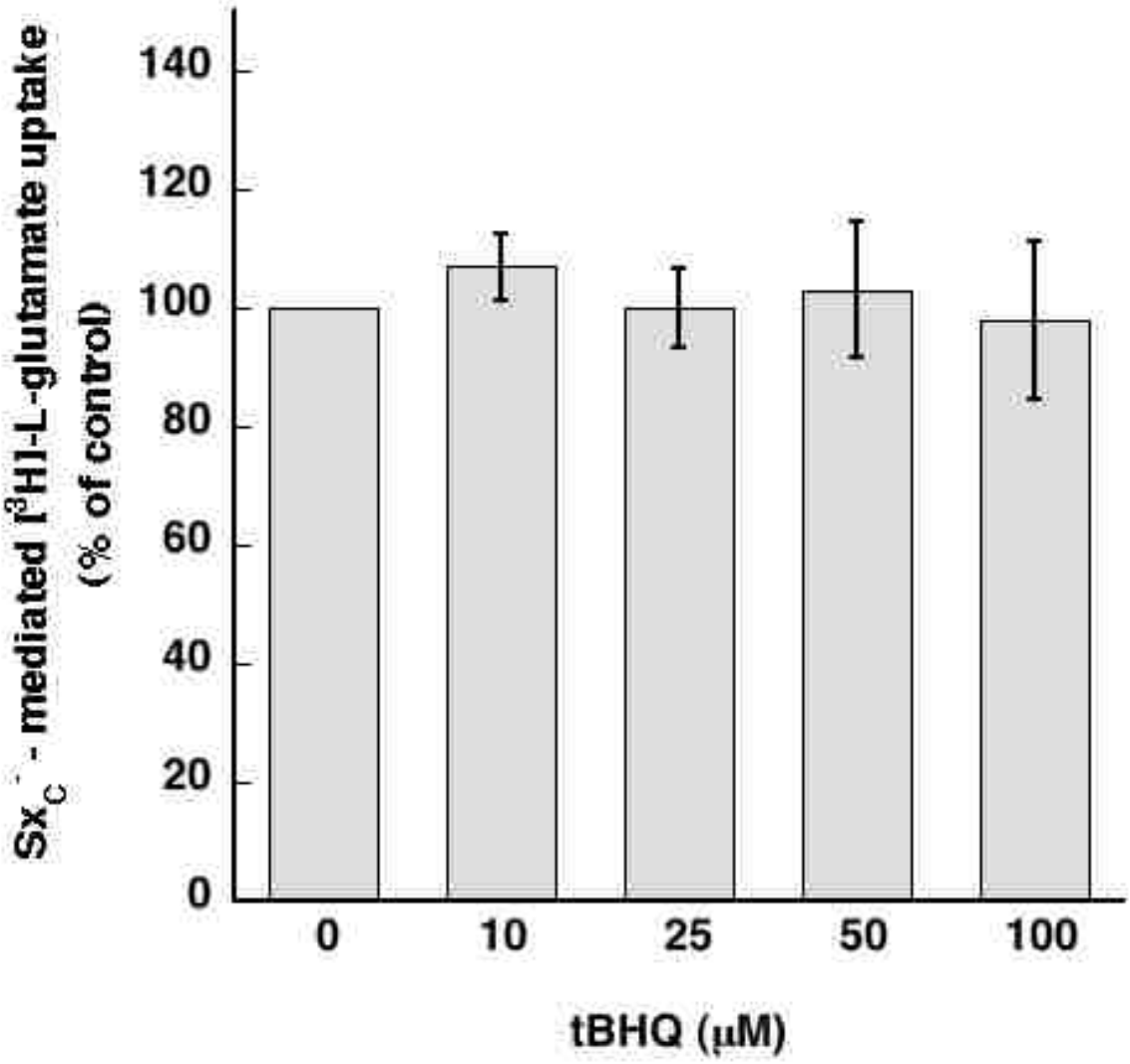

Figure 4.11. The effect of tBHQ on Sx_C^- -mediated uptake in primary astrocytes cultured in the presence of dbcAMP. Astrocytes cultured with dbcAMP for 7 days received various doses of tBHQ (0 -100 μM) for the final 24 hrs in culture and were assayed for Na^+ independent [^{3}H]-L-glutamate uptake (pmol/min/mg protein), n = 4-6.

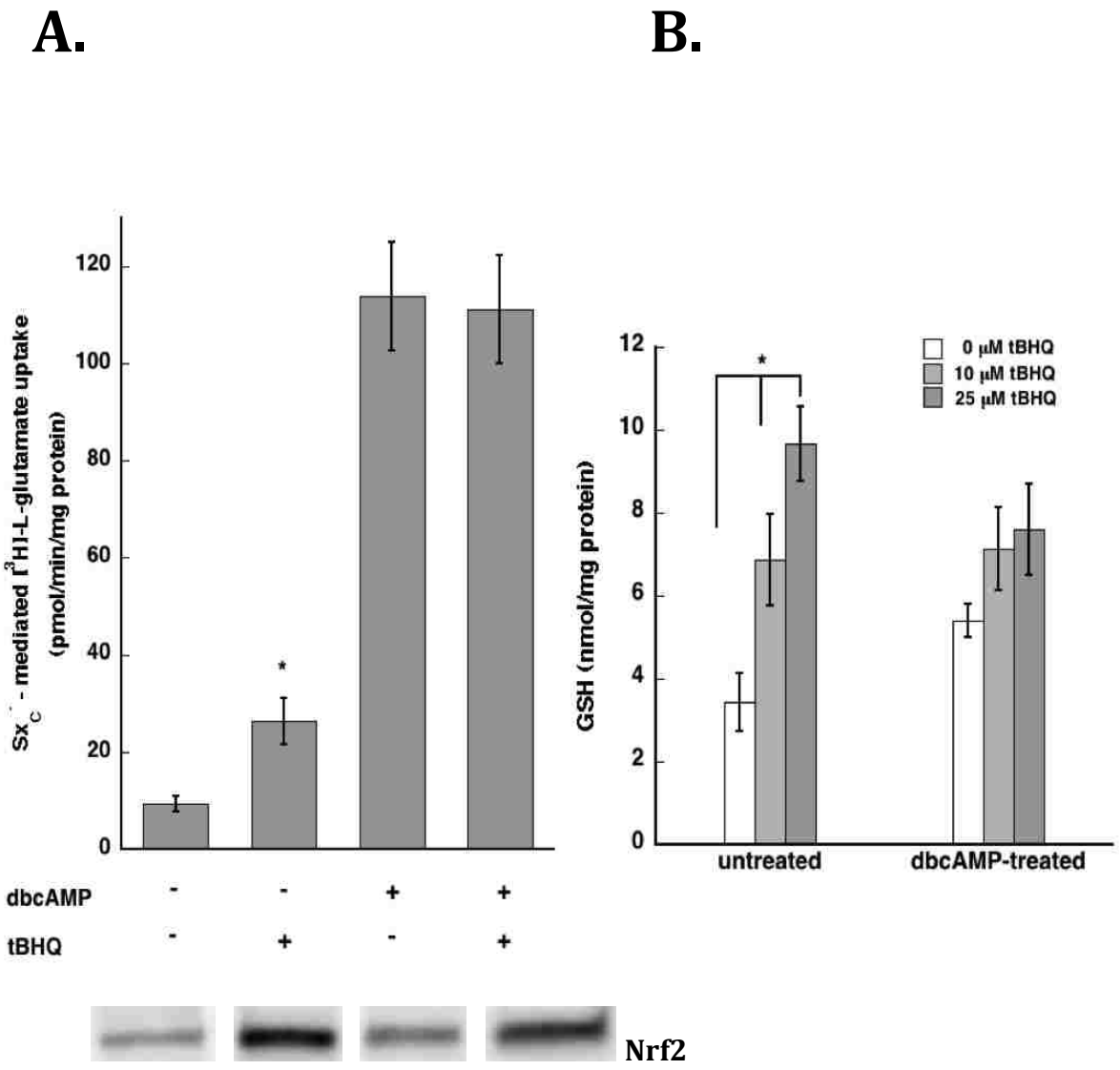

Figure 4.12. The effect of tBHQ on Sx_C^- activity and intracellular GSH levels in untreated and dbcAMP-treated astrocytes. Astrocytes cultured with and without dbcAMP for 7 days received various doses of tBHQ for the final 24 hrs in culture and Na^+-independent [^{3}H]-L-glutamate uptake (pmol/min/mg protein) or GSH content (nmol/mg protein) was measured as described in Methods. A. Sx_C^--mediated [^{3}H]-L-glutamate uptake in untreated and dbcAMP-treated astrocytes treated with tBHQ (25 μM). Immunoblots for nuclear Nrf2 correspond to conditions in graph. In all blots the Nrf2 antibody (Santa Cruz Biotechnology) revealed higher molecular weight bands (>100 kDa) than the predicted value (69 kDa), an observation consistent with other reports with this antibody (Alam et al. 1999; Danilov et al. 2009; Shih et al. 2003). B. GSH content in both untreated and dbcAMP-treated cells in response to tBHQ.

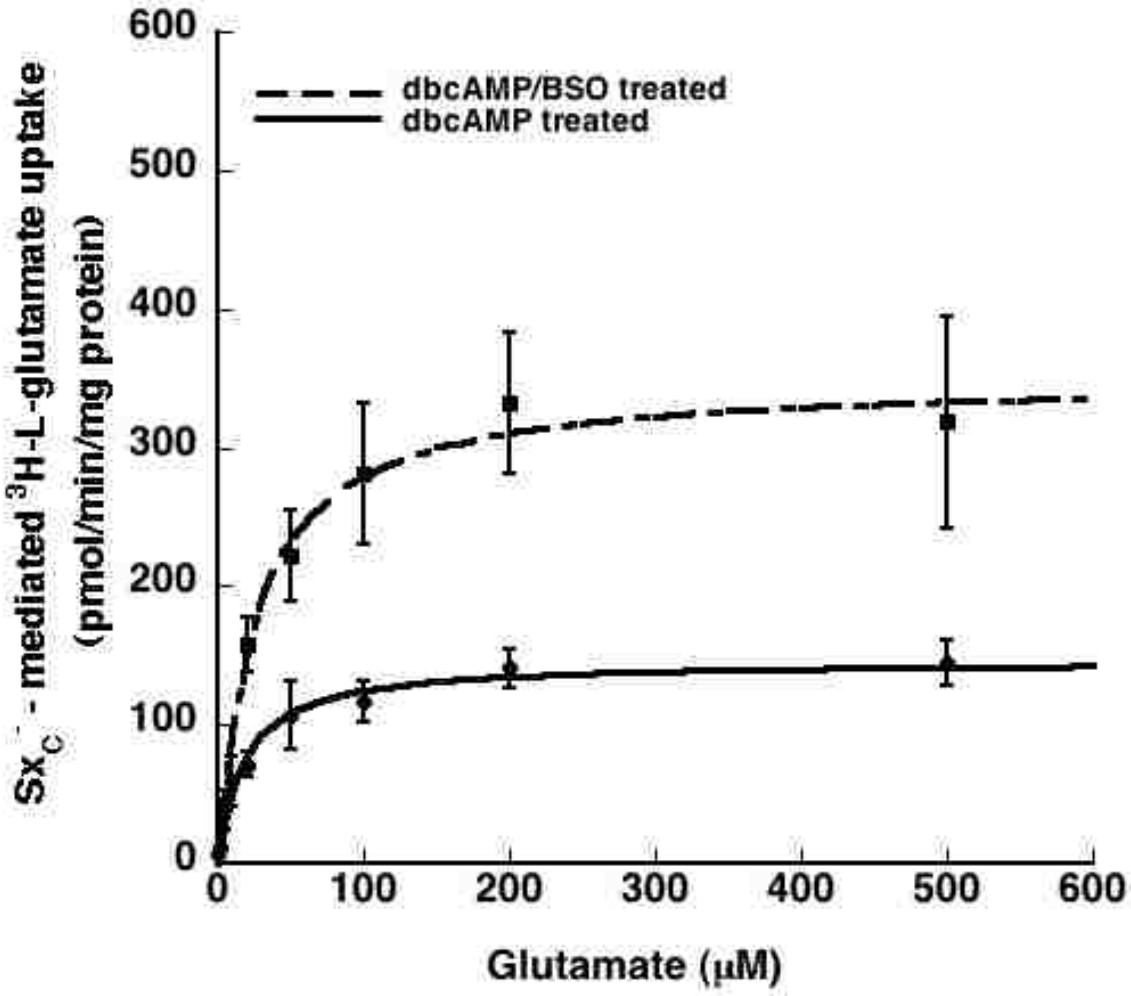

Figure 4.13. Kinetic analysis of [^{3}H]-L-glutamate uptake activity in primary astrocytes depleted of GSH with BSO. Data was fitted to y = m1*m0/(m2+m0) and followed Michaelis-Menten kinetics. The plot yielded a K_m of 17.4 ± 2.2 and V_{max} of 146.6 ± 4.6, (n = 6) in dbcAMP-treated astrocytes and a K_m of 25.1 ± 4.8 and V_{max} of 349.9 ± 15.0, (n = 5) for astrocytes treated with dbcAMP/BSO. We found no statistical difference between K_m values, P = 0.05 when comparing V_{max} values using the student's t-test

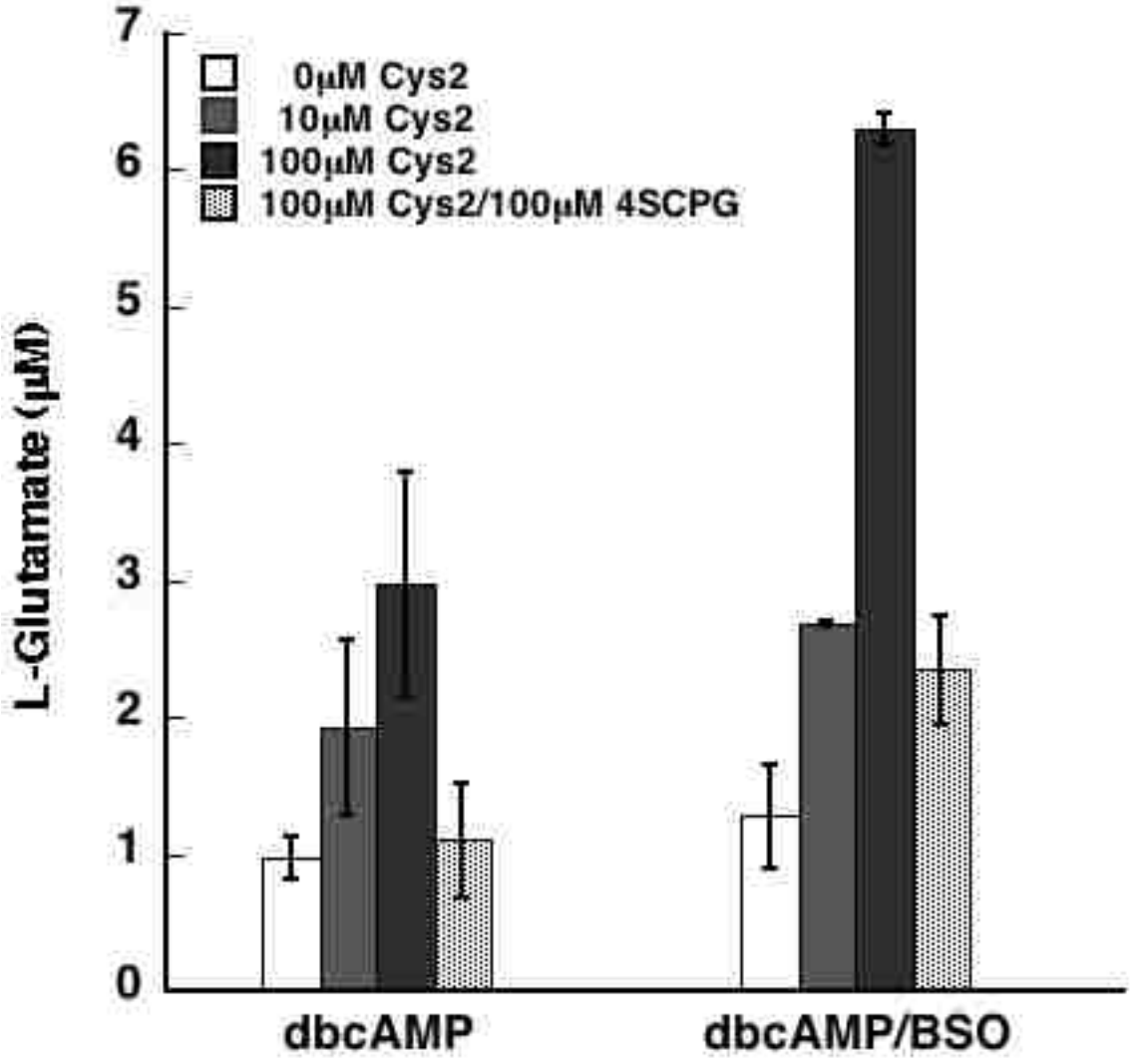

Figure 4.14. Fluorometric quantification of L-cystine induced L-glutamate efflux and accumulation via $NADP^+$ generation in astrocytes. Astrocyte cultures received 250 μM dbcAMP for 7 days and were treated with 500 μM BSO for the final 24hrs. Following a 15 minute incubation in Na^+-free buffer containing 0 μM, 10 μM, or 100 μM L-cystine, and 100 μM L-cystine + 100 μM 4SCPG, aliquots of buffer were analyzed for extracellular L-glutamate accumulation as described in Methods. Total L-glutamate from lysed cells treated with either dbcAMP or dbcAMP/BSO were 13.9 ± 4.5 and 14.6 ± 3.0 μM respectively.

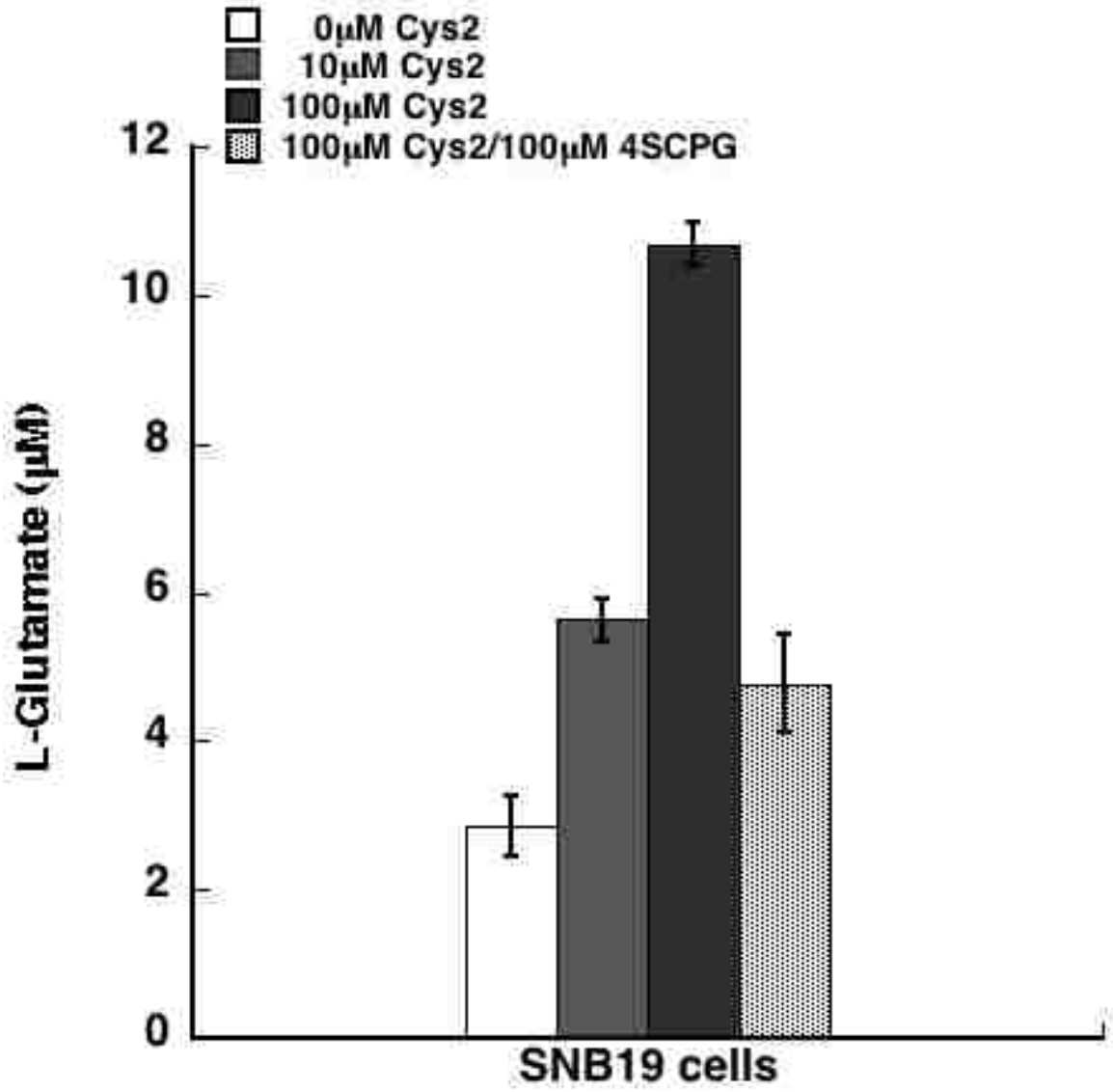

Figure 4.15. Fluorometric quantification of L-cystine induced L-glutamate efflux and accumulation via $NADP^+$ generation in SNB19 cells. Following a 15 minute incubation in NaCl buffer containing the EAAT inhibitor TBOA and 0 μM, 10 μM, or 100 μM L-cystine, and 100 μM L-cystine + 100 μM 4SCPG, aliquots of buffer were analyzed for extracellular L-glutamate accumulation as described in Methods, n = 3.

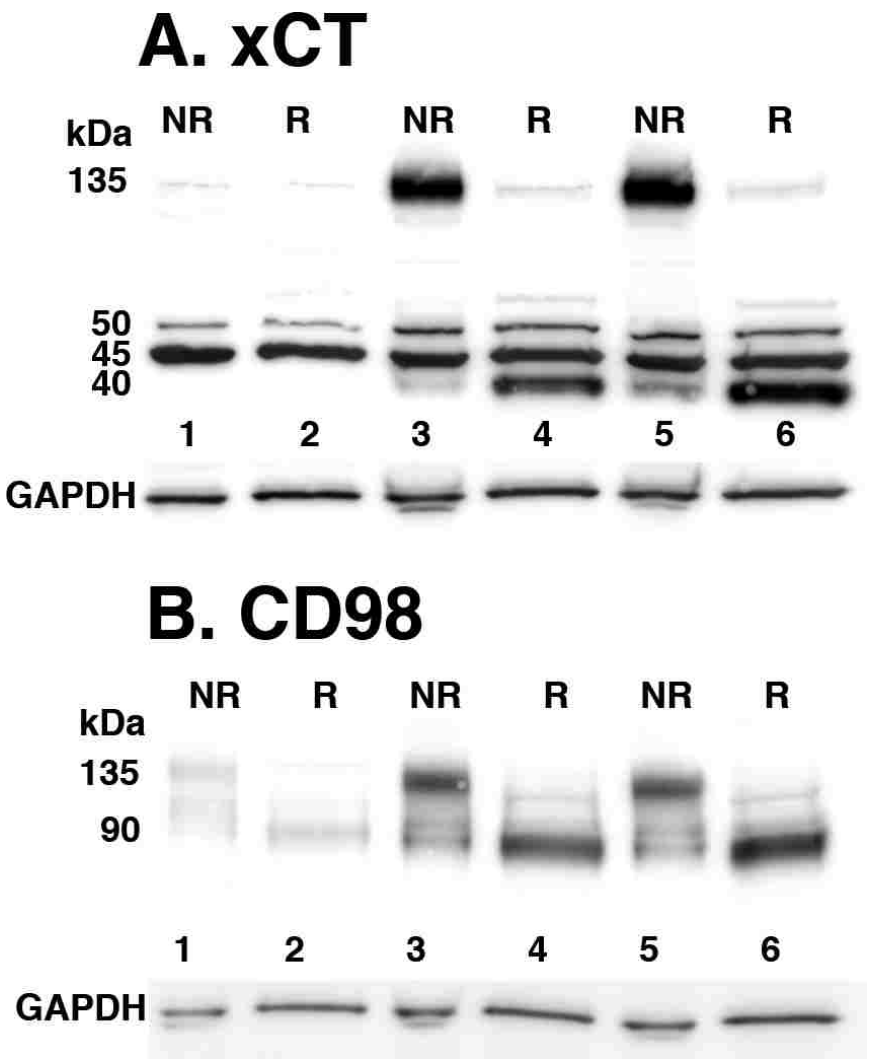

Figure 4.16. Immunoblot analysis of A. xCT and B**.** CD98 in primary astrocytes, R = reducing (355 mM 2ME) , NR = non-reducing conditions. Lanes 1,2: untreated astrocytes, 3,4: 250 μM dbcAMP–treated, 4,5: 250 μM dbcAMP-treated and incubated with 500 μM BSO for 24 hrs. The xCT antibody detected four bands specific to the xCT antibody as determined by peptide blocking, 135 kDa, 50 kDa , 45 kDa, and 40 kDa. The 135 kDa band is consistent with an xCT/CD98 dimer and appears only in blots under nonreducing conditions. xCT and CD98 heterodimerize through an extracellular disulphide bond that can be disrupted with 2ME. Immunoblotting for xCT under reducing conditions resulted in the disappearance of the higher mw band and the appearance of a band at 40 kDa, consistent with xCT. Likewise the 140 kDa band disappears in CD98 blots under reducing conditions and a band consistent with CD98 appears at 90 kDa. Representative blot of at least three experiments. xCT (1:500, 1% milk), CD98 ((SC-7094) 1:200, 0.1% milk), GAPDH (1:500 (SC-20357)), 20 μg loaded, 4-15% gel.

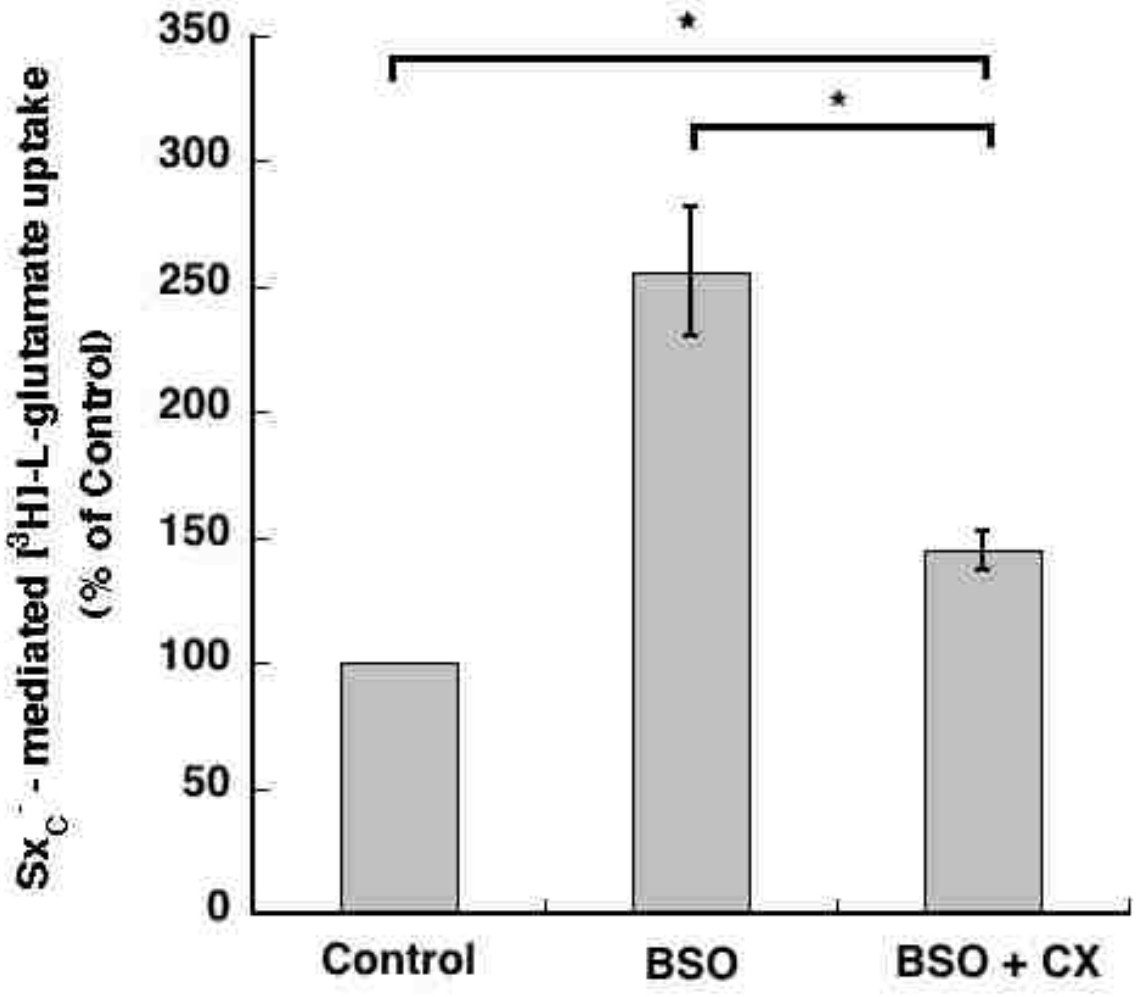

Figure 4.17. Inhibition of protein synthesis by cycloheximide (CX, 50 μM) treatment in GSH-depleted astrocytes. Astrocytes were cultured for 7 days in the presence of dbcAMP and treated with BSO or BSO+CX for the final 24 hrs. Data shown represents mean percents of control [^{3}H]-L-glutamate uptake, n =3-5. *P $\leq$ 0.01.

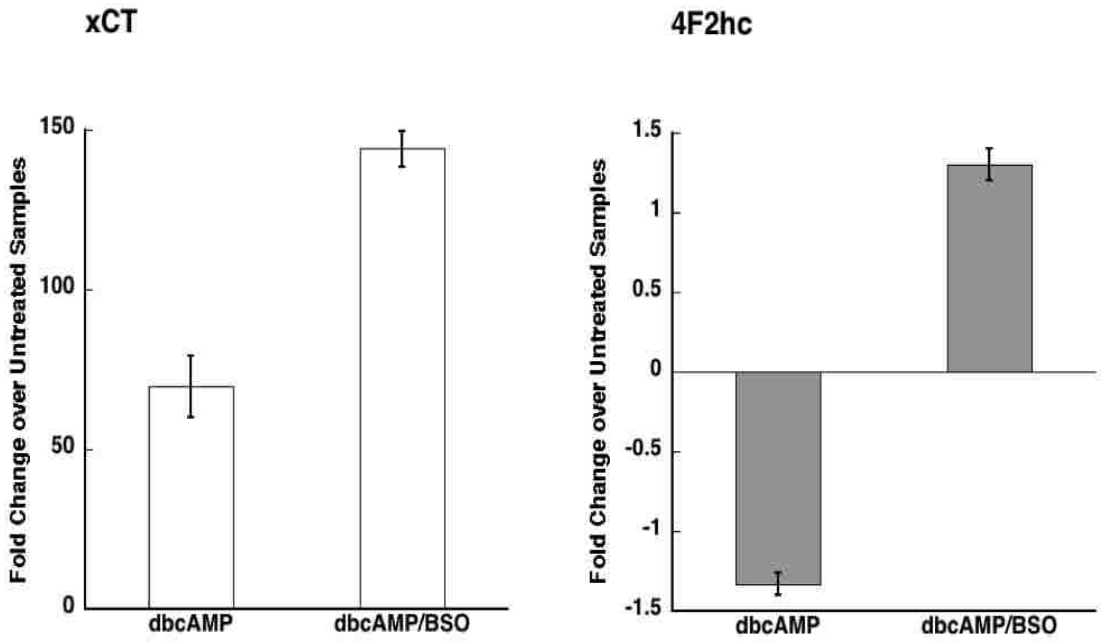

Figure 4.18. Q-PCR analysis of cDNA from untreated, cAMP-treated, and cAMP/BSO treated primary astrocytes for xCT and 4F2hc. Following 6 days in culture with or without dbcAMP, a subset of dbcAMP-treated cells were treated with 500 μM BSO for an additional 24hrs and RNA was extracted and PCR performed as described in Methods. The fold change was calculated by first normalizing against GAPDH Ct values, and then taking the difference of the ΔΔCT values for dbcAMP and dbcAMP/BSO from the ΔΔCT for untreated samples and calculating fold change with the following formula $2^{-\Delta\Delta CT}$. If this value was less than one, the fold change is represented as the negative reciprocal (i.e. a change of 0.75 from control is listed as a -1.3 fold change). The reported data are the average of two independent cultures. The low expression levels for xCT in untreated samples results in large fold-changes in dbcAMP and dbcAMP/BSO samples. It is perhaps more instructive to compare the fold-change of xCT expression in dbcAMP/BSO treated cells to dbcAMP-treated cells, which is 2.4 ± 0.1.

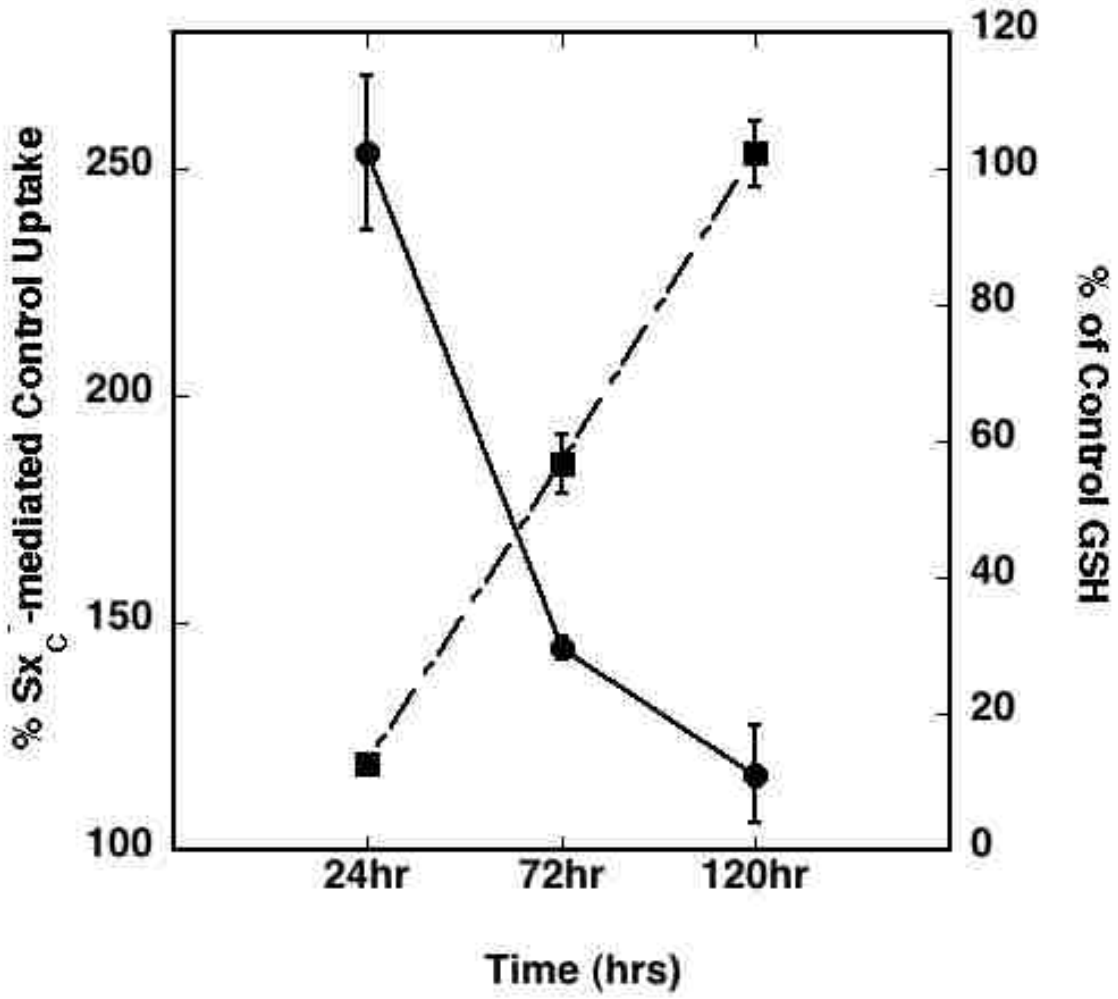

Figure 4.19. The recovery of system x_C^- activity and GSH levels following BSO washout. Following a 24 hr exposure to BSO, astrocytes received media changes daily and were assayed for intracellular GSH and [^{3}H]-L-glutamate uptake at the times indicated. n = 3-4. ●, % of control Sx_C^--mediated uptake; ■, % of control GSH

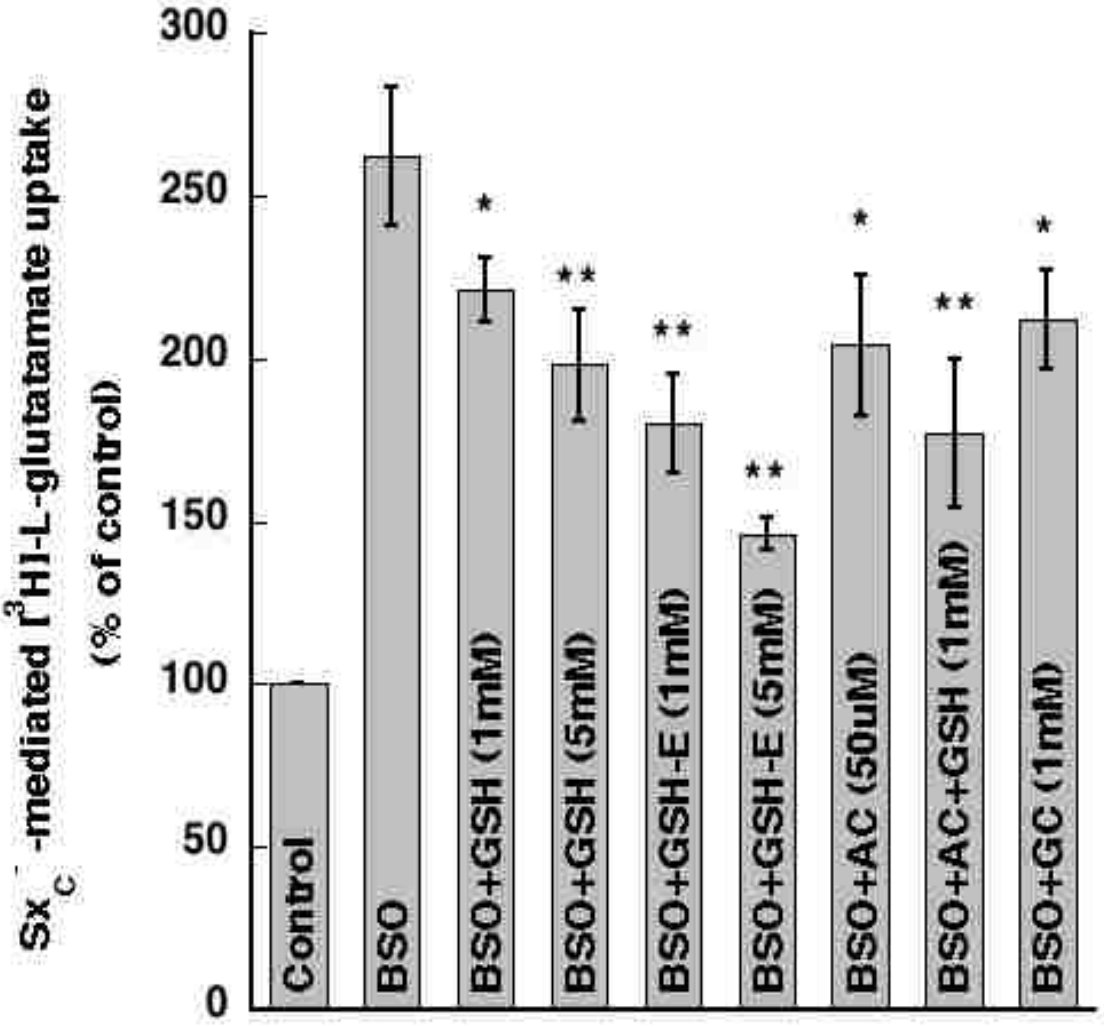

Figure 4.20. The ability of GSH to prevent the induction of system x_C^- activity in primary astrocytes. All agents were co-applied at the time of BSO-treatment. Data represents mean % of control ± SEM, n = 3-5, statistical significance is in relation to rates from BSO-treated astrocytes, *P $\leq$ 0.01, **P $\leq$ 0.0001 as determined by student t-test. Abbreviations are as follows: BSO, buthionine sulfoximine; GSH, glutathione; GSH-E, glutathione ethyl ester; AC, acivicin; GC, γ-glutamylcysteine.

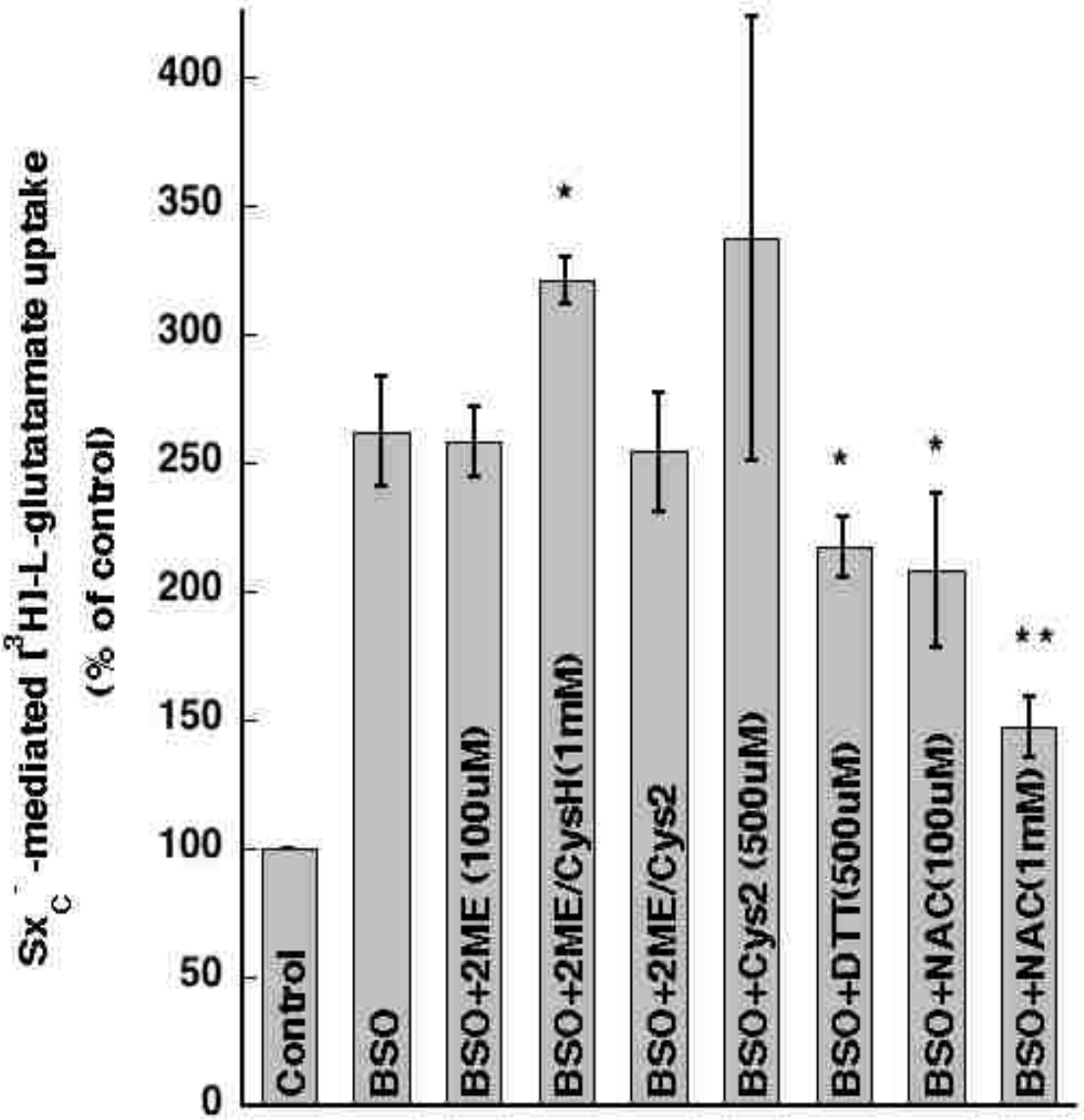

Figure 4.21. The ability of reducing agents and thiols to prevent the induction of system x_C^- activity in primary astrocytes. All agents were co-applied at the time of BSO-treatment. Data represents mean % of control ± SEM, n = 3-5, statistical significance is in relation to rates from BSO-treated astrocytes, *P $\leq$ 0.01, **P $\leq$ 0.0001 as determined by student t-test. Abbreviations are as follows: 2ME, 2-mercaptoethanol; CysH, L-cysteine; Cys2, L-cystine; DTT, dithiothreitol; NAC, N-acetylcysteine.

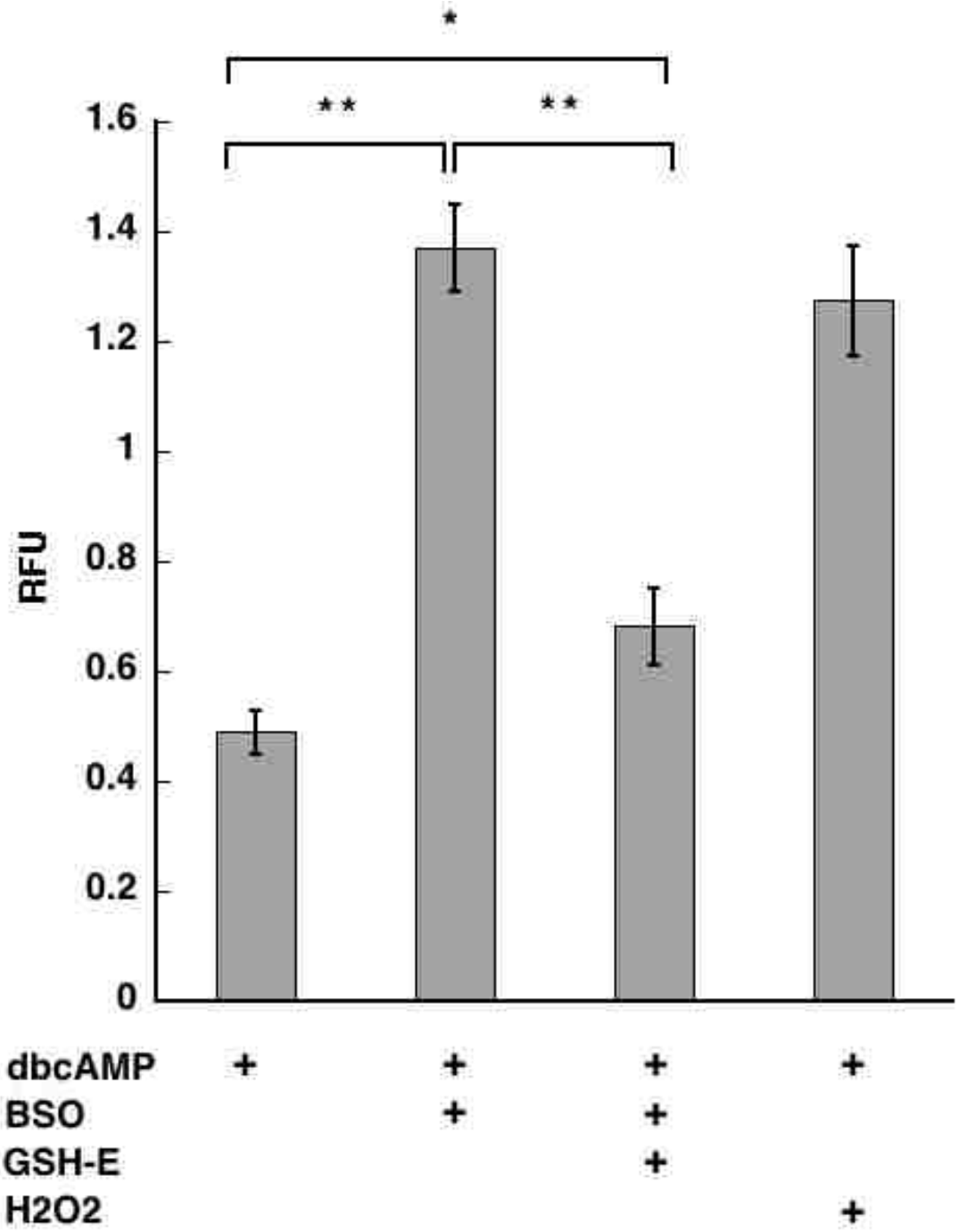

Figure 4.22. ROS-mediated fluorescence in primary astrocytes. Astrocytes were grown in 96-well plates and were treated with or without BSO for 24 hrs following 7 days of dbcAMP-treatment. An additional group of cells was also treated with GSH-ethyl ester (5 mM) in conjunction with BSO. The addition of H_2O_2 (50 μM) served as the positive control. Following the 24 hr treatments, cells were incubated for 25 minutes @ 37°C with carboxy-H2DCFDA (10 μM), rinsed with PBS, and read at Ex 485nm, Em 530nm. *P ≤ 0.03, ** ≤ 0.0001 as determined by student t-test. There is no significant difference between BSO and H_2O_2 treated samples. n = 4.

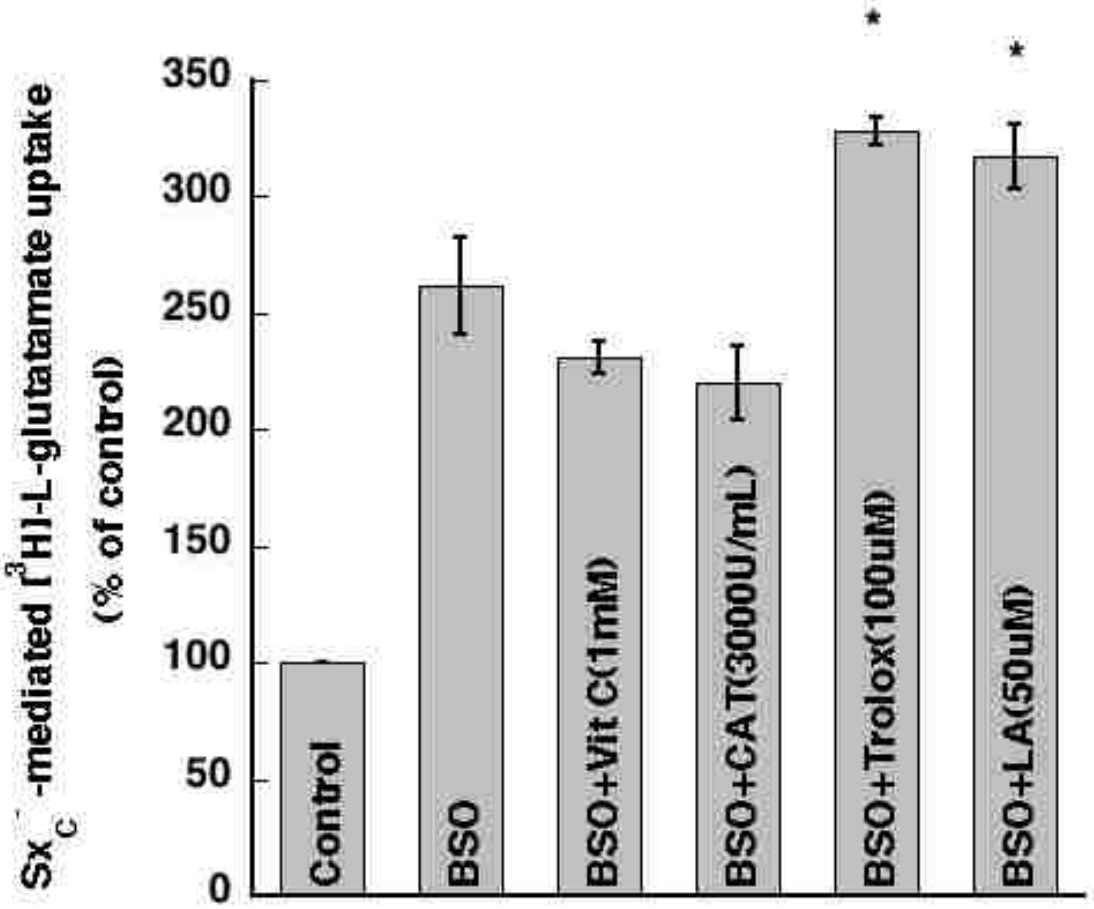

Figure 4.23. The ability of antioxidants to prevent the induction of system x_C^- activity in primary astrocytes. All agents were co-applied at the time of BSO-treatment. Data represents mean % of control ± SEM, n = 3-5, statistical significance is in relation to rates from BSO-treated astrocytes, *P $\leq$ 0.01, **P $\leq$ 0.0001 as determined by student t-test. Abbreviations are as follows: LA, R-α-lipoic acid; CAT, catalase.

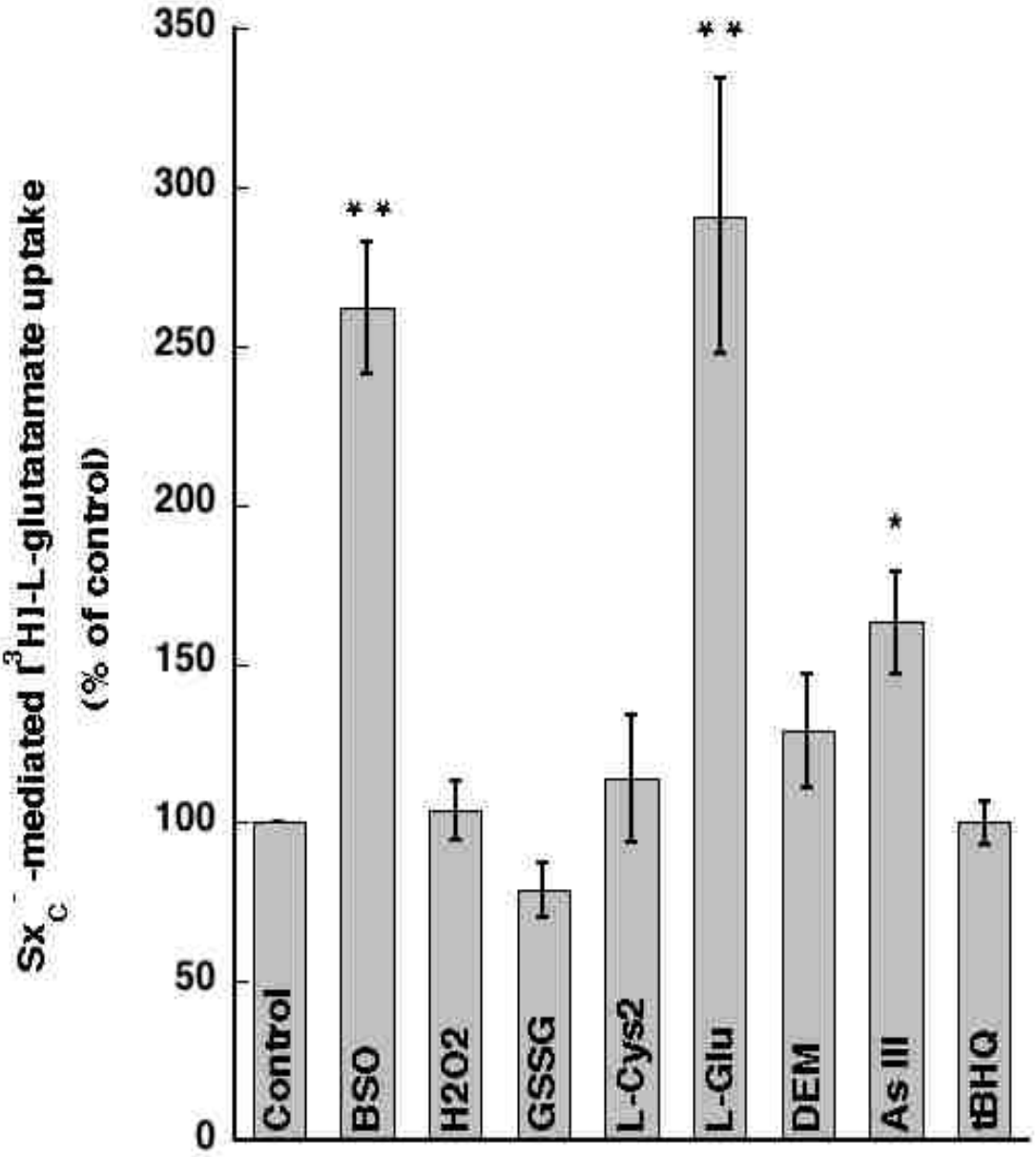

Figure 4.24. The ability of oxidants, electrophiles, and other agents to mimic the BSO-mediated induction of system x_C^- activity in primary astrocytes. Astrocytes were cultured for 7 days in the presence of dbcAMP and treated with BSO or other agents for the final 24 hrs. Data represents mean % of control ± SEM, n = 3-5, statistical significance is in relation to rates from control astrocytes (dbcAMP-treated), *P ≤ 0.01, **P ≤ 0.0001 as determined by student t-test. Abbreviations as follows: BSO, buthionine sulfoximine (500 μM); H2O2, hydrogen peroxide (50 μM); GSSG, oxidized glutathione (1 mM), L-Cys2, L-cystine (0.5 mM), L-Glu, L-glutamate (1 mM); DEM, diethylmaleate (100 μM); As III, sodium arsenite (2.5 μM); tBHQ, tert-butylhydroquinone (25 μM).

	GSH (% of control)	Sx_C^- activity (% of control)
No dbcAMP + BSO	86 ± 2.2	---
dbcAMP + BSO	62 ± 4.4*	121 ± 10

Table 4.1. Differences in total GSH levels following 2 hrs of BSO and the effect on Sx_C^- activity in dbcAMP-treated astrocytes. Total intracellular GSH levels were determined following a 2hr exposure to BSO in cultures treated with and without dbcAMP ($p = 0.002$). Sx_C^- -mediated [^{3}H]-L-glutamate uptake experiments were performed in parallel with cultures treated with dbcAMP. Data represents mean % of control values, *$P < 0.01$ as determined by student t-test, there is no statistically significant difference between % of control values for dbcAMP+BSO and dbcAMP controls (100%), n = 3-4.

	Total intracellular GSH (% of Control)		
	Exposure time	**No dbcAMP**	**dbcAMP**
Control	**0 hrs**	100% (4.2 ± 0.4 nmol/mg)	100% (6.4 ± 0.4 nmol/mg)
Control	**6hrs**	100% (5.2 ± 1.6 nmol/mg)	100% (9.64 ± 0.8 nmol/mg)
L-Cys2 (250 μM)		133 ± 9	95 ± 3
L-Cys2 (500 μM)		150 ± 15	91 ± 4
L-CysH (500 μM)		184 ± 50	96 ± 5
L-CysH (1000 μM)		176 ± 53	85 ± 10
4SCPG (100 μM)		53 ± 13	64 ± 2
Control	**12hrs**	100% (5.6 ± 1.2 nmol/mg)	100% (10.1 ± 2.5 nmol/mg)
L-Cys2 (250 μM)		124 ± 8	130 ± 26
L-Cys2 (500 μM)		152 ± 34	125 ± 26
L-CysH (500 μM)		169 ± 61	116 ± 26
L-CysH (1000 μM)		162 ± 45	102 ± 21
Control	**24 hrs**	100% (4.5 ± 0.7 nmol/mg)	100% (8.3 ± 0.7 nmol/mg)
L-Cys2 (250 μM)		110 ± 6	122 ± 3
L-Cys2 (500 μM)		125 ± 16	141 ± 11
L-CysH (500 μM)		133 ± 21	132 ± 7
L-CysH (1000 μM)		153 ± 29	139 ± 17

Table 4.2. GSH levels in astrocytes cultured in the presence of GSH precursors. Astrocytes cultured in the presence or absence of dbcAMP (250 μM) were supplied with fresh growth media and the amino acids at the final concentration listed above at the beginning of the incubation period. This concentration represents the amount added to the growth media and does not include the concentration of amino acids already contained in the media (0.1 mM L-cystine (L-Cys2) and 0.1 mM L-cysteine (L-CysH)). Data represents mean percent of control GSH for n = 3-4. Intracellular GSH content is shown (nmol/mg protein) for controls.

	Rate (pmol/min/mg protein ± SEM)		
	Sx_C^- mediated L-glutamate uptake	**EAAT-mediated D-aspartate uptake**	**Sx_C^-/ Sx_C^- + EAAT activity x 100**
No dbcAMP	**15 ± 4**	**240 ± 51**	**6%**
dbcAMP	**100 ± 21**	**685 ± 84**	**15%**
BSO	**25 ± 4**	**251 ± 58**	
dbcAMP + BSO	**253 ± 29**	**738 ± 76**	**26%**
dbcAMP + BSO + L-Cys2 as inhibitor	**32 ± 12**		
dbcAMP + BSO + 4SCPG as inhibitor	**36 ± 8**		

Table 4.3. Summary of Sx_C^- and EAAT mediated uptake in primary astrocytes cultured with and without dbcAMP in response to GSH-depletion by BSO (Figs. 4.6 and 4.8).

Chapter 5. Discussion

In a majority of mammalian cells, the Sx_C^--mediated exchange of intracellular L-Glu with extracellular L-Cys_2 and its subsequent reduction to L-CysH is a primary route through which this sulfur-containing amino acid enters cells as a rate-limiting precursor in the synthesis of the antioxidant GSH (Bannai 1984; Bannai and Kitamura 1980; Cho and Bannai 1990; Kranich et al. 1998; Sagara et al. 1993a). In the instance of astrocytes, this process takes on greater significance as it is needed not only for the maintenance of astrocytic GSH pools, but is also the first step in the Cys_2/CysH shuttle in which astrocytes supply the extracellular L-CysH needed to support GSH synthesis in neurons (Dringen et al. 2001; Dringen et al. 1999; Sagara et al. 1993b; Wang and Cynader 2000). Altered levels of GSH in the CNS have been associated with Parkinson's disease, schizophrenia, and glioma growth. These neuropathological outcomes could potentially involve an aberration in GSH-mediated feedback regulation of Sx_c^-. Just as significant, the efflux of L-Glu that occurs during the exchange with L-Cys_2 also provides a mechanism through which glial L-Glu can be exported from the cells, gain access to EAA receptors, and thereby contribute to either excitatory signaling (Baker et al. 2003; Baker et al. 2002a; Baker et al. 2002b) or excitotoxicity (Barger and Basile 2001; Piani and Fontana 1994; Piani et al. 1991; Ye and Sontheimer 1999). These studies, which detail the physiological consequences of both reductions (e.g., in neurodegeneration and susceptibility to relapse behavior in addiction models) and increases (e.g., in CNS infection,

glioblastomas, and relapse prevention) in Sx_C^- activity, highlight the importance of understanding how this transporter system is regulated.

In the present work we have used primary astrocyte cultures to study the relationship between GSH and the expression of Sx_C^- and find that the regulation of the transporter in astrocytes appears to be cell and phenotype-dependent. Thus, primary cells cultures treated with dbcAMP not only express higher levels of the transporter, the differentiated astrocytes also respond to low intracellular GSH levels by acutely and selectively increasing Sx_C^- activity in a manner not observed in control (untreated) cultures (Fig. 4.6). Using primary cultures as an experimental system permitted the direct quantification of Sx_C^- activity and the consequences of alterations in GSH levels to be selectively examined in astrocytes. Further, it also allowed GSH to be depleted by BSO-mediated inhibition of synthesis (BSO does not cross the blood-brain-barrier), thereby avoiding the complicating effects associated with using xenobiotics, electrophiles or toxins to alter GSH levels (Bannai 1984; Ishii et al. 2000; Meister 1991). That the observed increase in Sx_C^- expression that followed GSH depletion was most robust in those astrocytes that had been differentiated with dbcAMP is also notable, as these cells are believed to be more representative of an *in vivo* or activated phenotype with greater neuroprotective and neurotrophic functions (for reviews see Escartin and Bonvento 2008; Hertz et al. 1998; Juurlink and Hertz 1985). In particular, the expression of other key glutamate-associated glial proteins, including the EAAT transporters GLT-1 and GLAST and glutamine synthetase, are enhanced when glia are exposed to dbcAMP or

co-cultured with neurons (Schlag et al. 1998; Stanimirovic et al. 1999; Swanson et al. 1997).

5.1 The effect of dbcAMP treatment in astrocytes on Sx_c^-

As we and others have observed, the expression and functional activity of Sx_c^- in primary astrocytes is very low, so much so that the quantification of either L-Cys_2/L-Glu transport or intracellular GSH levels in these cells can be highly variable, even between individual experiments (Cho 1990, Dringen 1999, Kranich 1998, Sato 1995). Advantageously, we and others find that dbcAMP induces a significant increase in Sx_C^--mediated uptake of L-Glu (Gochenauer and Robinson 2001). That this activity is, indeed, attributable to Sx_C^- was confirmed using inhibitors (e.g., Cys_2 and 4-S-CPG), as well as a parallel assay directly quantifying Cys_2-mediated exchange with L-Glu (Fig. 4.6 and 4.14). This increase in transport activity also correlated with a marked increase in the 135 kDa Sx_C^- heterodimer as detected with antibodies to either the xCT or 4F2hc subunits (Fig. 4.16). When examined following reduction with 2ME, very prominent bands were observed at 40 kDa and 90 kDa, corresponding to the individual subunits of the heterodimer, xCT and 4F2hc, respectively. When examined in murine retinal Muller cells, Mysona et al. reported the presence of both a 50 kDa and 40 kDa isoform of xCT, of which only the latter increased in response to oxidative stress and accounted for the observed changes in activity (Mysona et al. 2009). Similarly, in the present investigation the 40 kDa isoform of xCT appears responsible for the significant increase in activity that

follows the phenotypic change induced by dbcAMP, as the it was only readily observable in the treated cultures. Isoforms of 50 kDa and 45 kDa were also observed in all of the cultures. However, as these subunits were equally present in the untreated cultures in which activity was difficult to distinguish from background, it would suggest that these subunits are much less functional than the 40 kDa isoform, possibly due to differences in structure and/or localization. Consistent with the activity and protein results, the astrocytes differentiated with the dbcAMP also exhibited about a 70-fold increase in xCT message as determined by Q-PCR. While parallel immunoblot assays with a 4F2hc antibody also demonstrated that the 90 kDa subunit was markedly increased in the differentiated astrocytes, this subunit was also detected in the untreated cells. It must be remembered that, as the 4F2hc subunit can associate with other "light chain" transporter subunits, its presences may or may not correlate closely with Sx_C^- activity. When examined by Q-PCR, the message levels for the 4F2hc subunit did not change with the dbcAMP induced phenotype. These findings indicate that Sx_C^- and, in particular, the expression of the 40 kDa xCT subunit, should be added to the list of glutamate-associated astrocytic proteins that are expressed in the dbcAMP-induced phenotype. The increased activity of this transport system might also contribute, in part, to the ability of these astrocytes to maintain intracellular GSH pools at higher concentrations (Fig. 4.5).

5.2 The phenotypic-specific effect of BSO on Sx_C^-

Sx_C^- activity increased by another 3-fold 24 hrs after BSO had been added to the dbcAMP-treated cultures to deplete intracellular GSH levels. This response appeared to be phenotype/cell specific, as the addition of BSO had little effect on Sx_C^- activity in untreated astrocytes (i.e., grown in the absence of dbcAMP), and has been reported to be ineffective in BHK21 cells (Sasaki et al. 2002) and rat kidney fibroblasts (Kang and Enger 1992).

In previous studies of astrocytes cultured in the absence of dbcAMP, BSO treatment had been reported to result in a modest increase (140% of control) in activity (Allen et al. 2001), consistent with our data (Fig. 4.6) and the range of variability characteristic of this phenotype. However, in another study of astrocytes treated with both dbcAMP and BSO, the authors reported a non-significant down-regulation of L-Cys_2 transport (Bender et al. 2000), a distinctly different result from the work presented here. It is likely that differences in experimental protocols in this latter study (e.g., exposure time to BSO (3hrs) and use of NaCl-containing uptake buffer) are partly responsible for the inconsistencies. In agreement with the data observed in our dbcAMP-treated astrocytes, GSH-depletion in C1 cells (simian virus 40 large T-antigen immortalized line) has lead to increased levels of xCT (Qiang et al. 2004) and the i.p. administration of BSO, while ineffective at entering the brain intact and altering GSH levels there, also leads to increases in xCT mRNA in whole brain homogenates (likely reflecting changes at or near the BBB) (Limon-Pacheco et al. 2007).

Our data demonstrate that the increased activity in response to BSO could be ascribed specifically to Sx_C^- based upon both pharmacological inhibition (Fig. 4.6) and parallel L-Cys_2/L-Glu exchange assays (Fig. 4.14). Several findings lead to the conclusion that the increase in transporter activity following GSH depletion is primarily attributable to an enhanced expression of Sx_C^-, including: kinetic studies demonstrating an increase in V_{max} without a significant change in K_m (Fig. 4.13), increased presence of both mRNA (Fig. 4.18) and protein (Fig. 4.16) for the xCT subunit, and the attenuation of the increase by co-administration of cycloheximide (Fig. 4.17). In contrast to changes in the xCT subunit, the BSO-induced depletion of the GSH levels did not appear to alter the expression of the 4F2hc subunit at either the message or protein levels. 4F2hc, like other heavy chain subunits, associates with a variety of light chains in the HAT family of transporters, where it plays a critical role in surface expression (Nakamura et al. 1999). Given the increase in both Sx_C^- activity and the expression of the xCT subunit, our findings could indicate that while the absolute amount of the 4F2hc subunit did not change, a greater proportion of it is associated with xCT in Sx_C^- heterodimers as part of the cellular response to decreased GSH levels.

5.3 The biochemical trigger of the BSO-mediated effect on Sx_C^-

While it was the treatment of the astrocyte cultures with BSO that led to the phenotype-specific induction of Sx_C^-, there are any number of biochemical events that may have actually triggered the response, especially given that the transport

system is upregulated by amino acid starvation, electrophiles, xenobiotics, toxins, and oxidative stress (Bannai 1984; Bannai et al. 1989; Ishii et al. 2000; Sato et al. 1995). Thus, beyond the ability of BSO to deplete intracellular GSH levels by inhibiting γ-glutamylcysteine synthetase, secondary effects could include an influence on extracellular GSH levels, intracellular or extracellular levels of L-Glu or L-CysH, the production or accumulation of ROS, or the redox state of signaling proteins.

To sort through these possibilities and try to elucidate the signal that triggered the induction, we first examined the well-characterized EpRE/ARE-associated pathway through which electrophiles or oxidative stress up-regulate Sx_c^- *via* an Nrf2-dependent mechanism. The cytoskeletal protein Keap1 is thought to negatively regulate Nrf2-mediated gene activation by retaining Nrf2 in the cytoplasm and targeting it for ubiquinization and degradation. Likely through a thiol-sensing mechanism (Keap1 contains 25 L-CysH residues), Keap1 releases Nrf2 which then migrates to the nucleus, forms heterodimers with other transcription factors (ATF4, Jun, Maf proteins) and initiates the transcriptional activation of target genes (He et al. 2001; for review see Itoh et al. 2004).

We find that the classic EpRE-gene inducer tBHQ did indeed produce a similar increase in the nuclear presence of Nrf2 when added to either control or dbcAMP treated astrocytes (Fig 4.12). Interestingly, however, tBHQ only produced the expected increase in Sx_c^- activity and GSH levels in the untreated astrocytes. The failure of tBHQ to produce any further increase in transporter activity over the

much higher basal levels present in the dbcAMP-differentiated cells infers that the signaling pathway is different in this phenotype or that the tBHQ induced increase was small enough to be masked by the higher levels of activity. Either way, it suggests that the upregulation of the transporter observed with dbcAMP and GSH depletion is unlikely attributable simply to the classic EpRE/ARE-associated pathway, a notion supported by similar data reported in a mammary cell line (Wang et al. 2006) and mouse embryonic fibroblasts (Sasaki et al. 2002). Notably, in the latter study, electrophiles and known inducers (arsenic, cadmium, hydroquinone, and DEM) of the EpRE were shown to be effective at upregulating Sx_C^-, advancing the argument that BSO and electrophiles may act independently to regulate L-Cys_2 transport. Further, GSH levels in glia of Nrf2 $^{-/-}$ animals are not different than that from wildtypes (Shih et al. 2005), suggesting other mechanisms in control of GSH homeostasis in these animals. Aside from Nrf2, the transcription factor ATF4 (aka Creb2) has also been shown to induce Sx_c^- activity (Lewerenz and Maher 2009), specifically in response to L-Cys_2 deprivation (Sato et al. 2004). Indeed, consistent with these results it has been demonstrated here that astrocyte cultures exposed to high levels of L-Glu (5 mM) (effectively outcompeting the transport of L-Cys_2) also exhibit increased levels of Sx_c^- activity (Fig. 4.24). However, unlike amino acid deprivation scenarios, treatment with BSO would be expected to lead to an increase in intracellular L-Cys_2/L-CysH and L-Glu, as these amino acids would not be utilized by the synthetase. Therefore, in the model of BSO-mediated GSH-depletion it is unlikely that the increase in Sx_c^- is related to ATF4-mediated activation of the AARE. Interestingly, the induction of xCT by the reactive tocopherol metabolite γ-

tocopheryl quinone has been shown to be attenuated by siRNA for ATF4 but not Nrf2 in PC-12 cells (Ogawa et al. 2008). This suggests that ATF4 can mediate the transcriptional control of xCT via the AARE in ways potentially distinct from amino acid deprivation or through a means independent of the AARE.

Alternatively, given the presence of Nrf2 in the nuclei of the dbcAMP + BSO – treated astrocytes and the heterodimeric nature of Nrf2-mediated gene activation, it is feasible that the stimulation of a converging signaling pathway may be involved in Sx_C^- regulation. In a model of systemic GSH-depletion in mice it was found that the upregulation of Sx_C^- was linked to p38MAPK and ERK2 signaling cascades (Limon-Pacheco et al. 2007), potentially leading to the activation/synthesis of any number of additional transcription factors linked to either the Nrf2-associated activation of Sx_C^- or an as yet unspecified Nrf2-independent pathway of gene activation. Thus, there may be other points along the pathway to EpRE stimulation on which BSO could be having its effect apart from the release of cytoplasmic sequestered Nrf2. This type of regulatory control is observed in the cases of arsenic (sodium arsenite) exposure in hepa1c1c7 cells (He et al. 2006). In this study, arsenic, but not tBHQ treatment, was associated with the disruption of Nrf2-keap1-Cu3 complexes and dimerization of Nrf2 and Maf proteins in the nucleus, resulting in increased EpRE-dependent transcription of the NQO1 gene. This observation of the differential actions of arsenic and tBHQ on EpRE-mediated gene expression may be relevant to the results presented here. Specifically, while tBHQ did not have an effect on dbcAMP-treated astrocytes, arsenic did have a modest inductive effect in this

phenotype (Fig. 24), again lending credence to the concept of multi-point regulatory control over genes containing EpRE response elements, in particular, Sx_c^-.

Additionally, in our model of GSH-depletion, ROS levels may be postulated to play a role in the regulation of Sx_c^-. However, ROS levels were comparable in astrocytes treated with either BSO or H_2O_2, although it was only the addition of BSO that led to an increase in Sx_c^- activity. Similarly, antioxidant treatment was ineffective at preventing the effect of GSH-depletion. There is evidence for the induction of MAP kinase pathways by oxidative stress and H_2O_2, specifically the activation of p38 MAPK and ERK (Rosenberger et al. 2001). As these pathways can lead to the activation of CREB, thereby mimicking the action of dbcAMP, it is possible that cells treated with H_2O_2 could induce Sx_c^- in a manner similar to dbcAMP. One explanation then is that astrocytes were already close to if not at their maximal level of dbcAMP-mediated Sx_c^- expression prior to the addition of H_2O_2 and therefore could not be further stimulated. These findings tie the induction of Sx_c^- more directly to changes in GSH itself, rather than secondary effects, such as a general increase in oxidative stress or ROS. Such a relationship would also be consistent with the close temporal correlation observed between Sx_c^- activity and GSH levels as both returned to basal levels following the washout of BSO (Fig. 4.19).

The strongest evidence that the induction of Sx_c^- was actually triggered by changes in intracellular GSH levels came from experiments demonstrating that the ethyl-ester of GSH (GSH-E) was able to prevent the increase in activity when added in combination with BSO. GSH-E is considered a "pro-drug" that enhances

permeability and intracellular accumulation of GSH and does so in a manner that bypasses the inhibition of γ-glutamylcysteine synthetase by BSO. The finding that additions of GSH (which cannot be transported into cells intact), L-CysH or L-Cys_2 failed to mimic the effectiveness of GSH-E in preventing the induction is not surprising, as the capacity of these precursors to replenish GSH levels would be dependent upon the activity of γ-glutamylcysteine synthetase. Further, the observation that γ-glutamylcysteine did have a modest effect on attenuating the increase Sx_c^- activity, provides an explanation as to how GSH may have produced its effect. The ineffectiveness of GSH, L-CysH or L-Cys_2 also suggests that the induction of Sx_c^- was not triggered by an extracellular decrease in any of these three, which would be expected to follow a reduction in the synthesis and export of intracellular GSH. The surprise among the compounds tested was, however, the other pro-drug N-acetyl-CysH (NAC), which was as effective as GSH-E in counteracting the action of BSO. When interpreted in view of the inactivity of L-CysH, it suggests that NAC may have been acting as a GSH mimic, rather than a source of intracellular of L-CysH. In this respect, NAC may more closely resemble L-CysH as it is embedded within the GSH tri-peptide. Following internalization and deacylation, this effect would be expected to be lost however. The potential for NAC to be acting extracellularly to alter the redox status on the surface of glia is a possibility. Alternatively, it may indicate that the induction of Sx_c^- was triggered by a more general loss of intracellular free thiols (whether GSH or L-CysH) and that the extracellular addition of NAC was more effective in this regard than L-CysH.

While the exact mechanism involved in the induction of Sx_c^- by the GSH/thiol trigger is unknown, recent evidence suggests that the redox state of protein sulfhydryl moieties can serve as signaling intermediates in a number of transcriptional activation events (Ahn and Thiele 2003; Delaunay et al. 2002; Limon-Pacheco et al. 2007; Tachibana et al. 2009). The role of GSH in these signaling events may involve interacting with cysteines located in the modulatory or active site of kinases, phosphatases, and transcription factors. As mentioned above, Nrf2 activation involves the redox status of cysteine moieties within the Keap1-Nrf2 complex. Other examples of redox-related activation exist as well. For instance, the HSF1 transcription factor is activated to the trimeric form in response to stress through the formation of disulfide bonds, and is inactivated by GSH, NAC, and DTT (Ahn and Thiele 2003). Along a similar vein, a decrease in liver, kidney, and brain GSH has led to varying levels of p38MAPK and ERK activation leading to NF-KB, ATF-2, and c-Jun phosphorylation (Limon-Pacheco et al. 2007). Also, the formation of disulphide bonds is responsible for the activation of Yap1 (a tf involved in oxidative stress in budding yeast) (Tachibana et al. 2009). Conversely, increases in the cellular reducing environment also serve to initiate signaling cascades. The application of reducing voltages to Caco-2 cells doubled the rate of BrDU incorporation and was found to increase EGF receptor phosphorylation and subsequently p44/42 MAPK activation (Nkabyo et al. 2005).

5.4 Physiological significance of the depletion of GSH

Perhaps the best correlation of our GSH-depletion model with known diseases is with inborn deficiencies in synthesis and GSH regeneration. GSSG reductase and GSH synthetase deficiencies have been associated with increased tendency to hemolytic disease, cataracts, and CNS function (Meister 1991). GSH synthetase deficiencies are interesting as they often involve a cascade of secondary effects related to normal GSH feedback and metabolism. Specifically, under normal conditions, GSH feedback inhibits γ-glutamylcysteine synthetase (γGCS), which catalyzes dipeptide (γ-glutamylcysteine) formation at sub-maximal rates. Without GSH synthetase activity, GSH levels are low, thus releasing γGCS inhibition. Excess formation of γ-glutamylcysteine (something that wouldn't occur in our BSO regimen), leads to the increased formation of 5-oxoproline as γ-glutamylcysteine is a good substrate for γ-glutamylcyclotransferase. 5-oxoproline accumulates in the blood as it overwhelms the degradation ability of 5-oxoprolinase. This causes acidosis which can be life threatening (Meister 1991). As an aside, in this case inhibition of Sx_C^- or BSO treatment could possibly have therapeutic effects.

In light of our findings, the functional link between GSH and Sx_c^- may also be relevant to a variety of pathologies characterized by decreases in GSH, such as Parkinsonian disorders (Chinta et al. 2007; Schulz et al. 2000a; Wullner et al. 1996) and schizophrenia (Berk et al. 2008; Do et al. 2000; Grima et al. 2003; Hirrlinger et al. 2002) as disease development and/or progression may conceivably be linked to an aberration in the GSH-mediated regulation of Sx_c^- described here.

In Parkinson's disease, sufficient GSH concentrations in astrocytes are critical for the survival of dopaminergic neurons, and neuronal GSH loss tends to correlate with PD severity (Schulz et al. 2000b). Interestingly, GSH is also decreased during the preclinical asymptomatic phase of the disease, suggesting an early role for GSH in pathogenesis of PD. Although GSH depletion is not sufficient to mimic PD in the healthy substantia nigra, it does lead to greater dopaminergic neurodegeneration (Chinta et al. 2007) and neurotoxicity upon subsequent exposure to MPTP, a meperidine analog that mimics the idiopathic effects of PD (Wullner et al. 1996). In addition to GSH loss, the potential generation of ROS as a result of dopamine metabolism by MAO is also thought to contribute to dopaminergic cell death and pathogenesis. In fact, the inhibition of MAO in Parkinson's patients remains an important therapeutic approach (Chen et al. 2008). Dopamine release from presynaptic neurons has been shown to be negatively regulated by the binding of glutamate released from Sx_C^- to mGlur2/3 (Baker et al. 2002b). Therefore, attenuated Sx_C^- could potentially lead to excess dopamine release and extensive MAO metabolism, with potentially significant ROS generation. The current data on this topic is intriguing however the exact role of GSH or Sx_C^- in PD pathogenesis has not been fully elucidated.

Schizophrenia is a disorder of the CNS for which the etiology is currently incomplete, but for which there is evidence of both dopaminergic hyperfunction (Howes et al. 2009; Howes and Kapur 2009)and glutamatergic hypofunction (Carlsson et al. 2001; Carlsson and Carlsson 1989; Olney 1990). Decreases in GSH have been observed in schizophrenics *in vivo* as well as in *in vitro* models (Do et al.

2000) and polymorphisms in GSH-metabolism and synthesis genes (i.e. GSTT1, GCLC, and GCLM) are associated with increased susceptibility to the disorder for review see: (Berk et al. 2008). GSH depletion is now thought to be a consequence of increased levels of dopamine (DA) in the CNS of schizophrenics. Free radicals and reactive oxygen species (namely superoxide and hydrogen peroxide) are produced as a result of dopamine metabolism (Chen et al. 2008; Hirrlinger et al. 2002), and consequently deplete cellular levels of GSH (Hirrlinger et al. 2002). In addition to increased DA metabolism, a number alterations in brain energy metabolism occur in schizophrenia, including polymorphisms in mitochondrial genes and proteins involved in the electron transport chain, potentially leading to ever greater production of oxidative species(Karry et al. 2004). Therefore, glutathione and, by association, Sx_C^-, may play a critical role in protecting cells from damage by ROS generated in schizophrenia. In fact, GSH-deficiency sensitizes neurons to DA-induced dendritic degeneration (Grima et al. 2003). Considering the connection between oxidative stress and psychiatric disorders, GSH may represent a novel target for treatment (Berk et al. 2008). In support of this, N-acetylcysteine (NAC) treatment led to higher ratings than placebo in a variety of categories. As the acetylated precursor of L-cysteine, NAC likely enters the cell through neutral amino acid transporters and once deacetylated supplies cysteine, the rate-limiting precursor to GSH synthesis. Along these lines, clinical data have demonstrated that the antioxidant effects of certain antipsychotic drugs may play a role in their therapeutic effect as they are capable of decreasing the oxidative stress reported in schizophrenia, bipolar, and major depressive disorders (Berk et al. 2008).

Decreases in cellular GSH could also alter the function of the glutamatergic system, in particular the NMDA receptor (NMDAR). In vitro, the NMDAR is positively modulated by reductants, including GSH (Aizenman et al. 1989; Janaky et al. 1993; Regan and Guo 1999a; Regan and Guo 1999b). Thus, a decrease in GSH could result in a reduction in NMDAR function. Indeed NMDAR dysfunction has been proposed as part of schizophrenia etiology as NMDAR antagonists like phencyclidine (PCP) and ketamine can induce schizophreniform psychotic symptoms in healthy human volunteers (Moghaddam 2003). Studies have also demonstrated that NMDA receptor dysfunction may underlie the increases in dopamine release seen in schizophrenic patients (Kegeles et al. 2000), supporting the notion that both the hyperdopaminergic and hypoglutamatergic theories may in fact overlap. From an experimental-model perspective, as compared to untreated astrocytes the dbcAMP-treated glial phenotype may represent a useful model for the study of Sxc regulation as it could represent how astrocytes, either in the presence of neurons or in response to disease (Daginakatte et al. 2008), uniquely respond to changes in GSH status.

5.5 Concluding remarks

Collectively, these findings support the conclusion that, like other glial proteins involved in the regulation of L-Glu (e.g., GLT1, GLAST, glutamine synthetase), the expression of Sx_c^- in astrocytes is phenotype dependent and markedly increases when the cells are differentiated with dbcAMP into a phenotype more

representative of that found *in vivo* or following injury-induced activation. Further, the depletion of GSH levels in these astrocytes appears to serve as a trigger for the rapid induction of Sx_c^-, a pathway not observed in other cell types. The ability of these cells to regulate Sx_c^- in this manner likely reflects the specialized role of astrocytes and Sx_c^- in maintaining glial, as well as neuronal, GSH levels as a protective mechanism and the inherent vulnerability of the CNS to oxidative injury. Ironically, while this pathway allows the CNS to rapidly up-regulate Sx_c^- in response to an oxidative or toxic challenge, it also holds the potential to exacerbate CNS pathology as a consequence of increasing extracellular L-Glu levels and the risk of excitotoxicity. Whether related to the progression of a disease or a therapeutic intervention, it is the balance between these two possible outcomes that must always be kept in mind when considering the physiological consequences of alterations in Sx_c^-.

Appendix I: Nrf2 involvement in the regulation of Sx_C^-, a history

Early work with DEM, L-Cys2 deprivation, and LPS

Given the link between GSH production and Sx_C^- activity, it is perhaps not surprising that some of the first investigations into the induction of Sx_C^- involved the treatment of cells with electrophilic agents in an attempt to deplete GSH (Bannai 1984). At that time it was known that electrophiles (most commonly diethyl maleate or DEM) interact with sulphydryl groups and accordingly deplete GSH levels both *in vivo* and *in vitro* through GSH conjugation reactions (Boyland and Chasseaud 1970; Brodie et al. 1982; Chuang et al. 1978; Early and Schnell 1982; Tietze 1969). The results of Shiro Bannai's 1984 study are striking however in that GSH depletion was not correlated with an upregulation of Sx_C^-. The treatment of human lung fibroblasts with DEM at concentrations high enough to deplete GSH (above 250 μM) resulted in a decrease in L-cystine/L-glutamate exchange activity, but at lower concentrations (<100 μM) both GSH and Sx_C^- activity increased (Bannai 1984). In this same study, and consistent with a negative feedback mechanism of regulation, it was also found that L-cystine deprivation led to a similar increase in Sx_C^- activity (a phenomenon now known to be mediated by the transcription factor ATF4 and the amino acid response element (AARE) (Lewerenz and Maher 2009; Sato et al. 2004)). Soon thereafter, fibroblasts were shown to respond to increased oxygen tension by upregulating Sx_C^-, likely in a manner distinct from DEM (Bannai et al. 1989). Then, in 1995, Sato et al demonstrated that lipopolysaccharide (LPS), like DEM, was capable of increasing both the activity of the transporter and GSH levels in peritoneal

macrophages (Sato et al. 1995). Interestingly these same changes in system x_C^- were not observed when fibroblasts were treated with LPS. This and the fact that the effect of LPS and DEM were additive suggested not only cell-type specific regulation but also another possible means by which system x_C^- may respond to environmental factors.

Two of the most common transcription factors known to respond to the cellular redox status are nuclear factor-kB (NF-κB) and activator protein-1 (AP1). NF-κB and AP-1 have been implicated in the inducible expression of a wide range of genes involved in oxidative stress and NF-κB is known to be activated by a wide spectrum of agents (eg. bacteria, oxidants, pathogens, viruses, UV radiation, phorbol esters, TNF-alpha, and others) (see Sen and Packer 1996 for review). GSH depletion has been shown to inactivate (Wu and Cederbaum 2004) whereas L-Glu (500 μM) is known to activate (Caccamo et al. 2005) NF-κB and DNA binding. Interestingly, LPS, a toxic product of bacterial infection, does not activate AP-1 nor NF-κB (Sato 1995, Sato 2001), a finding that at the time hinted at the presence of other transcription factors responsible for the control of Sx_C^- expression.

ARE/EpRE – the results of studies with electrophiles

In the late 1980's and early 1990's research began to link the ability of electrophilic compounds (oxidizable phenols, quinines, Michael reaction acceptors, isothiocyanates, peroxides, vicinal dimercaptans, divalent mercury derivatives, and

trivalent arsenicals) to induce phase II enzymes such as glutathione-S-transferases (GSTs), NAD(P)H: quinone oxidoreductase (NQO1), epoxide hydrolase, and UDP glucuronosyltransferases (Prochaska et al. 1985; Spencer et al. 1991; Talalay 1989; Talalay et al. 1988). These enzymes reportedly detoxify electrophiles through various mechanisms, including increasing GSH synthesis and conjugation, which protects against the toxic and neoplastic effect of carcinogens. The protective effects of these compounds is demonstrated by the isothiocyanate sulphoraphane (a potent NQO1 inducer found in broccoli). Sulphoraphane or broccoli sprout extracts reduced the incidence, multiplicity, tumor progression, and weight of mammary tumors in rats (Fahey et al. 1997; Zhang et al. 1994). Around the same time, upstream enhancer elements of mouse and rat liver GST genes that respond to these electrophilic inducers were identified as nearly identical 41-bp segments termed the EpRE (electrophile response element and the antioxidant-response element (ARE) respectively (Prestera et al. 1993; Prestera and Talalay 1995). These sites were shown to be distinct from AP-1 binding sites and tert-butylhydroquinone (tBHQ) was identified as one of a number of electrophiles shown to activate the EpRE (Prestera and Talalay 1995).

Nrf2- identified as link to electrophilic activation

Other groups were beginning to suspect proteins other than AP-1 were mediating transcription of genes in response to stress. It appears that while AP-1 and AP-1-like sites exist in ARE/EpREs, AP-1 proteins do not induce the genes under the

ARE/EpRE control in all cases (Alam et al. 1999; Venugopal and Jaiswal 1996). The nuclear erythroid specific transcription factor 2 (NE-F2) related factors 1-3 (Nrf1-3) were first suspected as potential mediator of ARE/EpRE activation as a result of both the similar tissue expression as genes regulated by ARE/EpRE, and for exhibiting similar binding site sequences consistent with ARE/EpRE (Chan et al. 1993; Moi et al. 1994). Additionally, mutation studies of AP-1-like enhancer regions of other phase II genes revealed that the sequences responsible for activation were in fact NF-E2 binding sites (Inamdar et al. 1996). The NF-E2 protein is a dimer consisting of Maf and other proteins. Maf, Nrf1, Nrf2, Nrf3 are basic leucine zipper (bZIP) proteins that contain a Cap'nCollar (CNC) domain and are collectively referred to as CNC-bZIP proteins.

One of the first lines of evidence for the involvement of Nrf proteins came when the ARE contained within the NQO1 gene was studied (this region contains one perfect and one imperfect AP1 element) (Venugopal and Jaiswal 1996). A gene expression reporter assay was performed in which Hep-G2 cells were co-transfected with a reporter plasmid containing the ARE of the NQO1 gene and either AP-1 proteins (c-Fos and Fra1,c-Jun, Jun-B, and Jun-D) or Nrf1 and Nrf2. They found that plasmids expressing c-Fos and Fra1 had a repressive effect on transcription and observed no effect with the Jun proteins. Interestingly, over-expression of Nrf1 and Nrf2 significantly increased gene expression and these cells responded similarly to b-naphthoflavone and tBHQ.

Similar experiments were performed to test the ability of AP-1, Maf, and CNC-bZIP families of transcription factors on the activation of the HO-1 gene. RAW264.7 and L929 cells (mouse macrophage and fibroblast lines) were transfected with a reporter plasmid containing the HO gene enhancer along with plasmids for AP-1 proteins (c-Jun and c-Fos), Maf, and CNC-bZIP proteins. The Nrf2-expressing plasmid induced the reporter by 25-30 fold (trans-activation) (Alam et al. 1999). This effect was mimicked by heme, t-BHQ, cadmium, arsenite, and zinc and attenuated by overexpression of an Nrf2 mutant. Lending more support for the role of Nrf2 in Phase II gene regulation, Nrf2 knockout mice were shown to lack inducible expression of these defensive genes (Itoh et al. 1997).These results represent the early evidence that Nrf2 acts as a primary transcription factor for the induction ARE/EpRE controlled genes, and that in some instances, AP-1 plays a repressive role in the regulation of these genes.

Nrf2 is a member of the basic leucine zipper family of transcription factors. Nrf2 has homology with chicken ECH (Erythroid derived CNC homology protein). The conserved regions are referred to as Neh1 through Neh6 (Nrf2-ECH homology) (Itoh et al. 1999). The N-terminus contains a transactivation domain (Neh2) that is responsible for binding Kelch-like ECH associating protein 1 (Keap1). The C-terminus contains a basic leucine zipper structure responsible for dimerization with small Maf proteins and for DNA-binding. Nrf2 resides in cytoplasm, associated with the chaperone Keap1. Keap1 is in turn associated with the cytoskeleton, and is thought to negatively regulate Nrf2 mediated gene activation by retaining Nrf2 in the cytoplasm and targeting it for ubiquination and degradation. As Keap1 is known

to contain 25 cysteine residues and given the reactivity of electrophiles and other Nrf2-activators with thiols, Keap1 is thought to act through a thiol sensing mechanism to initiate gene transcription by Nrf2. Cysteine mutation studies and experiments with Keap1 knock-outs support this hypothesis (Wakabayashi et al. 2004).

After exposure of cells to electrophiles or oxidative stress-generating agents, the Keap1 cytoplasmic retention mechanism is inactivated, and Nrf2 is transported to the nucleus. Once within the nucleus, Nrf2 activates the transcription of target genes by binding in heterodimeric forms with other transcription factors (Maf proteins, ATF4, Jun) to distinct DNA elements, including the EpRE enhancer regions of phase II genes (He et al. 2001; for review see Itoh et al. 2004). Accumulating evidence has shown Nrf2 mediated transcription to be protective from electrophilic drug-induced damage (Copple et al. 2008a; Copple et al. 2008b; Enomoto et al. 2001) and in carcinogenesis (Dinkova-Kostova 2002; Dinkova-Kostova et al. 2001; Fahey et al. 1997; Ramos-Gomez et al. 2001)

Sx_C^- is regulated through Nrf2 activation of the EpRE

The discovery of the Nrf2 protein helped explain previous results involving electrophilic induction (i.e. observation with DEM) of protective genes, including Sx_C^-. By using peritoneal macrophages from Nrf2-deficient mice, Ishii et al demonstrated that the Nrf2 protein mediated the inducible expression and activity

of Sx_C^- and other protective genes (e.g. HO-1, peroxiredoxin) by electrophiles and other agents (DEM, tBHQ, paraquat, cadmium, arsenic) (Ishii et al. 2000).

To further investigate the mechanism of transcriptional regulation of Sx_C^- by electrophiles, 5' deletion mutants of the EpRE-like sequences of xCT gene were cloned into a luciferase reporter and transfected into BHK21 cells (Sasaki et al. 2002). Separate sequences were found to control the basal and inducible expression of xCT mRNA and induction by electrophiles (arsenic, cadmium, hydroquinone, DEM) was mediated by Nrf2 (Sasaki et al. 2002). Similar to earlier findings, GSH levels increased with DEM treatment along with Sx_C^- (Sasaki et al. 2002). Unlike what has been shown in macrophages (Sato et al. 1995), PMA and LPS had no effect on Sx_C^- activity in these cells.

The EpRE driven gene expression has been found in macrophages, hepatocytes, BHK21 cells, fibroblasts, and the brain. By using a reporter gene and co-labeling Murphy et al demonstrated in both slice cultures and mixed cell cultures that glia (but not neurons) exhibit EpRE mediated gene expression (Murphy et al. 2001). Since EpRE-mediated gene expression is restricted to glial cells, they many represent a protective cell type in situations characterized by ROS and stress and respond by inducing EpRE-containing genes, including Sx_C^-.

Activation of the genes under control of EpRE, including Sx_C^-, is neuroprotective

In vitro and *in vivo* work has shown that the upregulation of Sx_C^- and other genes by Nrf2, specifically those involved in GSH synthesis and release, results in considerable protection of neurons from oxidative stress and glutamate toxicity (Kraft et al. 2004; Lee et al. 2003a; Lee et al. 2003b; Shih et al. 2005; Shih et al. 2003). Using microarray, mixed glia/neuronal cultures infected with Nrf2 adenovirus are shown to upregulate NQO1, GST, HO-1, MT, xCT, GCS, GSH synthetase, GGT, GSH reductase, and MRP1, confirming the ability of Nrf2 to control the coordinated expression of many important antioxidant and detoxification genes. Nrf2-infected cells have increased Sx_C^- activity and GSH content. To test if Nrf2-induced gene expression mediates protection of neurons from glutamate toxicity, mixed cultures were exposed to neurotoxic levels of L-glutamate (3mM) and grown either with or without Nrf2-infected glia. When glia, either infected with Nrf2 or exposed to the prototypical Nrf2 activator t-BHQ, were grown on top of mixed cultures, they were able to protect the neurons from glutamate toxicity. This protection was potent (only requiring a 1 to 100 ratio of glia to neurons) and shown to result from increased GSH synthesis and release by glia (Shih et al. 2003). Similar protection of neurons by Nrf2 expression has also been demonstrated in vivo (Shih et al. 2005). To further ascertain the role of xCT in this protection, Shih et al. examined the ability of cultured astrocytes, normally expressing nearly undetectable levels of Sx_C^-, astrocytes expressing a mutant non-functional xCT (sut/sut mouse), and astrocytes infected with xCT, to protect neurons from

oxidative glutamate toxicity. Only xCT infected astrocytes were protective (Shih et al. 2006). Implicit in the neuronal protection is the ability of Sx_C^- to control glial GSH levels, made available for release, and further metabolism and utilization by neurons. The regulation of Sx_C^-, by Nrf2 or other means, therefore represents an important thiol-mediated strategy of protection from the potentially neurotoxic episodes initiated by electrophiles, reactive oxidative species, and excitotoxicity.

Unresolved questions remain, LPS as example

The inseparable link between cystine entry via system x_C^- and GSH synthesis capacity presents the potential for a negative feedback loop for GSH levels to regulate Sx_C^- activity, potentially via Nrf2. However, this level of regulatory control appears to differ among cell types suggesting that not all cases of GSH-depletion lead to Nrf2 mediated gene activation. For example while arsenic, DEM, cadmium, and hydroquinone all induced Sx_C^- activity and xCT mRNA in an EpRE-driven luciferase reporter in BHK21 embryonic fibroblasts, treatment with either BSO or LPS did not (Sasaki et al. 2002). GSH-depletion by BSO also did not induce Nrf2 in a mammary cell line (Wang et al. 2006). Conversely, GSH-depletion did lead to increased levels of Nrf2 and xCT in C1 cells (simian virus 40 large T-antigen immortalized line) (Qiang et al. 2004). Interestingly, GSH levels in glia of Nrf2 -/- animals is not different than that from wildtypes (Shih et al. 2005), suggesting other mechanisms in control of GSH homeostasis in these animals. Just as the effect of GSH-depletion on Nrf2 appear to be cell-type specific, so is the effect of BSO on Sx_C^-.

For example, GSH-depletion has been reported to have no effect on L-Cys_2 transport in BHK21 fibroblasts (Sasaki et al. 2002) and rat kidney fibroblasts (Kang and Enger 1992), an inductive-effect in astrocytes (no dbcAMP) (Allen et al. 2001), C1 cells (Qiang et al. 2004) and whole-brain homegenates (Limon-Pacheco et al. 2007), and a down-regulatory effect in astrocytes (treated with dbcAMP) (Bender et al. 2000) and HAIN-6 lung fibroblasts (Bannai 1984).

While evidence for universal Nrf2-mediated control over Sx_C^- is lacking, there lies the possibility that the EpRE driven gene regulation mediated by Nrf2 is a system of control that overlaps with the function of other transcription factors. In a model of systemic GSH-depletion in mice it was found that the upregulation of Sx_C^- was linked to p38MAPK and ERK2 signaling cascades (Limon-Pacheco et al. 2007), potentially leading to the activation/synthesis of any number of additional transcription factors linked to either the Nrf2-associated activation of Sx_C^- or an as yet unspecified Nrf2-independent pathway of gene activation. Thus, there may be other points along the pathway to EpRE stimulation on which BSO could be having its effect apart from the release of cytoplasmic sequestered Nrf2. This type of regulatory control is observed in the cases of arsenic (sodium arsenite) exposure in hepa1c1c7 cells (He et al. 2006). In this study, arsenic, but not tBHQ treatment, was associated with the disruption of Nrf2-keap1-Cu3 complexes and dimerization of Nrf2 and Maf proteins in the nucleus, resulting in increased EpRE-dependent transcription of the NQO1 gene.

Additionally, there is now evidence that the up-regulation of Sx_C^- through L-Cys_2 deprivation and potentially other inducers, assumed to be mediated by the amino acid response element (AARE), is mediated not by Nrf2 but by the transcription factor ATF4 (aka Creb2)(Lewerenz and Maher 2009; Ogawa et al. 2008; Sato et al. 2004), specifically in response to L-Cys_2 deprivation (Sato et al. 2004). Interestingly, the induction of xCT by the reactive tocopherol metabolite γ-tocopheryl quinone has been shown to be attenuated by siRNA for ATF4 but not Nrf2 in PC-12 cells (Ogawa et al. 2008). This suggests that ATF4 can mediate the transcriptional control of xCT via the AARE in ways potentially distinct from amino acid deprivation or through a means independent of the AARE.

It is reasonable that the whole of Sx_C^- regulation cannot be explained by the activation of the ARE/EpRE by Nrf2. Most notably, studies with LPS suggest that other regulatory mechanisms exist. Like tBHQ, DEM, arsenic and other electrophilic agents, LPS is capable of inducing Sx_C^- in macrophages (Sato et al. 1995). However, this same induction is also observed in macrophages from mice deficient in Nrf2 (Ishii et al. 2000). In addition to Nrf2, The increase in Sx_C^- activity and intracellular levels of GSH in macrophages following LPS treatment has also been shown to be independent of AP1 and NFκB and dependent on oxygen (Sato et al. 1995). This effect of LPS is also cell-type specific, as the induction ability on Sx_C^- is not observed in fibroblasts (Sato et al. 1995) or BHK21 cells (Sasaki et al. 2002). Interestingly, there is a lack of data examining LPS treatment on Sx_C^- in the CNS, and some of it sounds contradictory. For instance, indirect evidence suggests that LPS in the CNS may involve the downregulaton of Sx_C^-. While some evidence suggests a lack of

effect of LPS on GSH levels in glia (McNaught and Jenner 2000), LPS exposure in other *in vitro* (mesencephalic cultures) and *in vivo* (subranigral injection) studies results in a loss of GSH, which suggests a down-regulatory effect by LPS on Sx_C^- function (Bharath et al. 2002; Kramer et al. 2002; Zhu et al. 2007).

Concluding Remarks

In summary, electrophile exposure and oxidative stress elicits an adaptive response aimed at maintaining redox homeostasis and reducing cellular damage. This response involves the activation of genes encoding detoxification and antioxidant proteins (e.g. γGCS,GST, NQO1, HO-1). Gene activation is mediated in part by a cis-acting element referred to as the ARE or EpRE located in the regulatory region within target genes. Nrf2 is now considered to be the major transcription factor responsible for regulating EpRE-mediated gene expression. Nrf2 is one transcription factor known to control the expression and activity of Sx_C^-, the proper functioning of which is neuroprotective. The intermediate events that tie GSH-depletion, electrophile exposure, and LPS treatments to Sx_C^- remain unclear, do not universally involve Nrf2, and deserve further study. As the effectiveness of these induction strategies appear to be dependent on cell type, studies that incorporate animal and cell-type considerations into the experimental design are likely to yield important new information for the field.

References

Aandahl EM, Moretto WJ, Haslett PA, Vang T, Bryn T, Tasken K, Nixon DF. 2002. Inhibition of antigen-specific T cell proliferation and cytokine production by protein kinase A type I. J Immunol 169(2):802-8.

Ahn SG, Thiele DJ. 2003. Redox regulation of mammalian heat shock factor 1 is essential for Hsp gene activation and protection from stress. Genes Dev 17(4):516-28.

Aizenman E, Lipton SA, Loring RH. 1989. Selective modulation of NMDA responses by reduction and oxidation. Neuron 2(3):1257-63.

Alam J, Stewart D, Touchard C, Boinapally S, Choi AM, Cook JL. 1999. Nrf2, a Cap'n'Collar transcription factor, regulates induction of the heme oxygenase-1 gene. J Biol Chem 274(37):26071-8.

Allen JW, Shanker G, Aschner M. 2001. Methylmercury inhibits the in vitro uptake of the glutathione precursor, cystine, in astrocytes, but not in neurons. Brain Res 894(1):131-40.

Anderson ME. 1985. Determination of glutathione and glutathione disulfide in biological samples. Methods in Enzymology 113:548-564.

Baker DA, McFarland K, Lake RW, Shen H, Tang XC, Toda S, Kalivas PW. 2003. Neuroadaptations in cystine-glutamate exchange underlie cocaine relapse. Nat Neurosci 6(7):743-9.

Baker DA, Shen H, Kalivas PW. 2002a. Cystine/glutamate exchange serves as the source for extracellular glutamate: modifications by repeated cocaine administration. Amino Acids 23(1-3):161-2.

Baker DA, Xi ZX, Shen H, Swanson CJ, Kalivas PW. 2002b. The origin and neuronal function of in vivo nonsynaptic glutamate. J Neurosci 22(20):9134-41.

Balazs R, Bridges R, Cotman C, Cotman C. 2006. Excitatory Amino Acid Transmission in Health and Disease. New York: Oxford University Press.

Bannai S. 1984. Transport of cystine and cysteine in mammalian cells. Biochim Biophys Acta 779(3):289-306.

Bannai S. 1986a. Exchange of cystine and glutamate across plasma membrane of human fibroblasts. J Biol Chem 261(5):2256-63.

Bannai S. 1986b. Exchange of Cystine and Glutamate across Plasma Membrane of Human Fibroblasts. The Journal of Biological Chemistry 261(5):2256-2263.

Bannai S, Kitamura E. 1980. Transport interaction of L-cystine and L-glutamate in human diploid fibroblasts in culture. J Biol Chem 255(6):2372-6.

Bannai S, Kitamura E. 1981. Role of proton dissociation in the transport of cystine and glutamate in human diploid fibroblasts in culture. J Biol Chem 256(11):5770-2.

Bannai S, Sato H, Ishii T, Sugita Y. 1989. Induction of cystine transport activity in human fibroblasts by oxygen. J Biol Chem 264(31):18480-4.

Barger SW, Basile AS. 2001. Activation of microglia by secreted amyloid precursor protein evokes release of glutamate by cystine exchange and attenuates synaptic function. J Neurochem 76(3):846-54.

Bassi MT, Gasol E, Manzoni M, Pineda M, Riboni M, Martin R, Zorzano A, Borsani G, Palacin M. 2001. Identification and characterisation of human xCT that co-expresses, with 4F2 heavy chain, the amino acid transport activity system xc. Pflugers Arch 442(2):286-96.

Bedingfield JS, Kemp MC, Jane DE, Tse HW, Roberts PJ, Watkins JC. 1995. Structure-activity relationships for a series of phenylglycine derivatives acting at metabotropic glutamate receptors (mGluRs). Br J Pharmacol 116(8):3323-9.

Ben-Yoseph O, Boxer PA, Ross BD. 1996. Assessment of the role of the glutathione and pentose phosphate pathways in the protection of primary cerebrocortical cultures from oxidative stress. J Neurochem 66(6):2329-37.

Bender AS, Reichelt W, Norenberg MD. 2000. Characterization of cystine uptake in cultured astrocytes. Neurochem Int 37(2-3):269-76.

Berk M, Ng F, Dean O, Dodd S, Bush AI. 2008. Glutathione: a novel treatment target in psychiatry. Trends Pharmacol Sci 29(7):346-51.

Bharath S, Hsu M, Kaur D, Rajagopalan S, Andersen JK. 2002. Glutathione, iron and Parkinson's disease. Biochem Pharmacol 64(5-6):1037-48.

Boyland E, Chasseaud LF. 1970. The effect of some carbonyl compounds on rat liver glutathione levels. Biochem Pharmacol 19(4):1526-8.

Bridges CC, Zalups RK. 2005. Cystine and glutamate transport in renal epithelial cells transfected with human system x(-) (c). Kidney Int 68(2):653-64.

Bridges RJ, Patel SA. 2009. Pharmacology of Glutamate Transport in the CNS: Substrates and Inhibitors of Excitatory Amino Acid Transporters (EAATs) and the Glutamate/Cystine Exchanger System xc-. In: Napier S, Bingham M, editors. Topics in Medicinal Chemistry: Transporters as Targets for Drugs. NY, NY: Springer. p 187-222.

Brodie AE, Potter J, Reed DJ. 1982. Unique characteristics of rat spleen lymphocyte, L1210 lymphoma and HeLa cells in glutathione biosynthesis from sulfur-containing amino acids. Eur J Biochem 123(1):159-64.

Caccamo D, Campisi A, Marini H, Adamo EB, Li Volti G, Squadrito F, Ientile R. 2005. Glutamate promotes NF-kappaB pathway in primary astrocytes: protective effects of IRFI 016, a synthetic vitamin E analogue. Exp Neurol 193(2):377-83.

Carlsson A, Waters N, Holm-Waters S, Tedroff J, Nilsson M, Carlsson ML. 2001. Interactions between monoamines, glutamate, and GABA in schizophrenia: new evidence. Annu Rev Pharmacol Toxicol 41:237-60.

Carlsson M, Carlsson A. 1989. Dramatic synergism between MK-801 and clonidine with respect to locomotor stimulatory effect in monoamine-depleted mice. J Neural Transm 77(1):65-71.

Chan JY, Han XL, Kan YW. 1993. Isolation of cDNA encoding the human NF-E2 protein. Proc Natl Acad Sci U S A 90(23):11366-70.

Chen L, Ding Y, Cagniard B, Van Laar AD, Mortimer A, Chi W, Hastings TG, Kang UJ, Zhuang X. 2008. Unregulated cytosolic dopamine causes neurodegeneration associated with oxidative stress in mice. J Neurosci 28(2):425-33.

Chen Y, Vartiainen etal. 2001. Astrocytes protect neurons from nitric oxide toxicity by a glutathione dependent mechanism. J Neurochem 77:1601-1610.

Chinta SJ, Kumar MJ, Hsu M, Rajagopalan S, Kaur D, Rane A, Nicholls DG, Choi J, Andersen JK. 2007. Inducible alterations of glutathione levels in adult dopaminergic midbrain neurons result in nigrostriatal degeneration. J Neurosci 27(51):13997-4006.

Chintala S, Li W, Lamoreux ML, Ito S, Wakamatsu K, Sviderskaya EV, Bennett DC, Park YM, Gahl WA, Huizing M and others. 2005. Slc7a11 gene controls production of pheomelanin pigment and proliferation of cultured cells. Proc Natl Acad Sci U S A 102(31):10964-9.

Cho Y, Bannai S. 1990. Uptake of glutamate and cysteine in C-6 glioma cells and in cultured astrocytes. J Neurochem 55(6):2091-7.

Choi DW. 1990. Cerebral hypoxia: some new approaches and unanswered questions. J Neurosci 10(8):2493-2501.

Choi DW, Rothman SM. 1990. The role of glutamate neurotoxicity in hypoxic-ischemic neuronal death. Annu Rev Neurosci 13:171-182.

Chuang AH, Mukhtar H, Bresnick E. 1978. Effects of diethyl maleate on aryl hydrocarbon hydroxylase and on 3-methyl-cholanthrene-induced skin tumorigenesis in rats and mice. J Natl Cancer Inst 60(2):321-5.

Chung WJ, Lyons SA, Nelson GM, Hamza H, Gladson CL, Gillespie GY, Sontheimer H. 2005. Inhibition of cystine uptake disrupts the growth of primary brain tumors. J Neurosci 25(31):7101-10.

Chung WJ, Sontheimer H. 2009. Sulfasalazine inhibits the growth of primary brain tumors independent of nuclear factor-kappaB. J Neurochem 110(1):182-93.

Copple IM, Goldring CE, Jenkins RE, Chia AJ, Randle LE, Hayes JD, Kitteringham NR, Park BK. 2008a. The hepatotoxic metabolite of acetaminophen directly activates the Keap1-Nrf2 cell defense system. Hepatology 48(4):1292-301.

Copple IM, Goldring CE, Kitteringham NR, Park BK. 2008b. The Nrf2-Keap1 defence pathway: role in protection against drug-induced toxicity. Toxicology 246(1):24-33.

Daginakatte GC, Gadzinski A, Emnett RJ, Stark JL, Gonzales ER, Yan P, Lee JM, Cross AH, Gutmann DH. 2008. Expression profiling identifies a molecular signature of reactive astrocytes stimulated by cyclic AMP or proinflammatory cytokines. Exp Neurol 210(1):261-7.

Danbolt NC. 2001. Glutamate Uptake. Prog in Neurobio 65:1-105.

Daniel PB, Walker WH, Habener JF. 1998. Cyclic AMP signaling and gene regulation. Annu Rev Nutr 18:353-83.

Danilov CA, Chandrasekaran K, Racz J, Soane L, Zielke C, Fiskum G. 2009. Sulforaphane protects astrocytes against oxidative stress and delayed death caused by oxygen and glucose deprivation. Glia 57(6):645-56.

Delaunay A, Pflieger D, Barrault MB, Vinh J, Toledano MB. 2002. A thiol peroxidase is an H2O2 receptor and redox-transducer in gene activation. Cell 111(4):471-81.

Desagher S, Glowinski, J etal. 1996. Astrocytes Protect Neurons from Hydrogen Peroxide Toxicity. J Neurosci 16(8):2553-2562.

Deves R, Boyd CA. 2000. Surface antigen CD98(4F2): not a single membrane protein, but a family of proteins with multiple functions. J Membr Biol 173(3):165-77.

Dinkova-Kostova AT. 2002. Protection against cancer by plant phenylpropenoids: induction of mammalian anticarcinogenic enzymes. Mini Rev Med Chem 2(6):595-610.

Dinkova-Kostova AT, Massiah MA, Bozak RE, Hicks RJ, Talalay P. 2001. Potency of Michael reaction acceptors as inducers of enzymes that protect against carcinogenesis depends on their reactivity with sulfhydryl groups. Proc Natl Acad Sci U S A 98(6):3404-9.

Do KQ, Trabesinger AH, Kirsten-Kruger M, Lauer CJ, Dydak U, Hell D, Holsboer F, Boesiger P, Cuenod M. 2000. Schizophrenia: glutathione deficit in cerebrospinal fluid and prefrontal cortex in vivo. Eur J Neurosci 12(10):3721-8.

Dringen R, Gutterer JM, Gros C, Hirrlinger J. 2001. Aminopeptidase N mediates the utilization of the GSH precursor CysGly by cultured neurons. J Neurosci Res 66(5):1003-8.

Dringen R, Gutterer JM, Hirrlinger J. 2000. Glutathione metabolism in brain. European Journal of Biochemistry 267:4912-4916.

Dringen R, Pfeiffer B, Hamprecht B. 1999. Synthesis of the antioxidant glutathione in neurons: supply by astrocytes of CysGly as precursor for neuronal glutathione. J Neurosci 19(2):562-9.

Drukarch B, Schepens E, Jongenelen CAM, Stoof JC, Langeveld CH. 1997. Astrocyte-mediated enhancement fo neuronal survival is abolished by glutathione deficiency. Brain Research 770:123-130.

Early JL, Schnell RC. 1982. Effect of glutathione depletion on selenium lethality and hepatic drug metabolism in male rats. Toxicol Lett 11(3-4):253-7.

Ebert B, Madsen U, Johansen TN, Krogsgaard-Larsen P. 1991. NMDA receptor agonists: relationships between structure and biological activity. Adv Exp Med Biol 287:483-7.

Enomoto A, Itoh K, Nagayoshi E, Haruta J, Kimura T, O'Connor T, Harada T, Yamamoto M. 2001. High sensitivity of Nrf2 knockout mice to acetaminophen hepatotoxicity associated with decreased expression of ARE-regulated drug metabolizing enzymes and antioxidant genes. Toxicol Sci 59(1):169-77.

Escartin C, Bonvento G. 2008. Targeted activation of astrocytes: a potential neuroprotective strategy. Mol Neurobiol 38(3):231-41.

Fahey JW, Zhang Y, Talalay P. 1997. Broccoli sprouts: an exceptionally rich source of inducers of enzymes that protect against chemical carcinogens. Proc Natl Acad Sci U S A 94(19):10367-72.

Figiel M, Engele J. 2000. Pituitary adenylate cyclase-activating polypeptide (PACAP), a neuron-derived peptide regulating glial glutamate transport and metabolism. J Neurosci 20(10):3596-605.

Gasol E, Jimenez-Vidal M, Chillaron J, Zorzano A, Palacin M. 2004. Membrane topology of system xc- light subunit reveals a re-entrant loop with substrate-restricted accessibility. J Biol Chem 279(30):31228-36.

Gegg ME, Clark JB, Heales SJ. 2005. Co-culture of neurones with glutathione deficient astrocytes leads to increased neuronal susceptibility to nitric oxide and increased glutamate-cysteine ligase activity. Brain Res 1036(1-2):1-6.

Gochenauer GE, Robinson MB. 2001. Dibutyryl-cAMP (dbcAMP) up-regulates astrocytic chloride-dependent L- [3H]glutamate transport and expression of both system xc(-) subunits. J Neurochem 78(2):276-86.

Griffith OW. 1982. Mechanism of action, metabolism, and toxicity of buthionine sulfoximine and its higher homologs, potent inhibitors of glutathione synthesis. J Biol Chem 257(22):13704-12.

Grima G, Benz B, Parpura V, Cuenod M, Do KQ. 2003. Dopamine-induced oxidative stress in neurons with glutathione deficit: implication for schizophrenia. Schizophr Res 62(3):213-24.

Guebel DV, Torres NV. 2004. Dynamics of sulfur amino acids in mammalian brain: assessment of the astrocytic-neuronal cysteine interaction by a mathematical hybrid model. Biochim Biophys Acta 1674(1):12-28.

Halliwell B. 1992. Reactive Oxygten Species and the Central nervous system. J Neurochem 59:1609-1623.

Haslett C, Savill JS, Meagher L. 1989. The neutrophil. Curr Opin Immunol 2(1):10-8.

Hayes JD, Flanagan JU, Jowsey IR. 2005. Glutathione transferases. Annu Rev Pharmacol Toxicol 45:51-88.

He CH, Gong P, Hu B, Stewart D, Choi ME, Choi AM, Alam J. 2001. Identification of activating transcription factor 4 (ATF4) as an Nrf2-interacting protein. Implication for heme oxygenase-1 gene regulation. J Biol Chem 276(24):20858-65.

He X, Chen MG, Lin GX, Ma Q. 2006. Arsenic induces NAD(P)H-quinone oxidoreductase I by disrupting the Nrf2 x Keap1 x Cul3 complex and recruiting Nrf2 x Maf to the antioxidant response element enhancer. J Biol Chem 281(33):23620-31.

Hertz L, Peng L, Lai JC. 1998. Functional studies in cultured astrocytes. Methods 16(3):293-310.

Hirrlinger J, Schulz JB, Dringen R. 2002. Effects of dopamine on the glutathione metabolism of cultured astroglial cells: implications for Parkinson's disease. J Neurochem 82(3):458-67.

Hosli E, Otten U, Hosli L. 1997. Expression of GABA(A) receptors by reactive astrocytes in explant and primary cultures of rat CNS. Int J Dev Neurosci 15(8):949-60.

Hosoya K, Tomi M, Ohtsuki S, Takanaga H, Saeki S, Kanai Y, Endou H, Naito M, Tsuruo T, Terasaki T. 2002. Enhancement of L-cystine transport activity and its relation to xCT gene induction at the blood-brain barrier by diethyl maleate treatment. J Pharmacol Exp Ther 302(1):225-31.

Howes OD, Egerton A, Allan V, McGuire P, Stokes P, Kapur S. 2009. Mechanisms underlying psychosis and antipsychotic treatment response in schizophrenia: insights from PET and SPECT imaging. Curr Pharm Des 15(22):2550-9.

Howes OD, Kapur S. 2009. The dopamine hypothesis of schizophrenia: version III--the final common pathway. Schizophr Bull 35(3):549-62.

Inamdar NM, Ahn YI, Alam J. 1996. The heme-responsive element of the mouse heme oxygenase-1 gene is an extended AP-1 binding site that resembles the recognition sequences for MAF and NF-E2 transcription factors. Biochem Biophys Res Commun 221(3):570-6.

Ishii T, Itoh K, Takahashi S, Sato H, Yanagawa T, Katoh Y, Bannai S, Yamamoto M. 2000. Transcription factor Nrf2 coordinately regulates a group of oxidative stress-inducible genes in macrophages. J Biol Chem 275(21):16023-9.

Itoh K, Chiba T, Takahashi S, Ishii T, Igarashi K, Katoh Y, Oyake T, Hayashi N, Satoh K, Hatayama I and others. 1997. An Nrf2/small Maf heterodimer mediates the induction of phase II detoxifying enzyme genes through antioxidant response elements. Biochem Biophys Res Commun 236(2):313-22.

Itoh K, Ishii T, Wakabayashi N, Yamamoto M. 1999. Regulatory mechanisms of cellular response to oxidative stress. Free Radic Res 31(4):319-24.

Itoh K, Tong KI, Yamamoto M. 2004. Molecular mechanism activating Nrf2-Keap1 pathway in regulation of adaptive response to electrophiles. Free Radic Biol Med 36(10):1208-13.

Janaky R, Varga V, Saransaari P, Oja SS. 1993. Glutathione modulates the N-methyl-D-aspartate receptor-activated calcium influx into cultured rat cerebellar granule cells. Neurosci Lett 156(1-2):153-7.

Jimenez-Vidal M, Gasol E, Zorzano A, Nunes V, Palacin M, Chillaron J. 2004. Thiol modification of cysteine 327 in the eighth transmembrane domain of the light subunit xCT of the heteromeric cystine/glutamate antiporter suggests close proximity to the substrate binding site/permeation pathway. J Biol Chem 279(12):11214-21.

Juurlink BH, Hertz L. 1985. Plasticity of astrocytes in primary cultures: an experimental tool and a reason for methodological caution. Dev Neurosci 7(5-6):263-77.

Juurlink BHJ, Patterson PG. 1998. Review of oxidative stress in brain and spinal cord injury: suggestions for pharmacological and nutritional management strategies. Journal of Spinal Cord Medicine 21(4):309-334.

Kang YJ, Enger MD. 1992. Buthionine sulfoximine-induced cytostasis does not correlate with glutathione depletion. Am J Physiol 262(1 Pt 1):C122-7.

Karry R, Klein E, Ben Shachar D. 2004. Mitochondrial complex I subunits expression is altered in schizophrenia: a postmortem study. Biol Psychiatry 55(7):676-84.

Kato S, Ishita S, Sugawara K, Mawatari K. 1993. Cystine/glutamate antiporter expression in retinal Muller glial cells: implications for DL-alpha-aminoadipate toxicity. Neuroscience 57(2):473-82.

Kegeles LS, Abi-Dargham A, Zea-Ponce Y, Rodenhiser-Hill J, Mann JJ, Van Heertum RL, Cooper TB, Carlsson A, Laruelle M. 2000. Modulation of amphetamine-induced striatal dopamine release by ketamine in humans: implications for schizophrenia. Biol Psychiatry 48(7):627-40.

Kim JY, Kanai Y, Chairoungdua A, Cha SH, Matsuo H, Kim DK, Inatomi J, Sawa H, Ida Y, Endou H. 2001. Human cystine/glutamate transporter: cDNA cloning and upregulation by oxidative stress in glioma cells. Biochim Biophys Acta 1512(2):335-44.

Koch HP, Kavanaugh MP, Esslinger CS, Zerangue N, Humphrey JM, Amara SG, Chamberlin AR, Bridges RJ. 1999. Differentiation of substrate and nonsubstrate inhibitors of the high-affinity, sodium-dependent glutamate transporters. Mol Pharmacol 56(6):1095-104.

Kraft AD, Johnson DA, Johnson JA. 2004. Nuclear factor E2-related factor 2-dependent antioxidant response element activation by tert-butylhydroquinone and sulforaphane occurring preferentially in astrocytes conditions neurons against oxidative insult. J Neurosci 24(5):1101-12.

Kramer BC, Yabut JA, Cheong J, JnoBaptiste R, Robakis T, Olanow CW, Mytilineou C. 2002. Lipopolysaccharide prevents cell death caused by glutathione depletion: possible mechanisms of protection. Neuroscience 114(2):361-72.

Kranich O, Dringen R, Sandberg M, Hamprecht B. 1998. Utilization of cysteine and cysteine precursors for the synthesis of glutathione in astroglial cultures: preference for cystine. Glia 22(1):11-8.

Lastro M, Kourtidis A, Farley K, Conklin DS. 2008. xCT expression reduces the early cell cycle requirement for calcium signaling. Cell Signal 20(2):390-9.

Le Prince G, Fages C, Rolland B, Nunez J, Tardy M. 1991. DBcAMP effect on the expression of GFAP and of its encoding mRNA in astroglial primary cultures. Glia 4(3):322-6.

Lee JM, Calkins MJ, Chan K, Kan YW, Johnson JA. 2003a. Identification of the NF-E2-related factor-2-dependent genes conferring protection against oxidative stress in primary cortical astrocytes using oligonucleotide microarray analysis. J Biol Chem 278(14):12029-38.

Lee JM, Shih AY, Murphy TH, Johnson JA. 2003b. NF-E2-related factor-2 mediates neuroprotection against mitochondrial complex I inhibitors and increased concentrations of intracellular calcium in primary cortical neurons. J Biol Chem 278(39):37948-56.

Lewerenz J, Maher P. 2009. Basal levels of eIF2alpha phosphorylation determine cellular antioxidant status by regulating ATF4 and xCT expression. J Biol Chem 284(2):1106-15.

Lim J, Lam YC, Kistler J, Donaldson PJ. 2005. Molecular characterization of the cystine/glutamate exchanger and the excitatory amino acid transporters in the rat lens. Invest Ophthalmol Vis Sci 46(8):2869-77.

Limon-Pacheco JH, Hernandez NA, Fanjul-Moles ML, Gonsebatt ME. 2007. Glutathione depletion activates mitogen-activated protein kinase (MAPK) pathways that display organ-specific responses and brain protection in mice. Free Radic Biol Med 43(9):1335-47.

Lo M, Wang YZ, Gout PW. 2008. The x(c)- cystine/glutamate antiporter: a potential target for therapy of cancer and other diseases. J Cell Physiol 215(3):593-602.

Lyons SA, Chung WJ, Weaver AK, Ogunrinu T, Sontheimer H. 2007. Autocrine glutamate signaling promotes glioma cell invasion. Cancer Res 67(19):9463-71.

Matyszak MK. 1998. Inflammation in the CNS: balance between immunological privilege and immune responses. Prog Neurobiol 56(1):19-35.

McCarthy KD, de Vellis J. 1980. Preparation of separate astroglial and oligodendroglial cell cultures from rat cerebral tissue. Journal of Cell Biology 85:890-902.

McNaught KS, Jenner P. 2000. Extracellular accumulation of nitric oxide, hydrogen peroxide, and glutamate in astrocytic cultures following glutathione

depletion, complex I inhibition, and/or lipopolysaccharide-induced activation. Biochem Pharmacol 60(7):979-88.
Meister A. 1991. Glutathione deficiency produced by inhibition of its synthesis, and its reversal; applications in research and therapy. Pharmacol Ther 51(2):155-94.
Meister AM, Anderson ME. 1983. Glutathione. Ann Rev Biochem 52:711.
Miller C, Tsatas O, David S. 1994. Dibutyryl cAMP, interleukin-1 beta, and macrophage conditioned medium enhance the ability of astrocytes to promote neurite growth. J Neurosci Res 38(1):56-63.
Moghaddam B. 2003. Bringing order to the glutamate chaos in schizophrenia. Neuron 40(5):881-4.
Moi P, Chan K, Asunis I, Cao A, Kan YW. 1994. Isolation of NF-E2-related factor 2 (Nrf2), a NF-E2-like basic leucine zipper transcriptional activator that binds to the tandem NF-E2/AP1 repeat of the beta-globin locus control region. Proc Natl Acad Sci U S A 91(21):9926-30.
Moran MM, McFarland K, Melendez RI, Kalivas PW, Seamans JK. 2005. Cystine/glutamate exchange regulates metabotropic glutamate receptor presynaptic inhibition of excitatory transmission and vulnerability to cocaine seeking. J Neurosci 25(27):6389-93.
Murphy TH, Schnaar RL, Coyle JT. 1990. Immature cortical neurons are uniquely sensitive to glutamate toxicity by inhibition of cystine uptake. FASEB 4:1624-1633.
Murphy TH, Yu J, Ng R, Johnson DA, Shen H, Honey CR, Johnson JA. 2001. Preferential expression of antioxidant response element mediated gene expression in astrocytes. J Neurochem 76(6):1670-8.
Mysona B, Dun Y, Duplantier J, Ganapathy V, Smith SB. 2009. Effects of hyperglycemia and oxidative stress on the glutamate transporters GLAST and system xc- in mouse retinal Muller glial cells. Cell Tissue Res 335(3):477-88.
Nagasawa K, Ito S, Kakuda T, Nagai K, Tamai I, Tsuji A, Fujimoto S. 2005. Transport mechanism for aluminum citrate at the blood-brain barrier: kinetic evidence implies involvement of system Xc- in immortalized rat brain endothelial cells. Toxicol Lett 155(2):289-96.
Nakamura E, Sato M, Yang H, Miyagawa F, Harasaki M, Tomita K, Matsuoka S, Noma A, Iwai K, Minato N. 1999. 4F2 (CD98) heavy chain is associated covalently with an amino acid transporter and controls intracellular trafficking and membrane topology of 4F2 heterodimer. J Biol Chem 274(5):3009-16.
Nkabyo YS, Go YM, Ziegler TR, Jones DP. 2005. Extracellular cysteine/cystine redox regulates the p44/p42 MAPK pathway by metalloproteinase-dependent epidermal growth factor receptor signaling. Am J Physiol Gastrointest Liver Physiol 289(1):G70-8.
Ogawa Y, Saito Y, Nishio K, Yoshida Y, Ashida H, Niki E. 2008. Gamma-tocopheryl quinone, not alpha-tocopheryl quinone, induces adaptive response through up-regulation of cellular glutathione and cysteine availability via activation of ATF4. Free Radic Res 42(7):674-87.
Olney JW. 1990. Excitotoxic amino acids and neuropsychiatric disorders. Annu Rev Pharmacol Toxicol 30:47-71.

Orlowski M, Karkowsky A. 1976. Glutathione metabolism and some possible functions of glutathione in the nervous system. International Reviews of Neurobiology 19:75-121.

Pacheco R, Gallart T, Lluis C, Franco R. 2007. Role of glutamate on T-cell mediated immunity. J Neuroimmunol 185(1-2):9-19.

Pacheco R, Oliva H, Martinez-Navio JM, Climent N, Ciruela F, Gatell JM, Gallart T, Mallol J, Lluis C, Franco R. 2006. Glutamate released by dendritic cells as a novel modulator of T cell activation. J Immunol 177(10):6695-704.

Patel SA, Warren BA, Rhoderick JF, Bridges RJ. 2004. Differentiation of substrate and non-substrate inhibitors of transport system xc(-): an obligate exchanger of L-glutamate and L-cystine. Neuropharmacology 46(2):273-84.

Philbert MA, Beiswanger CM, Waters DK, Reuhle KR, Lowndes HE. 1991. Cellular and regional distribution of reduced glutathione in the nervous system of the rat: histochemical localization by mercury orange and o-phthaldialdehyde-induced histofluorescence. Toxicology and Applied Pharmacology 107:215-227.

Piani D, Fontana A. 1994. Involvement of the cystine transport system xc- in the macrophage-induced glutamate-dependent cytotoxicity to neurons. J Immunol 152(7):3578-85.

Piani D, Frei K, Do KQ, Cuenod M, Fontana A. 1991. Murine brain macrophages induced NMDA receptor mediated neurotoxicity in vitro by secreting glutamate. Neurosci Lett 133(2):159-62.

Prestera T, Holtzclaw WD, Zhang Y, Talalay P. 1993. Chemical and molecular regulation of enzymes that detoxify carcinogens. Proc Natl Acad Sci U S A 90(7):2965-9.

Prestera T, Talalay P. 1995. Electrophile and antioxidant regulation of enzymes that detoxify carcinogens. Proc Natl Acad Sci U S A 92(19):8965-9.

Prochaska HJ, De Long MJ, Talalay P. 1985. On the mechanisms of induction of cancer-protective enzymes: a unifying proposal. Proc Natl Acad Sci U S A 82(23):8232-6.

Qiang W, Cahill JM, Liu J, Kuang X, Liu N, Scofield VL, Voorhees JR, Reid AJ, Yan M, Lynn WS and others. 2004. Activation of transcription factor Nrf-2 and its downstream targets in response to moloney murine leukemia virus ts1-induced thiol depletion and oxidative stress in astrocytes. J Virol 78(21):11926-38.

Ramos-Gomez M, Kwak MK, Dolan PM, Itoh K, Yamamoto M, Talalay P, Kensler TW. 2001. Sensitivity to carcinogenesis is increased and chemoprotective efficacy of enzyme inducers is lost in nrf2 transcription factor-deficient mice. Proc Natl Acad Sci U S A 98(6):3410-5.

Raps SP, Lai JC, Hertz L, Cooper AJ. 1989. Glutathione is present in high concentrations in cultured astrocytes but not in cultured neurons. Brain Research 493(2):398-401.

Regan RF, Guo Y. 1999a. Extracellular reduced glutathione increases neuronal vulnerability to combined chemical hypoxia and glucose deprivation. Brain Res 817(1-2):145-50.

Regan RF, Guo YP. 1999b. Potentiation of excitotoxic injury by high concentrations of extracellular reduced glutathione. Neurosci 91(2):463-70.
Rosenberger J, Petrovics G, Buzas B. 2001. Oxidative stress induces proorphanin FQ and proenkephalin gene expression in astrocytes through p38- and ERK-MAP kinases and NF-kappaB. J Neurochem 79(1):35-44.
Ryan GB, Majno G. 1977. Acute inflammation. A review. Am J Pathol 86(1):183-276.
Sagara J, Miura K, Bannai S. 1993a. Cystine uptake and glutathione level in fetal brain cells in primary culture and in suspension. J Neurochem 61(5):1667-71.
Sagara J, Miura K, Bannai S. 1993b. Maintenance of neuronal glutathione by glial cells. J Neurochem 61:1672-1676.
Sasaki H, Sato H, Kuriyama-Matsumura K, Sato K, Maebara K, Wang H, Tamba M, Itoh K, Yamamoto M, Bannai S. 2002. Electrophile response element-mediated induction of the cystine/glutamate exchange transporter gene expression. J Biol Chem 277(47):44765-71.
Sato H, Fujiwara K, Sagara J, Bannai S. 1995. Induction of cystine transport activity in mouse peritoneal macrophages by bacterial lipopolysaccharide. Biochem J 310 (Pt 2):547-51.
Sato H, Nomura S, Maebara K, Sato K, Tamba M, Bannai S. 2004. Transcriptional control of cystine/glutamate transporter gene by amino acid deprivation. Biochem Biophys Res Commun 325(1):109-16.
Sato H, Shiiya A, Kimata M, Maebara K, Tamba M, Sakakura Y, Makino N, Sugiyama F, Yagami K, Moriguchi T and others. 2005. Redox imbalance in cystine/glutamate transporter-deficient mice. J Biol Chem 280(45):37423-9.
Sato H, Tamba M, Ishii T, Bannai S. 1999. Cloning and expression of a plasma membrane cystine/glutamate exchange transporter composed of two distinct proteins. J Biol Chem 274(17):11455-8.
Sato H, Tamba M, Kuriyama-Matsumura K, Okuno S, Bannai S. 2000. Molecular cloning and expression of human xCT, the light chain of amino acid transport system xc. Antioxid Redox Signal 2(4):665-71.
Sato H, Tamba M, Okuno S, Sato K, Keino-Masu K, Masu M, Bannai S. 2002. Distribution of Cystine/Glutamate Exchange Transporter, System Xc-, in the Mouse Brain. Journal of Neuroscience 22(18):8028-8033.
Schlag BD, Vondrasek JR, Munir M, Kalandadze A, Zelenaia OA, Rothstein JD, Robinson MB. 1998. Regulation of the glial Na+-dependent glutamate transporters by cyclic AMP analogs and neurons. Mol Pharmacol 53(3):355-69.
Schulz JB, Lindenau J, Seyfried J, Dichgans J. 2000a. Glutathione, oxidative stress and neurodegeneration. Eur J Biochem 267(16):4904-11.
Schulz JB, Lindenau J, Seyfried J, Dichgans J. 2000b. Glutathione, oxidative stress and neurodegeneration. European Journal of Biochemistry 267:4904-4911.
Sen CK, Packer L. 1996. Antioxidant and redox regulation of gene transcription. FASEB J 10(7):709-20.
Shih AY, Erb H, Sun X, Toda S, Kalivas PW, Murphy TH. 2006. Cystine/glutamate exchange modulates glutathione supply for neuroprotection from oxidative stress and cell proliferation. J Neurosci 26(41):10514-23.

Shih AY, Imbeault S, Barakauskas V, Erb H, Jiang L, Li P, Murphy TH. 2005. Induction of the Nrf2-driven antioxidant response confers neuroprotection during mitochondrial stress in vivo. J Biol Chem 280(24):22925-36.

Shih AY, Johnson DA, Wong G, Kraft AD, Jiang L, Erb H, Johnson JA, Murphy TH. 2003. Coordinate regulation of glutathione biosynthesis and release by Nrf2-expressing glia potently protects neurons from oxidative stress. J Neurosci 23(8):3394-406.

Skaper SD. 2007. The brain as a target for inflammatory processes and neuroprotective strategies. Ann N Y Acad Sci 1122:23-34.

Slivka A, Mytilineou C, Cohen G. 1987. Histochemical evaluation of glutathione in brain. Brain Research 409(2):275-84.

Sontheimer H. 2008. A role for glutamate in growth and invasion of primary brain tumors. J Neurochem 105(2):287-95.

Spencer SR, Xue LA, Klenz EM, Talalay P. 1991. The potency of inducers of NAD(P)H:(quinone-acceptor) oxidoreductase parallels their efficiency as substrates for glutathione transferases. Structural and electronic correlations. Biochem J 273 (Pt 3):711-7.

Stanimirovic DB, Ball R, Small DL, Muruganandam A. 1999. Developmental regulation of glutamate transporters and glutamine synthetase activity in astrocyte cultures differentiated in vitro. Int J Dev Neurosci 17(3):173-84.

Steindler DA. 2002. Neural stem cells, scaffolds, and chaperones. Nat Biotechnol 20(11):1091-3.

Swanson RA, Liu J, Miller JW, Rothstein JD, Farrell K, Stein BA, Longuemare MC. 1997. Neuronal regulation of glutamate transporter subtype expression in astrocytes. Journal of Neuroscience 17(3):932-940.

Tachibana T, Okazaki S, Murayama A, Naganuma A, Nomoto A, Kuge S. 2009. A major peroxiredoxin-induced activation of Yap1 transcription factor is mediated by reduction-sensitive disulfide bonds and reveals a low level of transcriptional activation. J Biol Chem 284(7):4464-72.

Talalay P. 1989. Mechanisms of induction of enzymes that protect against chemical carcinogenesis. Adv Enzyme Regul 28:237-50.

Talalay P, De Long MJ, Prochaska HJ. 1988. Identification of a common chemical signal regulating the induction of enzymes that protect against chemical carcinogenesis. Proc Natl Acad Sci U S A 85(21):8261-5.

Talalay P, Fahey JW, Holtzclaw WD, Prestera T, Zhang Y. 1995. Chemoprotection against cancer by phase 2 enzyme induction. Toxicol Lett 82-83:173-9.

Tate SS, Meister A. 1981. gamma-Glutamyl transpeptidase: catalytic, structural and functional aspects. Mol Cell Biochem 39:357-68.

Tietze F. 1969. Enzymic method for quantitative determination of nanogram amounts of total and oxidized glutathione: applications to mammalian blood and other tissues. Anal Biochem 27(3):502-22.

Venugopal R, Jaiswal AK. 1996. Nrf1 and Nrf2 positively and c-Fos and Fra1 negatively regulate the human antioxidant response element-mediated expression of NAD(P)H:quinone oxidoreductase1 gene. Proc Natl Acad Sci U S A 93(25):14960-5.

Verrey F, Closs EI, Wagner CA, Palacin M, Endou H, Kanai Y. 2004. CATs and HATs: the SLC7 family of amino acid transporters. Pflugers Arch 447(5):532-42.

Wakabayashi N, Dinkova-Kostova AT, Holtzclaw WD, Kang MI, Kobayashi A, Yamamoto M, Kensler TW, Talalay P. 2004. Protection against electrophile and oxidant stress by induction of the phase 2 response: fate of cysteines of the Keap1 sensor modified by inducers. Proc Natl Acad Sci U S A 101(7):2040-5.

Wang H, Tamba M, Kimata M, Sakamoto K, Bannai S, Sato H. 2003. Expression of the activity of cystine/glutamate exchange transporter, system x(c)(-), by xCT and rBAT. Biochem Biophys Res Commun 305(3):611-8.

Wang XF, Cynader MS. 2000. Astrocytes provide cysteine to neurons by releasing glutathione. J Neurochem 74(4):1434-42.

Wang XJ, Hayes JD, Wolf CR. 2006. Generation of a stable antioxidant response element-driven reporter gene cell line and its use to show redox-dependent activation of nrf2 by cancer chemotherapeutic agents. Cancer Res 66(22):10983-94.

Waniewski RA, Martin DL. 1984. Characterization of L-glutamic acid transport by glioma cells in culture: evidence for sodium-independent, chloride-dependent high affinity influx. J Neurosci 4(9):2237-46.

Warren BA, Patel SA, Nunn PB, Bridges RJ. 2004. The Lathyrus excitotoxin beta-N-oxalyl-L-alpha,beta-diaminopropionic acid is a substrate of the L-cystine/L-glutamate exchanger system xc. Toxicol Appl Pharmacol 200(2):83-92.

Wu D, Cederbaum A. 2004. Glutathione depletion in CYP2E1-expressing liver cells induces toxicity due to the activation of p38 mitogen-activated protein kinase and reduction of nuclear factor-kappaB DNA binding activity. Mol Pharmacol 66(3):749-60.

Wullner U, Loschmann PA, Schulz JB, Schmid A, Dringen R, Eblen F, Turski L, Klockgether T. 1996. Glutathione depletion potentiates MPTP and MPP+ toxicity in nigral dopaminergic neurones. Neuroreport 7(4):921-3.

Ye ZC, Rothstein JD, Sontheimer H. 1999. Compromised glutamate transport in human glioma cells: reduction-mislocalization of sodium-dependent glutamate transporters and enhanced activity of cystine-glutamate exchange. J Neurosci 19(24):10767-77.

Ye ZC, Sontheimer H. 1999. Glioma cells release excitotoxic concentrations of glutamate. Cancer Res 59(17):4383-91.

Zhang Y, Kensler TW, Cho CG, Posner GH, Talalay P. 1994. Anticarcinogenic activities of sulforaphane and structurally related synthetic norbornyl isothiocyanates. Proc Natl Acad Sci U S A 91(8):3147-50.

Zhu Y, Carvey PM, Ling Z. 2007. Altered glutathione homeostasis in animals prenatally exposed to lipopolysaccharide. Neurochem Int 50(4):671-80.